The University Of Sheffield.

The Molecular Mechanisms Underlying Gall Formation in *Plasmodiophora brassicae* Infected *Arabidopsis thaliana*

A thesis submitted in part fulfilment for the degree of Doctor of Philosophy.

Department of Animal and Plant Sciences,
The University of Sheffield.

Serina Ann Akhtar
MBiolSci (Hons) University of Sheffield

January 2014

Summary

Plasmodiophora brassicae is an obligate pathogen that causes clubroot disease. Infection occurs in plants of the *Brassica* genus including many economically important crops and the model organism *A. thaliana*. The disease results in a gall forming on infected root tissue. The gall is a consequence of extensive host cell division and expansion, additionally the disease leads to a disruption in cellular differentiation and organisation. The gall has a negative impact on shoot growth and leads to reductions in yields that can be up to 100 % in heavily infected fields. Currently there are no effective measures for the prevention or treatment of the disease.

The *A. thaliana* mutant *ein5-1* was shown to be tolerant to infection compared with wild-type, Col-0. *ein5-1* showed a delay in gall formation of approximately 7days, which was found to be a consequence of both delayed host symptom and pathogen development. ein5 encodes an exoribonuclease involved in ethylene signalling and miRNA-mediated cleavage. The role of these two pathways in infection was explored in order to further understand the tolerance response of *ein5-1*. Examination of the *ein2-1* mutant indicated that perturbations in ethylene signalling were not responsible for the tolerance response of *ein5-1*. The miRNA-biogenesis mutant, *hen1-5*, displayed a response to clubroot that was reminiscent of that seen in *ein5-1* indicating a possibly role for miRNA-silencing in clubroot infection.

A microarray analysis was conducted to examine changes in gene expression in Col-0 and *ein5-1* during infection. The analysis suggested that infection in both Col-0 and *ein5-1* impacted on gene expression in a similar manner. However, a role for salicylic acid and flavonoid related genes during infection of *ein5-1* was suggested. Further to this it was hypothesised that alterations in secondary metabolite content may play a role in *ein5-1* tolerance.

Acknowledgements

Firstly I liked to thank Dr Steve Rolfe and Professors Andrew Fleming and Julie Scholes for giving me the opportunity to undertake a PhD and for their supervision. Thanks in particular go to Steve for all his advice and help; getting to this point has been a difficult journey and I could not have done it without your encouragement, support and patience.

Thanks must go to all my C45 lab mates, past and present, for all the support both technical and emotional that you have given me over the past four years. You have all made working in the lab such a joy. Special thanks must go to Jody Smith and Anne-Laure Hepp, you guys are amazing! Thanks for all the support - you have kept me going! Thanks to Dr Robert Malinowski for all the clubroot technical help. I want to thank Maggi Killion for always being there for me when I needed to talk. Dr Jen Sloan, thanks for the coffee breaks, for being such great listener and for all the science help over the years. Carla Turner, I came upon you late in my PhD but you sure do make life fun, thanks for getting me through the worst bit. I must thank Professor Jeff Green for his continuing support long after I left MBB. Thanks also to past and present members of F10 for their friendship and advice over the years. Special mention to Dr Laura Smith, Nikki Whitting and Ashley Davies, it is hard to put into words how invaluable your friendships have been to me throughout my PhD, but I am so grateful to you all! A very special thank you to Dr Kay Guccione for getting me through the last couple of months and for being such a good friend to me from the minute I stepped into the lab - you are one in a million!

To Mum, Dad and Daniel, I could not be more grateful to you all for you unwavering love and support. Thanks for always believing in me.

Finally, Dr Adam Hayes: for the science help, for keeping me on track, for the confidence boosts, for your patience and for always being on hand to give me that stern talking to when I needed it. I could not have done this without you!

Abbreviations

DI	disease index
DPI	days post inoculation
ECD	European clubroot definition
ER	endoplasmic reticulum
IAA	indole-3-acetic acid
miRNA	microRNA
PCR	polymerase chain reaction
PGR	plant growth regulators
PTGS	post transcriptional gene silencing
RDRP	RNA-dependent RNA polymerase
RISC	RNA induced silencing complex
ROS	reactive oxygen species
siRNA	small-interfering RNA
VC	vascular cambium
WT	wild type

Contents Page

Chapter 1: General Introduction

Clubroot has been termed the most important disease affecting the brassica crops, this is because of its destructive nature and lack of effective control measures. The *Brassica* genus includes crops such as oilseed rape (*Brassica napus*), the *Brassica oleracea* cultivars (broccoli, cauliflower, Brussels sprouts etc.) and the *Brassica rapa* cultivars (turnip, Chinese cabbage etc.). It is thought that all members of the *Brassicaceae* family are susceptible to the disease (Dixon 2009). The disease has been reported in over 60 countries around the world and is reported to account for a reduction in yield of 10-15 % on a global scale; as the pressure for Brassica crops for food and industry has increased so has the incidence of clubroot disease (Dixon 2009).

Plasmodiophora brassicae, an obligate pathogen, is the organism responsible for the disease and was first identified as the cause of clubroot in 1878 by the Russian scientist M.S. Woronin. The organism has an unusual biology and cannot be cultured axenically. The pathogen is a eukaryotic microorganism placed within the class Phytomyxea (Plasmodiophorids) which is found in the phylum Cercozoa within the supergroup Rhizaria (Cavalier-Smith and Chao 2003; Burki et al. 2010). The organism has a complex life cycle which is detailed in Section 1.1.

The disease causes a gall to form on the root system of infected plants. Galls are formed as a consequence of extensive cell division (hyperplasia) and expansion (hypertrophy). The gall leads to a disruption in the normal root architecture which leads to an inhibition of water and nutrient uptake in turn leading to a loss of yield (Oxley 2007; Jubault et al. 2013). The shoot system becomes stressed as the disease progresses, plants are stunted and early flowering is initiated (Dixon 2009). These symptoms manifest in crops as, for example, the formation of poor-quality spears in cauliflower, Brussels sprouts becoming physically unstable and the seed and oil quality of oilseed rape being reduced (Dixon 2009). The disease typically results in a loss of 30 % and upwards of crop yield (Oxley, 2007; Leboldus et al. 2012). Yield, quality, aesthetics, taste, storability of crop and value of growing land are all impacted detrimentally by clubroot infection (Dixon 2009).

The disease is transmitted by the resting spores of *P. brassicae.* In fields with 100 % infestation, spores were shown to fall below detection level only after 17.3 years (Wallenhammar 1996). Soil contaminated with resting spores remains that way for many years, impeding the eradication of the disease from fields. Spread of the disease occurs via transfer of infected soil containing resting spores; on the shoes of farm

workers and on the machinery and tools used to farm the land (Cook and Swartz, 1930).

Traditional methods for controlling clubroot include liming, which helps to control the disease by increasing the soil pH and increasing the concentration of calcium ions in the soil (Oxley, 2007; Donald and Porter, 2009). Liming requires large quantities of lime and multiple applications, and is not suitable for all crop production, for example oilseed rape (Oxley, 2007; Leboldus et al. 2012). In severe infestations liming is inadequate and crop rotation with non-*Brassicas* is used to combat the disease, with breaks between *Brassicas* of 4 to 5 years ideally (Oxley, 2007; Rastas et al. 2012). *P. brassicae* has been found to colonise roots of non-brassicas but not cause infection or lead to gall formation in these plants (Ludwig-Muller et al. 1999). It is possible that infection of non-brassicas are a dead-end for the pathogen and they have no reproductive purpose, alternatively it has been suggested that infection of non-brassicas act as a reservoir of spores; increasing the inoculum potential of the pathogen (Dixon 2009). If this were the case it would add to the problems of inadequate control as plants used for crop rotations would have to be carefully controlled.

Some resistant cultivars are available; however these too are often insufficient, many having shown a break down in resistance after a limited period of use (Oxley 2007). For example, a resistant cultivar of oilseed rape: 'Mendel', has been available for commercial use in the UK since 2003 (Oxley, 2007 and Diederichsen et al 2009). However, by 2007 it was reported that 'Mendel' had been subjected to serious cases of clubroot disease, indicating a breakdown in resistance (Oxley 2007). It was noted that to be successful resistant cultivars needed to be used in conjunction with classical control methods, and that resistant cultivars were not a suitable rotation crop (Oxley, 2007 and Donald and Porter 2009).

The control of the disease is further complicated by the lack of chemical control measures (Donald and Porter 2009). Very few pesticides have been shown to be affective against clubroot. Often they are not widely used due to legislative issues and expense. For instance, no pesticides against clubroot are approved for use in the European Union region (Oxley 2007 and Donald and Porter 2009). There is therefore a great need for the development of new and effective measures for the control of clubroot.

A. thaliana is a model organism of choice in plant biology, due to its many useful traits which make it amenable to manipulations required for genetic and molecular analysis. These include its small and sequenced genome, its rapid life cycle and the ease with which it is transformed. *A. thaliana* has also been shown to be susceptible to clubroot infection (Koch et al. 1991). It has since been used by many researchers to further the understanding of clubroot infection. Due to the wealth of knowledge relating to clubroot infection and its useful traits discussed above *A. thaliana* was used in this work to studying mechanisms underlying gall formation during clubroot disease. Further aspects of plant-pathogen interactions are discussed below.

1.1 The Life Cycle of *Plasmodiophora brassicae*

Traditionally the life cycle of *P. brassicae* has been divided into two phases, termed the primary and secondary phases (Cook and Schwartz 1930). More recently the life cycle has been referred to in three stages; survival in the soil, root hair infection (primary phase) and the cortical infection (secondary phase). A schematic of the pathogen's life cycle is shown in Figure 1.1.

The life cycle is initiated by resting spores which reside in the soil. Resting spores of *P. brassicae* have a spiny wall and are approximately spherical in shape, with a diameter ranging from around 3 to 5 µm (Ingram and Tommerup 1972). The resting spores carry a single nucleus and are haploid (Tommerup and Ingram 1971; Ingram and Tommerup 1972). On germination a single motile primary zoospore emerges through a pore in the resting spore (Tommerup and Ingram 1971; Ingram and Tommerup 1972). The primary zoospore is slightly ovate in shape with two unequal anterior flagella; a shorter flagellum with a blunt end and a longer whiplash flagellum (Ingram and Tommerup 1972; Asano and Kageyama 2006). The primary zoospore then moves to the site of infection, it is thought that the zoospores require a film of water in soil to swim towards the root hairs (Hwang et al. 2012).

1.1.1 The Primary Phase of *P. brassicae* Life Cycle: Root Hair Infection

Following germination of the resting spore it attaches to and penetrates the host root hairs, a process which was described by Aist and Williams, 1971. The primary zoospores collide with the root hairs several times before they become attached via the opposite side to where their flagella reside, encystment then occurs. The flagella are retracted and the zoospore becomes flattened against the root hair wall, following this the parasite becomes a spherical cyst. Within the cyst is a tubular cavity name the

Rohr, and inside the Rohr lies the Stachel: a sharp-pointed rod. Penetration of the root hair wall occurs approximately 2.5 to 3.5 hours after encystment. The cyst begins to form a large internal vacuole and the Rohr orientates one end towards the root hair wall with a swelling formed at its end termed the “adhesorium”. The satchel penetrates the cell wall and a spherical uninucleate amoeba is injected inside. The adhesorium is formed from an invagination of the Rohr which results in the Stachel being forced through the host cell wall. It is thought that the adhesorium formation and injection of the parasite is a result of pressure created within the cyst vacuole, and that the adhesorium may contract to aid this process, the process appears to be primarily mechanical (Aist and Williams 1971).

Inside the root hair the pathogen forms primary plasmodia. On entering the host cytoplasm the uninucleate primary plasmodia undergoes several rounds of synchronous nuclear division to become multinucleate (Ingram and Tommerup 1972). The plasmodia enlarge and root hairs may be completely filled by plasmodia (Ingram and Tommerup 1972). The cytoplasm of the primary plasmodia cleaves to yield between 4 and 10 zoosporangia, each containing 3 to 16 nuclei (Tommerup and Inrgam 1971). These nuclei correspond to secondary zoospores, which are released from the zoosporangia. The primary phase of infection is not responsible for any of the macroscopic symptoms of the disease and does not cause any significant yield or quality losses (Hwang et al. 2012).

1.1.2 The Secondary Phase of *P. brassicae* Life Cycle: Infection of Cortical Cells

The secondary phase of infection is associated with the onset of disease symptoms; the host cell hypertrophy (cell expansion), hyperplasia (cell division) and loss of cell differentiation resulting in gall formation which is indicative of clubroot disease. The secondary phase of infection is initiated by secondary zoospores which cannot be visually distinguished from primary zoospores (Asano and Kageyama 2006). Secondary zoospores were found to be necessary for cortical infection, while primary zoospores were not (Dobson and Gabrielson 1983).

The role played by secondary zoospores during infection has been an area of the life cycle that has been debated greatly. It has been proposed by some authors that secondary zoospores are released from the root hairs (Buczacki 1983). Secondary zoospores have been observed in the process of moving from inside the root hair to the external environment (Buczacki, 1983). It could be that once in the external environment secondary zoospore act to the further infect more root hairs, thus

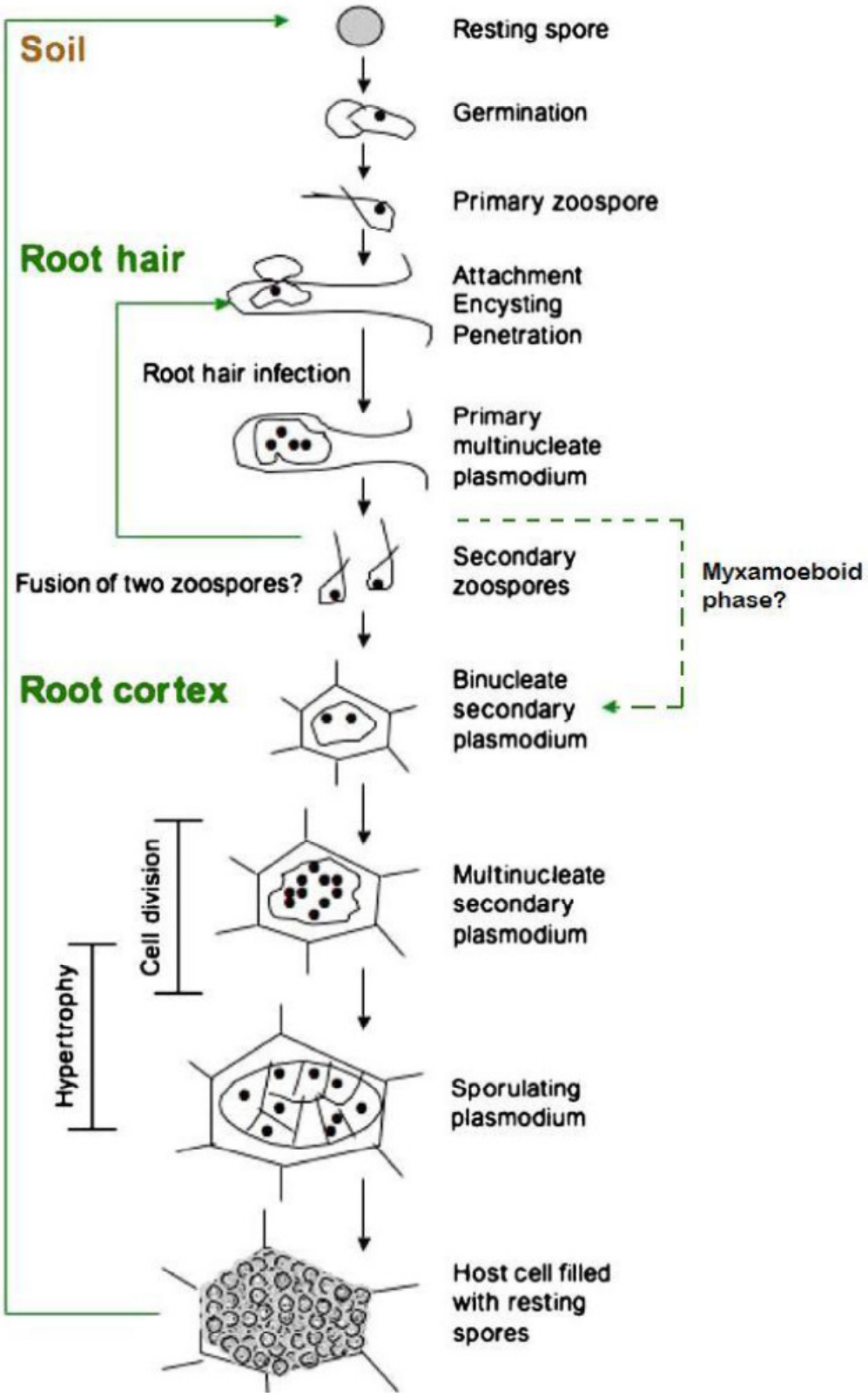

Figure 1.1 The Life Cycle of *Plasmodiophora brassicae.*
The life cycle consists of two phases; the primary phase which occurs in the root hairs of the host plant and the second phase which occurs in the cortical cells. Details can be found in the text. Adapted from Ludwig-Müller and Schuller (2008).

amplifying infection in a kind of micro-cycle (Buczacki, 1983). Aist and Williams reported that within the root hairs a few secondary zoospores encysted, developed a vacuole, formed a structure resembling the Rohr and also produced adhesoria (Aist and Williams, 1971). Although none of the secondary zoospores were seen to empty their contents, they suggested that secondary zoospores of *P. brassicae* are capable of penetrating the host cell wall in a manner similar to that used by primary zoospores, and they may encyst inside the base of the root hair cell and penetrate directly into the first layer of cortical cells (Aist and Williams, 1971). It has been suggested that the secondary zoopores are both released into the soil and are able to move from the root hair directly to the cortical cells, this would seem a reasonable explanation; some of the secondary spores initiating secondary infection while others act to perpetuate the primary infection (Kageyama and Asano, 2009). Mithen and Magrath suggested an alternative life cycle in which the role of secondary zoospores is solely to re-infect the root hairs producing more secondary zoospores. A myxamoeboid stage in the life cycle is suggested to initiate cortical infection leading to secondary plasmodia formation (Mithen and Magrath, 1992). The myxamoebae were seen to possess pseudopodia-like structures indicating they are able to actively move (Mithen and Magrath, 1992). Mithen and Magrath (1992) further suggested that *P. brassicae* is able to produce enzymes which digest host cell walls, facilitating myxamoebae movement to the cells of the cortex. This myxamoeboid stage has also been seen by Kobelt *et al* (2000) and Donald *et al* (2008), in *Arabidopsis* and *Brassica oleracea* respectively.

However cortical infection proceeds, binucleate secondary plasmodia form in the cortical cells. Secondary plasmodia enlarge and undergo a series of synchronous mitotic divisions to become multinucleate (Tommerup and Ingram 1971; Ingram and Tommerup 1972). Pairs of nuclei within the secondary plasmodia may fuse followed by immediate meiosis; this process has been suggested to form the sexual stages of *P. brassicae* life-cycle (Tommerup and Ingram, 1971). The plasmodial cytoplasm cleaves to yield numerous resting spores (Tommerup and Ingram, 1971; Ingram and Tommerup, 1972). Mature spores remain within host cells until the tissue begins to decay; as cell walls are ruptured the spores are released into the soil thus completing the disease cycle (Cook and Swartz, 1930).

1.2 Impact of Clubroot Infection on the Host

The first visible disease symptoms, swelling of the hypocotyl, appear 2 weeks after infection of *A. thaliana* with *P. brassicae* (Fuchs and Sacristan 1996). Ten to 14 days later typical clubroot symptoms are apparent; severe swelling of the hypocotyl, primary,

secondary and lateral roots (Mithen and Magrath 1992; Fuchs and Sacristan 1996). Sections of infected roots reveal the pathogen has promoted extensive cell division and cell expansion (Mithen and Magrath 1992; Fuchs and Sacristan 1996). As the gall forms as a consequence of cell division and expansion it has been suggested that both cytokinins and auxins are involved in symptom development, the role of both these plant growth regulators (PGRs) during clubroot infection is discussed below (Ludwig-Müller et al. 2009). A breakdown in the structural organisation of the root is seen, with the regions of the cortex, endodermis and stele no longer apparent (Mithen and Magrath 1992). The formation of galls proceeds rapidly and 6 weeks after inoculation the galls being to decompose (Mithen and Magrath 1992). Infection often leads to stunted plants and delayed flowering (Fuchs and Sacristan 1996). Premature deaths are also seen before flowering, usually preceded by the wilting and yellowing of leaves and rotting of the root system (Koch et al. 1991; Fuchs and Sacristan 1996). As an obligate pathogen *P. brassicae* is dependent on the host for its nutritional needs during infection (Ludwig-Müller et al., 2009). *P. brassicae* induced galls were found to act as sinks for carbon (Evans and Scholes 1995).

1.2.1 Does Clubroot Infection Cause *de novo* Meristem Formation or Make Use of Existing Meristems?

It was initially reported that clubroot infection caused cells to re-enter the cell cycle and thus cell division, leading to gall formation, was initiated (Devos et al. 2006). An increase in cytokinin levels was shown to proceed an increase in expression of the CYCLIN B1::GUS (CYCB1::GUS) reporter gene, a marker for cells undergoing mitosis, at 4DPI in infected *A. thaliana* roots (Devos et al. 2006). This re-initiation of cell division was said to be a consequence of secondary infection by *P. brassicae*, as cortical cells were seen to be dividing (Devos et al. 2006). The authors stated that *P. brassicae* induced a new meristem to form as a consequence of elevated levels of cytokinin, which were thought to be pathogen derived (Devos et al. 2006). It was concluded therefore that *de novo* meristem formation was driving gall development during infection (Devos et al. 2006).

Recent work however, found that *P. brassicae* induced cell division was occurring from 12DPI onwards (Malinowski et al. 2012). This is concurrent with the onset of secondary thickening, when a secondary meristem is formed, the vascular cambium (VC), which acts to provide cells for xylem and phloem production and increases the width of the hypocotyl/root. Use of the CYCB1::GUS construct showed that cell divisions were in fact occurring in the vicinity of the VC in infected tissue (Malinowski et al. 2012).

AINTEGUMENTA::GUS (ANT::GUS) marker expression, an indicator of meristem activity, overlapped with that of CYCB1:GUS expression in the VC (Malinowski et al. 2012). The timing and location of *P. brassicae* induced cell division indicated that a stimulation of an existing meristem, the VC, was occurring during secondary infection as opposed to an initiation of a new meristem (Malinowski et al. 2012). The pathogen hijacks the process of secondary thickening to access a reservoir of dividing cells which drive gall formation (Malinowski et al. 2012). Further to this it was found that the VC was necessary for gall formation (Malinowski et al. 2012). Blocking cell division with the use of the cell cycle inhibitor KRP1, lead to plants which were unable to form galls (Malinowski et al. 2012). Interestingly, the pathogen was still able to complete its lifecycle and produced infective spores in the absence of a gall, indicating that gall formation and pathogen development can be uncoupled (Malinowski et al. 2012). As KRP1 switches off all cell division these results did not rule out the Devos *et al de novo* meristem hypothesis. Therefore infection in the *cle41-1* mutant, which exhibits altered cambial activity, was examined to investigate the role of the VC during gall formation (Malinowski et al. 2012). Cell division and gall formation were greatly impaired in this mutant, indicating that an increase in VC activity is a major factor in gall formation in *A. thaliana* (Malinowski et al. 2012). This work has lead to the *de novo* meristem driving gall formation theory being put aside in favour of the notion that the existing meristem of the VC is used to drive gall formation.

As Devos *et al* used the same clubroot isolate as Malinowski *et al*, it is possible that differences in onset of cell division occurred as a consequence of the different tissue examined: root and hypocotyl respectively (Devos et al. 2006 and Malinowski et al. 2012). As the pathogen has to move from the root, the initial site of infection, to the hypocotyl it is feasible that there would be differences in the time secondary infection occurs in these two tissues, with the timing being delayed in hypocotyl tissue. Malinowski *et al* also included cross sections of infected and uninfected tissue which made visualisation of the cellular location of reporter gene expression easier than in the whole tissue images, at much lower magnifications, provided by Devos *et al* (Devos et al. 2006 and Malinowski et al. 2012). In addition pathogen development and location could not be visualised in the Devos *et al* data (Devos et al. 2006). As Malinowski *et al* used additional mutant and reporter gene lines to Devos *et al* they had an additional pool of evidence from which their conclusions could be drawn, leading to a more complete picture of the drivers behind gall formation being established (Devos et al. 2006 and Malinowski et al. 2012).

1.2.2 Transcriptome and Proteome Studies

To date two studies have looked to investigate changes in host gene expression during infection using a microarray analysis (Siemens et al. 2006; Agarwal et al. 2011). Siemens examined changes in gene expression in *Arabidopsis* at an early time point (10DPI) and at a later stage of infection in hypocotyls/roots (23DPI). At the early time point no disease symptoms were present and plasmodia were present only in the young vegetative state, at the late time point a gall had formed and resting spores had begun to form in the root. Mitochondrial-associated transcripts were found to be up-regulated at 10 DPI. Chloroplast-associated genes were found to be up-regulated 23DPI, the authors stated that this was a consequence of the tissue used for microarray analysis being green. This is likely due to the fact that as the gall forms in the hypocotyl it causes breaks to form in soil exposing the tissue to light as opposed to it being a consequence of infection. Few metabolic pathways were found to be differentially regulated at 10DPI, while at 23DPI starch, lipid and secondary metabolism was up-regulated. Many transport process were found to be differentially regulated at 23DPI compared to 10DPI. The authors indicated this was a consequence of reserve accumulation at the latter stages of the disease. The majority of defence-related proteins were found to not be differentially expressed during infection, consistent with *P. brassicae* survival in the host for a long period of time during infection. In line with the impact of disease on cell division and expansion many genes associated with growth and cell cycle control were induced during infection. Many plant hormone biosynthesis and signalling-associated genes were also found to be differentially expressed during infection, although it appeared there was no pattern in their regulation, as many of the hormone associated genes were found to be both up-regulated and down-regulated on infection. The Siemens study did not provide any statistical evidence to indicate whether genes that were found to increase or decrease on infection did so significantly, which makes the conclusions drawn from this study difficult to interpret (Siemens et al. 2006).

Agarwal *et al* investigated changes in host gene expression during the primary phase of infection in *A. thaliana* roots 4, 7 and 10DPI (Agarwal et al. 2011). A small subset of genes were found to be differentially regulated in the study (Agarwal et al. 2011). This is probably due to their being fewer physiological and morphological changes occurring during the primary stages of infection. The differentially expressed genes were found to fall into a range of functional categories, although due to the small number of genes differentially expressed the differentially regulated function categories may only have contained a few genes. At 4DPI genes involved in signalling transduction and

transcription were found to be up-regulation in infected plants. It is not surprising that infection would lead to alterations in host signalling and gene expression. Genes involved in cell wall modification and cell growth were also up-regulated at this early time point. Genes down-regulated at 4DPI included those associated with cellular transport, biosynthesis pathways and response to stimuli. Metabolism related genes also appeared differentially regulated although no pattern, either up or down-regulated, was established. Fewer genes were found to be differentially expressed at 7 and 10DPI which were grouped into fewer functional categories.

Two-dimensional gel electrophoresis was used to identify proteins differentially expressed during infection (Devos et al. 2006). Protein expression was examined in hypocotyl/roots of *A. thaliana* 4DPI (Devos et al. 2006). 7 % of those proteins differentially regulated were found to be associated with general metabolism, while 9 % of the differentially expressed proteins were related to energy metabolism. 26 % of differentially examined proteins were involved in cell rescue, defence and virulence including proteins corresponding to myrosinases and those involved in the detoxification of reactive oxygen species (ROS). 9 % of differentially expressed proteins were cell architecture related. Cao *et al* conducted a similar analysis of *Brassica napus* hypocotyls/roots 12, 24, 24 and 72 hours after inoculation (Cao et al. 2008). Proteins that were differentially regulated included those associated with detoxification of ROS, metabolic pathways, lignin biosynthesis, calcium homeostasis and signal transduction (Cao et al. 2008).

1.2.3 The Role of Cytokinins During Infection

An increase in the concentrations of cytokinins was found in infected *Brassica rapus* (turnip) tissue compared to uninfected tissue, levels of cytokinins were found to be 10 to 100 times that of those found in uninfected plants (Dekhuijzen and Overeem 1971). The cytokinins found to be increased were zeatin and zeatin riboside, the authors indicated that the cytokinins were derived from the host (Dekhuijzen and Overeem 1971). An additional study found that the concentration of cytokinins zeatin and zeatin riboside were increased by 30-50 % in infected turnips (Dekhuijzen 1980). It was also found that zeatin riboside was increased 6, 13 and 21DPI and isopentenyl adenosine was increased 21DPI in infected Brassica rapa spp. pekinensis (Chinese cabbage) roots/hypocotyls (Devos et al. 2005). Four cytokinin biosynthesis genes BrIPT1, 3, 5 and 7 were found to be up-regulated in Chinese cabbage 20DPI, and were not found to be up-regulated in resistant cultivars (Ando et al. 2006). This expression was found in tissue not yet displaying symptoms, indicating that early increases in cytokinin levels

initiate gall formation, as the genes were not up-regulated in tissue which had formed galls (Ando et al. 2006). Dekhuijzen found that plasmodia contained at least three different cytokinins; zeatin, zeatin riboside and the OH-glucoside of zeatin riboside (Dekhuijzen 1981). It was concluded that cytokinins are synthesised by *P. brassicae* and are then released into the host cytoplasm inducing cell division (Dekhuijzen 1981). In keeping with this conclusion it was found that secondary plasmodia of *P. brassiace* were able to incorporate ^{14}C-adenine into *trans*-zeatin (Müller and Hilgenberg 1986). Thus the increase in cytokinin concentration seen in infected roots/hypocotyls is partly a result of the ability of *P. brassicae* to actively synthesise zeatin. It is possible that both the host and the pathogen produce cytokinin which drives gall formation.

A cytokinin responsive reporter gene construct: ARR5::GUS, showed that altered cytokinin response was visible from 3DPI in *A. thaliana* roots (Devos et al. 2006). Two cytokinin metabolites: isopentenyl adenine and isopentenyl adenosine were found to be significantly increased in infected tissue compared to uninfected tissue, although other cytokinin metabolites were not found to be induced significantly during infection (Devos et al. 2006). The authors stated that the first indication of infection was an increase in cytokinin levels, which is in line with other studies which have found increases in cytokinin early in infection. Pathogen induced cell division is seen at the beginning of gall formation which correlates with the early increase in cytokinin level as a driver of this (Mithen and Magrath 1992). In addition it was found that the ADK protein, involved in cytokinin homeostasis, was down-regulated during the very early stages of infection in both *A. thaliana* and *B. napus* (Devos et al. 2006; Cao et al. 2008). This down-regulation was suggested to lead to an increase in active cytokinin levels (Devos et al. 2006; Cao et al. 2008). Agarwal *et al* also suggested that increased cytokinins levels were important during the early stages of infection (Agarwal et al. 2011).

Two out of a known seven putative cytokinin biosynthesis genes as well as two cytokinin oxidases/dehydrogenases (*CKX1* and *CKX6*) were found to be down-regulated on infection (Siemens et al. 2006). However, as stated above there was no statistical analysis included in the study and differences in gene expression were not reported as fold-changes. While a third cytokinin oxidase/dehydrogenase (*CKX4*) was reported to be up-regulated and the other *CKX* genes were found not to respond to clubroot infection. A reduction in specific *CKX* genes could lead to an increase in cytokinin levels. In addition a cytokinin receptor *CRE1/AHK4* was found to be up-regulated, an indication that clubroot infected tissue has an increased sensitivity to cytokinin. A reduction in expression of *CKX1* and 6 was seen using RT-PCR at 10 and 23DPI (Siemens et al. 2006). Using *GUS*:promoter gene fusions Siemens *et al* showed

that expression of *CKX1* and *2* was down-regulation during infection. *Arabidopsis* lines overproducing *CKX1*, *CKX2* and *CKX3* were used to examine the impact of over-expressing cytokinin degrading enzymes on clubroot disease (Siemens et al. 2006). Over-expression of *CKX1* and *CXK3* resulted in apparent resistance to clubroot isolate 'e_H' while over-expression of *CKX2* had only a limited impact on the disease. Infected plants over-expressing *CKX1* were said to be similar to uninfected plants in appearance and *CKX3* over-expressing plants were found to have a significantly different response to infection to Col-0 which is susceptible to the disease. Plants over-expressing *CKX1* and *CKX3* were also found to be tolerant to three additional clubroot isolates, indicating a more general resistance response to clubroot infection. Over-expression of *CKX1* was correlated to reduced cytokinin levels in the root, suggesting that the resistance to clubroot infection is a consequence of cytokinin levels being lowered. The study by Siemens *et al* provided additional evidence to the notion that cytokinins play a large role during infection. However, the study did lack any histological examination of tissue using only gall size as an indicator of resistance. While this is a useful measure, being combined with a histological survey would give a much greater view of the impact of the disease on mutant lines compared to wild-type, in terms of both host and pathogen development.

An *A. thaliana* quadruple mutant: *atipt1;3;5;7*, which has 4 cytokinin biosynthesis genes disrupted by a T-DNA insertion was found to be unable to form VC and displayed a reduction in root girth (Matsumoto-Kitano et al. 2008). In addition, application of exogenous cytokinin was found to reactivate the VC in these plants (Matsumoto-Kitano et al. 2008). It was therefore concluded that cytokinin is required for the formation of the VC and for secondary thickening to occur (Matsumoto-Kitano et al. 2008). As discussed above Malinowski *et al* found that activity of the VC and secondary thickening were required for gall formation during clubroot infection (Malinowski et al. 2012). Could it be that Siemens *et al* saw a reduced gall size in *CKX* mutants due to defects in cytokinin levels which led to a reduction in the VC activity? Even plants with moderately lower levels of cytokinin led to a reduction in root thickening and disruption of VC activity led to a significantly decreased gall size (Matsumoto-Kitano et al. 2008; Malinowski et al. 2012). A cytokinin responsive marker indicated that cytokinin levels were reduced in the *CKX1* root, therefore it is plausible that VC activity was possibly also reduced leading to reduced gall formation (Siemens et al. 2006). As a histological examination of the *CKX* mutants was not included in the study this hypothesis cannot be confirmed without further experiments being undertaken (Siemens et al. 2006). It does seem likely though that increases in cytokinin during infection occur in order to maintain the VC which in turn provides dividing cells to drive gall formation.

1.2.4 The Role of Auxins During Infection

Unlike cytokinins there is no evidence to suggest that *P. brassicae* has the ability to synthesise auxins (Ludwig-Müller et al. 2009). Several studies have investigated the auxin content of infected roots/hypocotyls (Raa 1971; Butcher et al. 1974; Mousdale 1981; Ludwig-müller et al. 1993). Auxin levels were found to be 50-100 times higher in infected cabbage roots compared with uninfected roots (Raa 1971). Further to this auxin activity increased in infected tissue of *B. rapa* (Butcher et al. 1974). The levels of indole-3-acetic acid (IAA) were found to be 66.5 % higher in infected Chinese cabbage plants than in non-infected plants 10DPI (Ludwig-müller et al. 1993). In contrast lower levels of IAA were found in the root/hypocotyls of infected swede (Brassica napus variant Danestone) plants compared to uninfected plants (Mousdale 1981). It has been suggested that this could be due to the older age of the tissue used in Mousdale's analysis or due to the plasmodia acting as sinks for IAA which is then difficult to extract from infected tissue (Ludwig-müller et al. 1993; Devos et al. 2006; Ludwig-Müller et al. 2009). It is generally though that there are elevated levels of auxin in infected tissue compare to uninfected tissue.

In-line with this the use of DR5::GUS showed increased auxin responsiveness in infected roots from 6DPI, indicating levels of auxin were up-regulated during infection (Devos et al. 2006). Myrosinase, IAR4 and GST proteins were all found to be up-regulated at 4DPI, these proteins are involved in the regulation of auxin biosynthesis (Devos et al. 2006). This evidence coupled with infected tissue having increased auxin responsiveness lead the authors to conclude that plasmodia act as a sink for auxin (Devos et al. 2006). Further to this they suggested that the initial increase in cytokinin they observed in infected tissue lead to the establishment of a sink for auxin, which is why an increase in cytokinin levels proceeded an increase in auxin levels (Devos et al. 2006).

A microarray analysis of infection tissue from Col-0 roots/hypocotyls found genes involved in auxin homeostasis were up-regulated (Siemens et al. 2006). Nitrilases 1 and 2 were found to be induced during infection, particularly at 23DPI (Siemens et al. 2006). Several members of the GH3 family, which are able to synthesise IAA-conjugates, were up-regulated during infection; indicating that both the free IAA levels and the auxin pool are important during infection (Siemens et al. 2006).

Nitrilase is an enzyme involved in the production of the auxin IAA in Brassica plants. Expression of *NIT1* and *2* were found to be up-regulated in *A. thaliana* during the later

stages of infection (Grsic-Rausch et al. 2000). The transcript of a nitrilase gene homolog from *B. rapa* (*BrNIT-T1*) was found to be induced 100-fold in infected roots compared to uninfected roots (Ishikawa et al. 2007). It has also been indicated that the expression of *NIT1* from *Brassica juncea* variant *tumida* is up-regulated from 20DPI and reaches levels 50x that seen in uninfected tissue, this further suggests a role for nitrilases in clubroot infection (Liu et al. 2012).

Additionally several auxin-associated *A. thaliana* mutants have been shown to display an altered response to clubroot, compared to wild type (WT), when infected. *alh1*, which is defective in cross-talk between ethylene and auxin- most likely at the site of auxin transport was found to be resistant to clubroot infection (Devos et al. 2006). It was hypothesised that this mutant is resistant because IAA could not reach site of infection and therefore fails to initiate gall formation (Devos et al. 2006). *nit1-3*, defective in *NIT1*, had a reduced infection rate and produced smaller galls when compared to the WT (Grsic-Rausch et al. 2000). *axr3-1* which is involved in auxin response was found to be less susceptible to clubroot infection (Alix et al. 2007). The authors concluded this was due to a negative regulation of auxin-induced genes in the mutant (Alix et al. 2007). Two TU mutants of *A. thaliana*, TU3 and 8, which have altered glucosinolate patterns, where shown to have reduced symptom development compared to WT when infected with clubroot (Ludwig-Müller et al. 1999). Glucosionolates have been implicated as precursors for auxin biosynthesis and in keeping with this the levels of IAA where found to be reduced in TU3 and 8 (Ludwig-Müller et al. 1999; Ludwig-Müller et al. 2009).

There is a great wealth of information available on the involvement of auxins during clubroot infection. The evidence suggests a major role for auxins in clubroot disease progression. However, more work is needed to gain a clearer understanding of the specific roles auxin plays in gall formation.

1.3 Aims, Objectives and Hypotheses of the Project

The aim of the work presented in this thesis was to understand the molecular mechanisms controlling gall formation in *A. thaliana* infected with *P. brassicae*. It is hypothesised that *P. brassicae* subverts the normal development and signalling pathways of the root and hypocotyl leading to gall formation. It had been previously suggested that the *ein5-1* mutant shows tolerance to clubroot infection (Penny-Evans 2000). The response of *ein5-1* to infection was therefore examined. Further to this it was investigated whether the tolerance response of *ein5-1* was due to its role in

ethylene signalling or its other roles in the microRNA (miRNA) pathway. Finally an analysis of gene expression during infection of *ein5-1* and Col-0 was conducted. Contrasting wild type and tolerant responses could lead to new avenues for disease control being highlighted.

The project objectives were:

1. To examine how the regulation of cell division, expansion and differentiation in hypocotyls is altered in *P. brassicae* infected wild type (WT) plants. Examining which cells within the root are affected and at which time points during infection the alterations occur.

2. To understand the mechanisms underlying the tolerance response of *ein5-1*, specifically to understand if perturbations in ethylene response or RNA silencing are responsible for the tolerance response.

3. To investigate how gene expression is altered in the *ein5-1* mutant compared with WT plants during infection with *P. brassicae.*

Chapter 2: Investigating the Role of *ein5-1* During Infection of *Arabidopsis thaliana* with *Plasmodiophora brassicae*

2.1 Introduction

As discussed in the opening chapter, the PGRs cytokinins and auxin have been shown to play a role during clubroot infection. Consequently a screen of various PGR *Arabidopsis* mutants was undertaken in this laboratory (Penny-Evans 2000). Penny-Evans screened various auxin and ethylene mutants, using gall size as the main measure of infection (Penny-Evans 2000). The auxin mutants screened showed little differential response when infected with clubroot compared with wild-type plants. The screen of the ethylene mutants however, yielded varied results. Some of the ethylene mutations examined, *ethylene insensitive 2-1* (*ein2-1*) and *ein3*, had little impact on the plants response to infection. One, *ethylene response 1-3* (*etr1-3*), was more susceptible to clubroot infection. Three of the ethylene mutants screened, *ein5-1*, *ein7* and *ein4-1*, were found to be more tolerant of clubroot infection, with *ein5-1* being particularly tolerant to infection. *ein5* and *ein7* were subsequently found to be allelic (Potuschak et al. 2006).

2.1.1 The Ethylene Signalling Pathway

Ethylene (C_2H_4) is a gaseous plant hormone which has been attributed to the control of many processes including seed germination, fruit ripening, responses to stress and pathogens. The gas is synthesised from methionine via several enzymatic steps, Figure 2.1. Plants exposed to ethylene in the dark exhibit the “triple response” which results in plants with short, thickened hypocotyl/roots and an exaggerated apical hook. The “triple response” has been exploited in order to discover members of the ethylene signalling pathway (Guzmán and Ecker 1990; Roman et al. 1995). Identifying, for example, plants that are insensitive to ethylene i.e. do not exhibit the “triple response” when exposed to ethylene and those that display a constitutive ethylene response i.e. displaying the “triple response” in the absence of ethylene. Ethylene signalling was initially thought to occur through a linear pathway, extensive research has however, uncovered a pathway with many levels of regulation, see Figure 2.2.

Ethylene is first perceived by five receptors which are found on the endoplasmic reticulum (ER): ETR1, ETR2, ETHYLENE SENSOR 1 (ERS1), ERS2 and EIN4 (Bleecker et al. 1988; Hua et al. 1995; Hua et al. 1998; Sakai et al. 1998). The receptors act to negatively regulate signalling with ethylene inactivating receptor

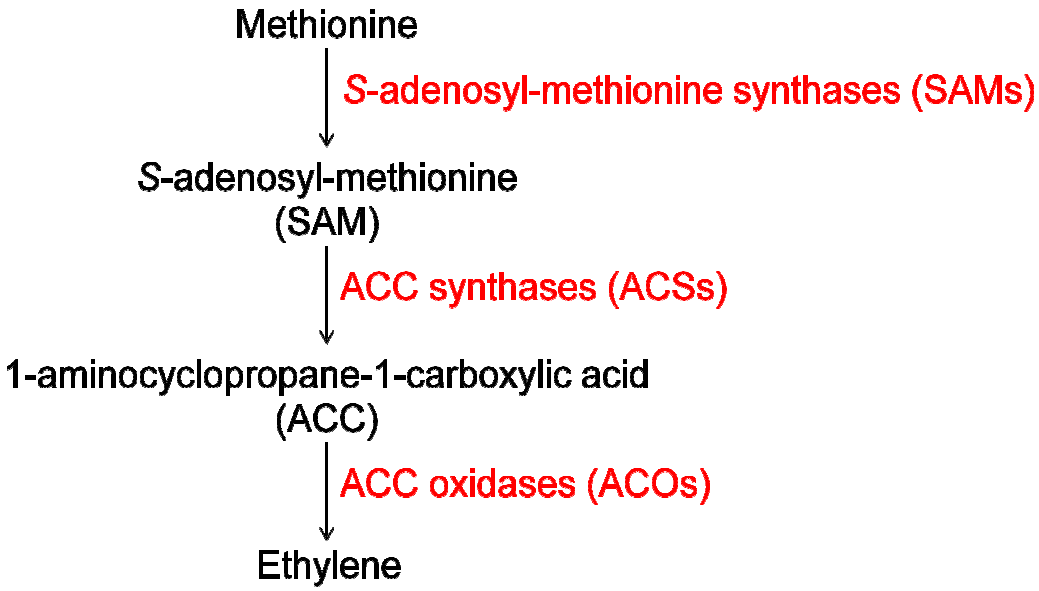

Figure 2.1 The ethylene biosynthesis pathway.
Ethylene is synthesised via a series of enzymatic reactions from methionine. Red = enzyme and black = substrate/product.

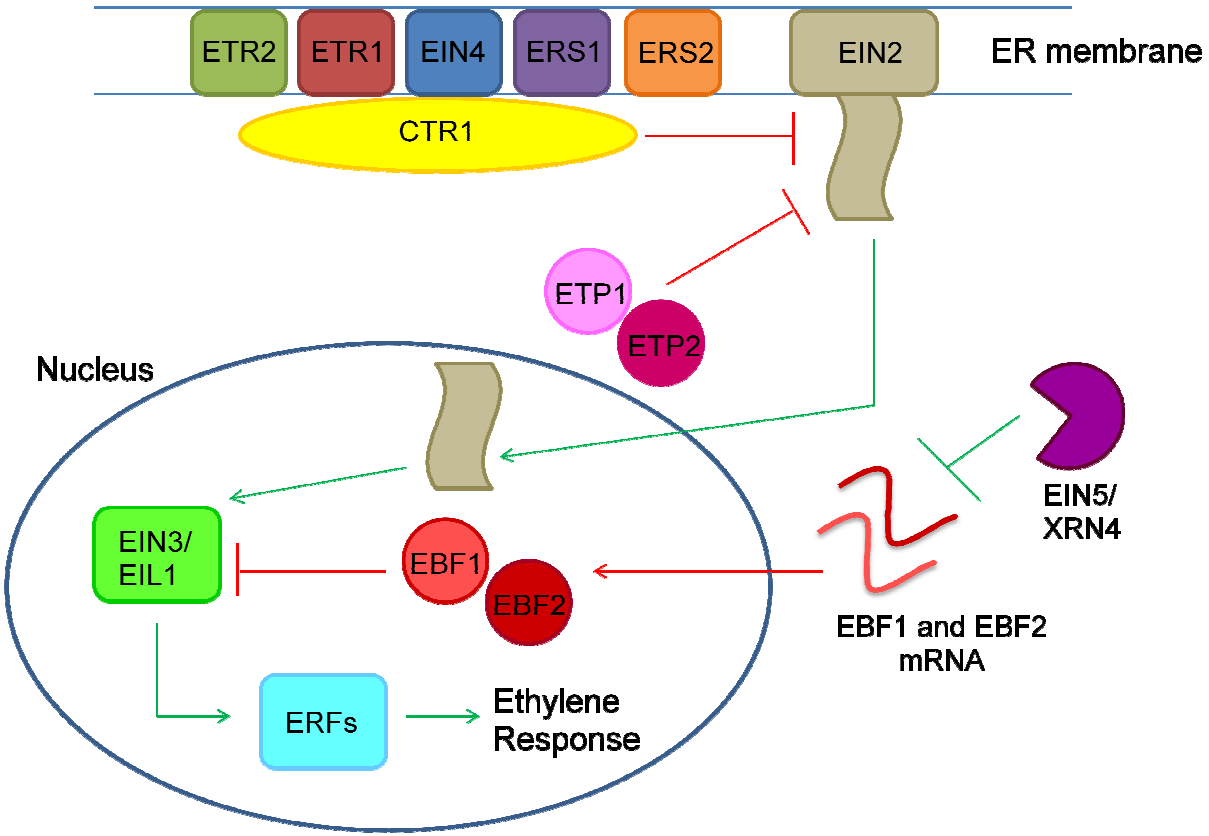

Figure 2.2 A simplified schematic of the ethylene signalling pathway.
Five ethylene receptors reside in the ER membrane, these are active in the absence of ethylene and subsequently activate the negative regulator CTR1. CTR1 acts to inhibit the function of EIN2 preventing downstream signalling. In the absence of ethylene EBF1 and EBF2 target EIN3/EIL1 for degradation. In the presence of ethylene inhibition of EIN2 is lifted, which undergoes cleavage of its C-terminal. This C-terminal translocates to the nucleus where it activates the ethylene response via EIN3/EIL1- that in turn activate ethylene response factors (ERFs). Also in the presence of ethylene EIN5 acts to target EBF1 and EBF2 mRNA for degradation, alleviating their repression of EIN3. Red arrows indicate signalling in the absence of ethylene and green arrows in the presence of ethylene.

signalling; the receptors are largely redundant although they do exhibit some functional specificity (Hua et al. 1998; Hua and Meyerowitz 1998; Merchante et al. 2013). The receptors show structural similarity to bacterial two-component histidine kinases (Chang et al. 1993). They consist of a membrane-bound N-terminal domain, a GAF domain which is involved in receptor-to-receptor interactions and a C-terminal signalling domain which physically interacts with CONSITUTIVE TRIPLE RESPONSE 1 (CTR) a downstream component of the signalling pathway (Clark et al. 1998). The receptors posses a copper co-factor which acts to bind ethylene, inactivating the receptor (Rodríguez 1999). When ethylene is absent the receptors are active and act as positive regulators of CTR1 (Hua and Meyerowitz 1998).

CTR1 is a Raf-like serine/threonine kinase protein which acts downstream of the ethylene receptors and upstream of EIN2 in the ethylene signalling pathway (Kieber et al. 1993; Roman et al. 1995). The protein is a negative regulator of the pathway with *ctr1* mutants displaying a constitutive ethylene response (Kieber et al. 1993). CTR1 interacts with the ethylene receptors at the ER membrane, which is critical for the induction of its kinase activity which induces downstream signalling (Clark et al. 1998; Gao et al. 2003).

The EIN2 membrane protein plays an irreplaceable role in the ethylene signalling pathway as a positive regulator, with loss of the protein leading to complete ethylene insensitivity; EIN3, a down-stream component of the pathway, fails to accumulate in the *ein2* mutant (Alonso et al. 1999; Guo and Ecker 2003). The protein consists of an N-terminal membrane bound domain and C-terminal domain (Alonso et al. 1999). EIN2 has for a long time been the least understood of all the components of the ethylene signalling pathway, but recently new insights into its role have been gained.

EIN2 was found to reside at the ER membrane and interact with the kinase domain of the ethylene receptors (Bisson et al. 2009; Bisson and Groth 2010). The C-terminal domain of EIN2 contains a nuclear localisation signal which is able to move to the nucleus in the presence of ethylene inducing downstream signalling via EIN3 (Ju et al. 2012; Qiao et al. 2012; Wen et al. 2012). In the absence of ethylene the kinase domain of CTR1 acts to phosphorylate the C-terminal of EIN2 preventing downstream signalling. When ethylene is present phosphorylation of EIN2 does not occur and proteolytic cleavage of EIN2 allows its C-terminal to translocate to the nucleus and initiate ethylene signalling via EIN3.

EIN2 is subject to regulation at the protein level. EIN2 has a short half-life but was found to be stabilised and to accumulate in the presence of ethylene (Qiao et al. 2009). Two F-box proteins EIN2-targetting protein 1 and 2 (ETP 1 and 2), which form the part of the SCF complex, a multiple-component E3 ubiquitin ligating enzyme involved in ubiquitin-mediated protein degradation were found to target EIN2 for degradation (Qiao et al. 2009). ETP1 and ETP2 protein levels were down-regulated on treatment with ethylene which is thought to alleviate their impact on EIN2 allowing signalling to proceed (Qiao et al. 2009).

Downstream of EIN2 is another positive regulator of the pathway, EIN3 a transcription factor which accumulates in response to ethylene (Chao et al. 1997; Guo and Ecker 2003). EIN3 was found to be sufficient and necessary for activation of all known ethylene induced responses (Chao et al. 1997). EIN3 belongs to a family of transcriptional proteins consisting of EIN3 and five EIN3-LIKE proteins, of which *EIL1* and *EIL2* are known to independently complement the *ein3* mutation (Chao et al. 1997). EIL1 is the most similar of EIN3's homologs and is also induced in response to ethylene (An et al. 2010). EIN3 and EIL1 were found to cooperatively regulate ethylene induced responses, having overlapping but distinct effects (An et al. 2010). Activation of EIN3 leads to a transcriptional cascade resulting in the myriad of ethylene responses produced by the plant. One of the transcription factors induced by EIN3 is ETHYLENE RESPONSE FACTOR 1 (ERF1), which is known to initiate a subset of ethylene responses (Solano et al. 1998).

EIN3 is a constitutively expressed short half life protein which in the absence of ethylene is continually degraded in order to prevent EIN3 reaching levels which would detrimentally impact the plant (Guo and Ecker 2003; Potuschak et al. 2003; Gagne et al. 2004). EIN3-BINDING F-BOX PROTEIN 1 (EBF1) and EBF2 were found to interact with EIN3 (Guo and Ecker 2003; Potuschak et al. 2003; Gagne et al. 2004). EBF 1 and EBF2 form part of an SCF complex; negatively regulating ethylene signalling by targeting EIN3 for ubiquitin-mediated degradation (Guo and Ecker 2003; Potuschak et al. 2003; Gagne et al. 2004). In the presence of ethylene EIN3 is stabilised and is able to act on its target genes, thus ethylene signalling proceeds. In addition to this it was found that EBF1 plays a role in constitutively targeting EIN3 for degradation at low levels, preventing signalling in the absence of ethylene (Binder et al. 2007). EBF2 is itself a target of EIN3 and increases in response to ethylene, this creates a negative feedback loop allowing tight regulation of the response by preventing excess accumulation of EIN3 and quickly shutting off signalling when ethylene is no longer present (Potuschak et al. 2003; Binder et al. 2007; Konishi and Yanagisawa 2008).

EIN2 was found to promote accumulation of EIN3/EIL1 in response to ethylene by inducing the proteasomal degradation of EBF1 and EBF2, thus repressing degradation of EIN3 (An et al. 2010). EIL1 was also found to be targeted for degradation via the $SCF^{EBF1/EBF2}$ complex in the same manner as EIN3 (Binder et al. 2007; An et al. 2010).

EIN5 is allelic to the 5' → 3' exoribonuclease XRN4, known to be involved in mRNA decay (Souret et al. 2004; Olmedo et al. 2006; Potuschak et al. 2006). In the ethylene signalling pathway EIN5 acts downstream of CTR1 and upstream of EBF1/2 (Olmedo et al. 2006; Potuschak et al. 2006). *EBF1* and *EBF2* transcripts were found to accumulate in *ein5/xrn4* mutants and as a result no EIN3 protein accumulated (Olmedo et al. 2006; Potuschak et al. 2006). It was concluded that EIN5 acts to regulate EBF1 and EBF2 levels, albeit in an unknown manner. It is thought that in the presence of ethylene EIN5 acts to indirectly decrease the levels of EBF1/2 thus alleviating their effect on EIN3/EIL1, allowing ethylene signalling to proceed (Olmedo et al. 2006; Potuschak et al. 2006). As this is an indirect response it is suggested that EIN5 may act to promote a repressor of *EBF1* and *EBF2* transcription (Kendrick and Chang 2008).

2.1.2 Hypotheses, Aims, Objectives and Rationale

Since Penny-Evan's initial screen EIN5/XRN4 has been found to be not just involved in the ethylene response but also in general mRNA decay and has been implicated in both the miRNA and siRNA-mediated decay pathways and is now know to be involved in the regulation of numerous transcripts (Gazzani et al. 2004; Souret et al. 2004; Rymarquis et al. 2011).

In light of this new evidence and together with Penny-Evan's initial observation that not all ethylene mutants responded in a similar manner to clubroot infection, it is hypothesised that the tolerance response exhibited by *ein5-1* is due to its roles outside of ethylene signalling and is not a consequence of perturbations in ethylene signalling. To test this hypothesis a series of experiments were carried out using the *ein5-1* mutant and an EIN2 mutant, *ein2-1*. EIN2 is a pivotal component of the ethylene signalling pathway and mutations in this gene lead to a complete loss of the ethylene response which is not seen in other ethylene signalling mutants (Alonso et al. 1999). Mutations in EIN5 lead to a less severe ethylene-insensitive phenotype, with *ein5* being one of the least insensitive to ethylene *ein* mutations (Roman et al. 1995). In *ein2* mutants there is no accumulation of EIN3 protein in response to ethylene, while in *ein5* mutants there is a delay and a reduction in EIN3 accumulation, these differences could

account for the different ethylene insensitivities of the two mutants (Guo and Ecker 2003). Previously *ein5-1* and *ein2-1* have been shown to exhibit different responses from one another when exposed to the bacterial protein harpin (Dong et al. 2004). It is known however, that EIN2 and EIN5 are required for ethylene signalling via EIN3, which is necessary and sufficient for the ethylene response, so examining both here should help to establish if the ethylene response is playing a role during clubroot infection (Guo and Ecker 2003). If ethylene does play a role in clubroot infection it would be expected that *ein2-1* would be tolerant as *ein5-1* was; this response would be more pronounced in *ein2-1* due to its complete lack of ethylene insensitivity. If however, ethylene signalling does not play a marked role in clubroot infection (and therefore *ein5-1* is tolerant due to other factors), it would be expected that *ein5-1* and *ein2-1* would present different responses to clubroot infection.

The first part of the chapter looks to investigate whether the initial findings of Penny-Evans (2000) are repeatable. To address this; a growth analysis was carried out to analyse the impact of infection on the growth and morphology of Col-0, *ein5-1* and *ein2-1*, this would also begin to unravel the mechanisms behind the tolerance, specifically if ethylene signalling plays a role. The experiments covered in the second part of this chapter details an in-depth microscopic analysis of the infection process in *ein5-1* and contrast this with infection in Col-0 and *ein2-1*. This type of analysis, was lacking in Penny-Evans' (2000) study, and will allow further understanding of the mechanisms behind *ein5-1* tolerance response to clubroot infection and whether it is a consequence of perturbations in ethylene signalling or due to one of the other roles EIN5 carries out within the plant.

The aims and objectives of this chapter are:

Aims:

1. To examine whether the initial observation that *ein5-1* is tolerant to clubroot disease was repeatable and to contrast infection in *ein5-1* and *ein2-1* in order to examine whether ethylene signalling plays a role in infection.

2. To understand developmental changes in the host and pathogen that occur as a consequence of infection in three different genetic backgrounds, Col-0, *ein5-1* and *ein2-1*.

Objectives:

1. To conduct a growth analysis of infected and uninfected Col-0, *ein5-1* and *ein2-1*.

2. To undertake a detailed microscopic analysis of infected and uninfected Col-0, *ein5-1* and *ein2-1* with a focus on changes in secondary thickening and pathogen development and distribution.

2.2 Materials and Methods

2.2.1 Preparation of *P. brassicae* Resting Spore Inoculum

Initial galls were obtained from clubroot-infected *Brassica oleracea* from Penyrheol, South Wales (European Clubroot Definition set 16/2/12). Subsequent galls were produced on a frequent basis, by Ms J. Smith, University of Sheffield, in order to maintain stocks of *P. brassicae* inoculum. In order to maintain stocks, Chinese cabbage seeds were sown on moist M3 compost (Levington) and placed into a growth chamber with a temperature of 20 ^{o}C, a photoperiod of 9 hours and an irradiance of 100 µmol m^{-2} s^{-1}. Plants were watered from the bottom on a frequent basis so that the compost was never allowed to dry out. Seven days after germination seedlings were transplanted individually into moist M3 compost in pots and returned to the growth room. Fourteen days after germination plants were inoculated with a *P. brassicae* spore suspension by pipetting 2 ml of spore suspension onto the soil around the base of the plant. Six to eight weeks post inoculation galls were collected, rinsed and subsequently stored at -20 ^{o}C until required.

An infected gall from *Brassica rapa* (Chinese cabbage) was placed in an electrical blender and homogenised with 300 ml of distilled H_2O until no large pieces of tissue remained. The homogenate was passed through three layers of muslin and the resulting filtrate was centrifuged at 23 500 x g for 15 minutes at 4 ^{o}C. Following centrifugation the supernatant was discarded and soil, starch and other plant material was removed from the pellet using a spatula. The remaining layer of spores was re-suspended in 40 ml distilled H_2O. The spore solution was then re-centrifuged as previously described and again non-spore material was removed from the pellet. Spores were re-suspended in 40 ml distilled H_2O. Spore concentration was calculated with the use of a haemocytometer. The spore suspension was stored at 4 ^{o}C. Spores were diluted to a working concentration of 1 x 10^6 spore ml^{-1}, prior to inoculation of plants, using distilled H_2O.

2.2.2 *A. thaliana* Growth Conditions and Inoculation with *P. brassicae* Spores

Seeds of *A. thaliana* were sown on moist M3 compost. To ensure even germination following sowing seeds were placed in the dark at 4 ^{o}C for five days. Following stratification, seeds were transferred to a growth room, with a temperature of 20 ^{o}C, a photoperiod of 9 hours and an irradiance of 100 µmol m^{-2} s^{-1}, and covered with a transparent plastic lid. Plants were watered, from the bottom, for the duration of the experiment on a frequent basis to ensure compost never dried out. Seven days after germination seedlings were transplanted individually into pots containing a mix of moistened M3 compost and perlite at a 3:1 ratio. Following transplantation plants were returned to the growth room uncovered.

One week after transplantation (14 days after germination) plants were inoculated with a *P. brassicae* spore suspension, see Section 2.2.1, by pipetting 2 ml of spore suspension onto the soil at the base of the plant. As a control, plants that were to remain uninfected were inoculated with 2ml of distilled H_2O.

2.2.3 Measurement of *A. thaliana* Growth and Biomass

Wild type *A. thaliana* (Col-0) and the ethylene insensitive mutants (*ein5-1* and *ein2-1*) (Guzman and Ecker, 1990; Roman et al. 1994) were grown and inoculated as described in Section 2.2.2.

Ten infected plants and ten uninfected plants were harvested at 7, 14, 21 and 28 days post inoculation (DPI). A series of measurements of plant growth and biomass were taken. The rosette diameter of each plant was recorded and digital callipers were used to measure the hypocotyl width of each plant. Plants were then separated into roots and shoots. Due to the difficult nature of harvesting the whole root systems intact, the hypocotyl/root described here consisted of the hypocotyl plus 1 cm of root tissue. Photographs of the rosette of each plant and the hypocotyl plus the upper part of the root system were taken before separation of plants into roots and shoot parts. The root and shoot were dried at 46 ^{o}C and their dry weights were recorded. The dry weights of plants 7DPI were excluded from the analysis over concerns about accuracy of measurements due to their small size.

2.2.4 Statistical Analysis

Statistical analysis was carried out using Minitab® statistical software (Minitab Inc.). Graphs were produced using SigmaPlot (Systat Software, San Jose, CA).

2.2.5 Technovit Sectioning of Hypocotyl Samples

Col-0, *ein5-1* and *ein2-1* plants were grown and infected as described in Section 2.2.2.

Three hypocotyl samples were taken from uninfected and infected plants of the three lines 7, 14, 21 and 28 DPI. Samples were fixed in approximately 2 ml ethanol:acetic acid at a ratio of 4:1 and vacuum infiltrated for 20 minutes.

After at least 1 day samples were transferred to 100 % ethanol for at least 30 minutes, the ethanol was removed and replaced with fresh ethanol for at least 30 minutes. A Technovit 7100 kit (TAAB, Berkshire, UK) was used for embedding of the samples. In preparation for embedding samples were gradually infiltrated with Technovit 1 solution, prepared as directed in the kit. Samples were changed from ethanol to ethanol:Technovit 1 solution at a ratio of 1:1 for approximately 1 day, then to 100 % Technovit 1 solution for approximately 3 days.

Samples were divided into smaller sections, approximately 5 mm in length before embedding. Samples were individually embedded in 1.5 ml Eppendorf lids in a solution of Hardener 2 and Technovit 1 mixed as detailed in the kit instructions. Approximately 250 µl of embedding solution was pipetted into an eppendorf lid and samples were placed vertically into the lid containing embedding solution. Embedded samples were left overnight to allow the resin to set.

The embedded samples were removed from the eppendorf lids and mounted individually on ‘Histoblocs’ using the mounting media provided in a Technovit 3040 kit (TAAB, Berkshire, UK). Samples were mounted using approximately 500 µl of mounting media, and left to set for approximately 30 minutes. Mounting media was prepared using 3040 powder:3040 liquid at a ratio of 3:1. ‘histoblocs’ were pre-prepared using the mounting media to create a flat surface on which samples could be mounted.

Mounted samples were sectioned using a Leica RM 2145 rotation microtome. Sections were cut at a thickness of 5 µm and transferred directly to a pool of water on a

microscope slide. Slides were dried at 65 ^{o}C on a hot plate overnight, before staining with a drop of 0.1 % (w/v) toluidine blue in 100 mM phosphate buffer at pH 7 (Sigma Aldrich, Dorset, UK) for 2 minutes at 65 ^{o}C. Toluidine blue was washed from the samples with dH_2O and the sample was incubated at room temperature for 10 minutes under a drop of dH_2O to remove stain from the background. Remaining liquid was rinsed off with further dH_2O and samples were dried at 65 ^{o}C overnight.

Coverslips were mounted on the slides using a small amount of DePex mounting media (VWR International) and allowed to set overnight. A BX51 Olympus microscope and a DP71 Olympus camera were used to photograph the sections.

2.3 Results

2.3.1 Analysis of the Impact of *P. brassicae* Infection on the Growth and Morphology of *A. thaliana* Col-0, *ein2-1* and *ein5-1*

The impact of clubroot infection on the growth and biomass of wild-type Col-0 and two ethylene insensitive mutants, *ein5-1* and *ein2-1*, was examined, Figures 2.3-2.5.

Following infection Col-0, *ein5-1* and *ein2-1* plants displayed the characteristic symptoms of clubroot disease, with gall formation occurring in the hypocotyl and upper root system. The root/hypocotyls of all lines 21 DPI can be seen in Figure 2.3. Digital callipers were used to determine hypocotyl width which was used as an indicator of gall size, Figure 2.4. Infected Col-0 plants exhibited a significant increase in hypocotyl width from 21DPI, with infected plants having a hypocotyl width 3.5 times bigger than their respective uninfected plants by 28DPI. A similar response was seen in *ein2-1* plants, with a significant increase in hypocotyl width of infected plants also seen from 21DPI. The increase in hypocotyl width induced by clubroot infection was delayed in the *ein5-1* mutant; at 21DPI there was no significant difference between the hypocotyl widths of infected and uninfected plants. By 28DPI the hypocotyl width of infected plants was only 2.2 times that of uninfected plants.

No significant difference was observed between the rosette diameters of infected and control Col-0 plants, Figure 2.5. The rosette diameters of infected *ein2-1* plants were significantly smaller than that of uninfected plants from 21DPI onwards, Figure 2.5. At 28DPI infected rosettes were 1.3 times smaller than uninfected rosettes. In *ein5-1* plants the rosette diameters increased in size at the same rate as uninfected plants and were not significantly different until 28DPI, when rosettes of infected plants were

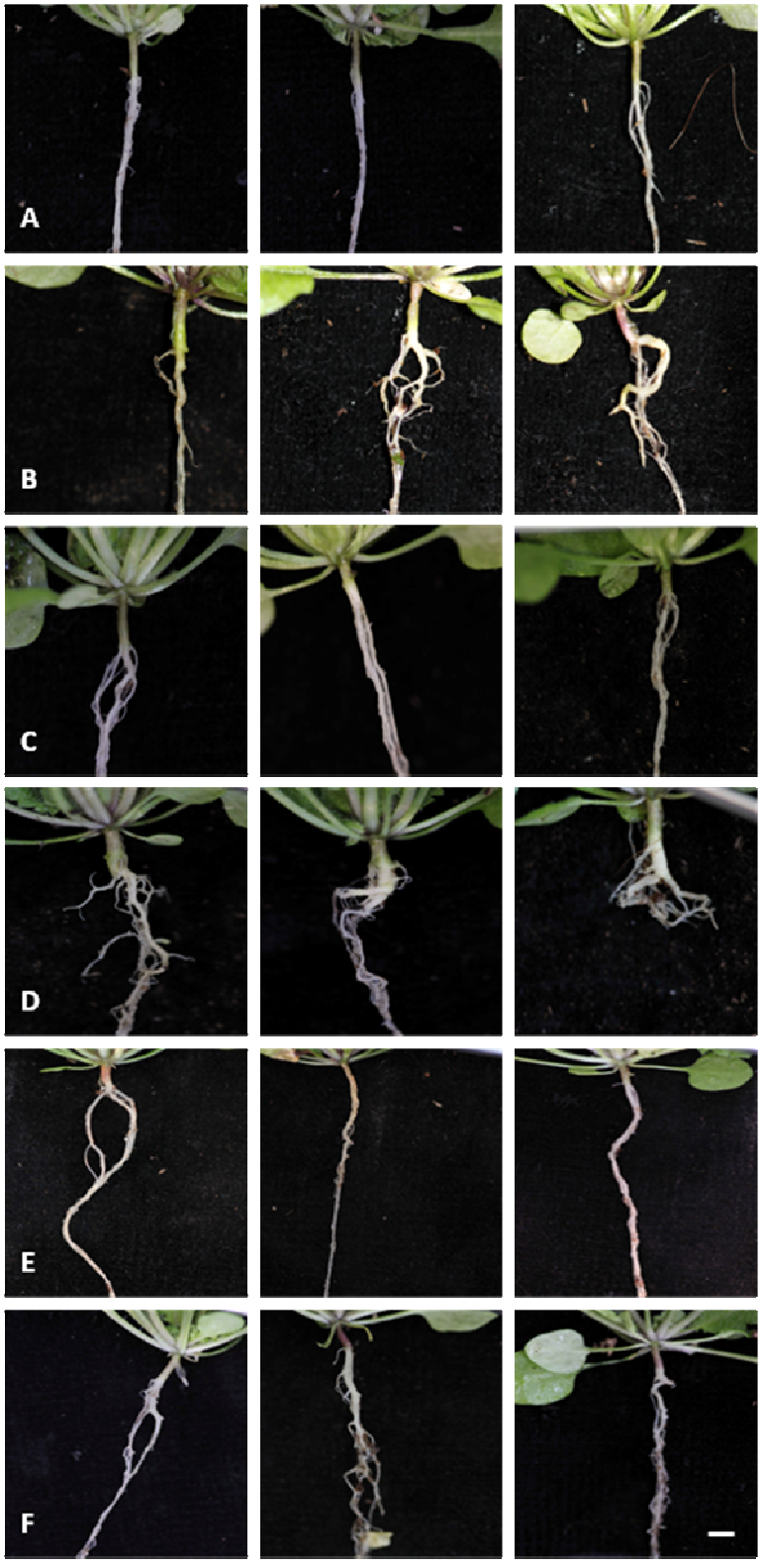

Figure 2.3. Hypocotyl/roots of uninfected and infected Col-0, *ein2-1* and *ein2-1* 21DPI. Hypocotyl/root of (**A**) uninfected Col-0, (**B**) infected Col-0, (**C**) uninfected *ein2-1*, (**D**) infected *ein2-1*, (**E**) uninfected *ein5-1* and (**F**) infected *ein5-1* 21DAI with *P. brassicae*. Three examples of the root/hypocotyl are shown for each line. Scale bar = 2 mm.

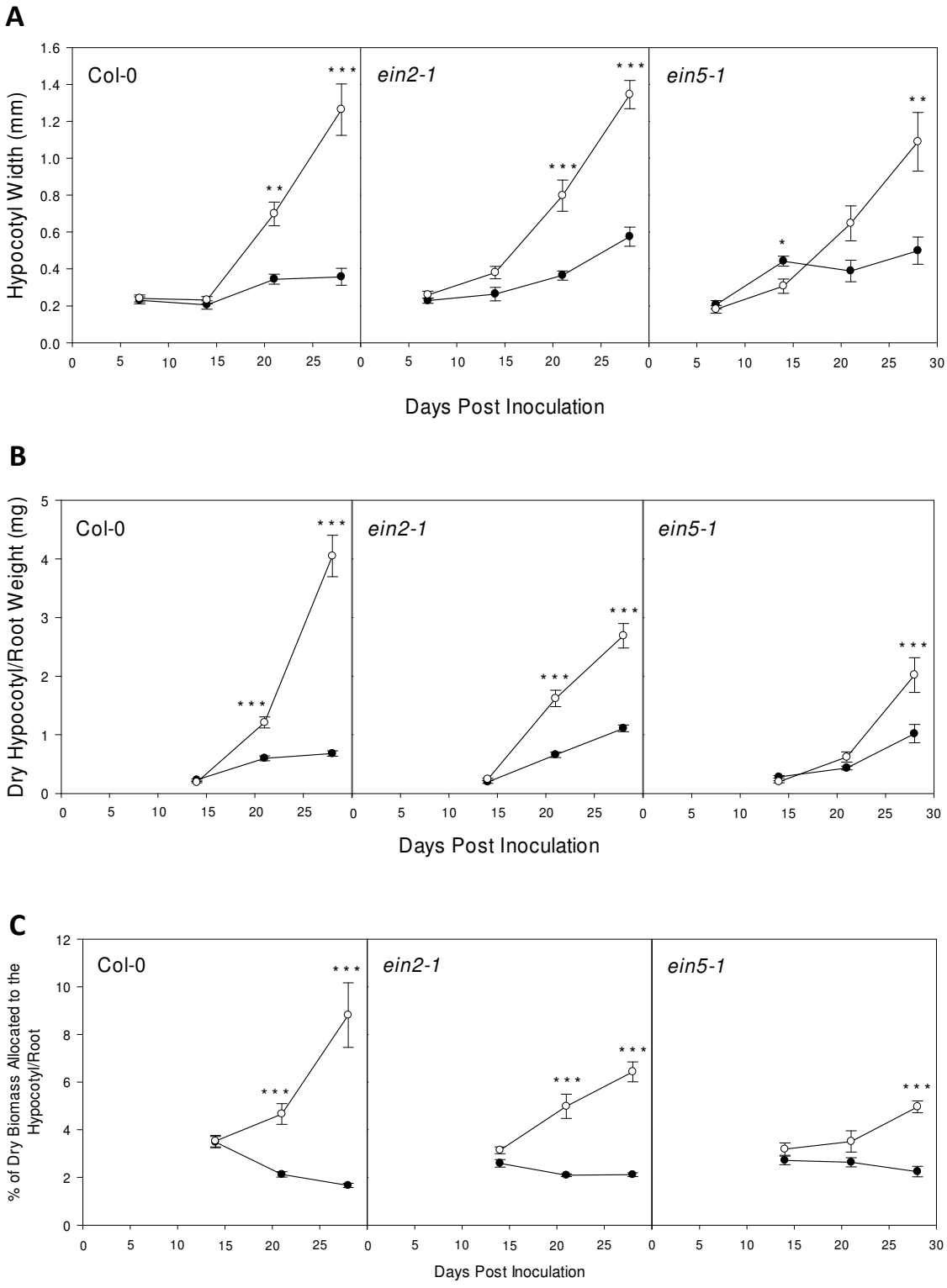

Figure 2.4. Impact of *P. brassicae* infection on the hypocotyl/root of Col-0, *ein2-1* and *ein5-1*.
The effect of *P. brassicae* infection on (**A**) hypocotyl width (**B**) the dry hypocotyl/root weight and (**C**) % dry biomass allocated to the hypocotyl/root of *A. thaliana*. Uninfected controls (filled circles), *P. brassicae* infected plants (open circles). Results are means ± S.E. of 6-10 plants. Data were (**B**) natural log and (**C**) arcsine square root transformed prior to statistical analysis. (Tukey multi-comparison test *$p \leq 0.05$, ** $p \leq 0.01$, *** $p \leq 0.001$).

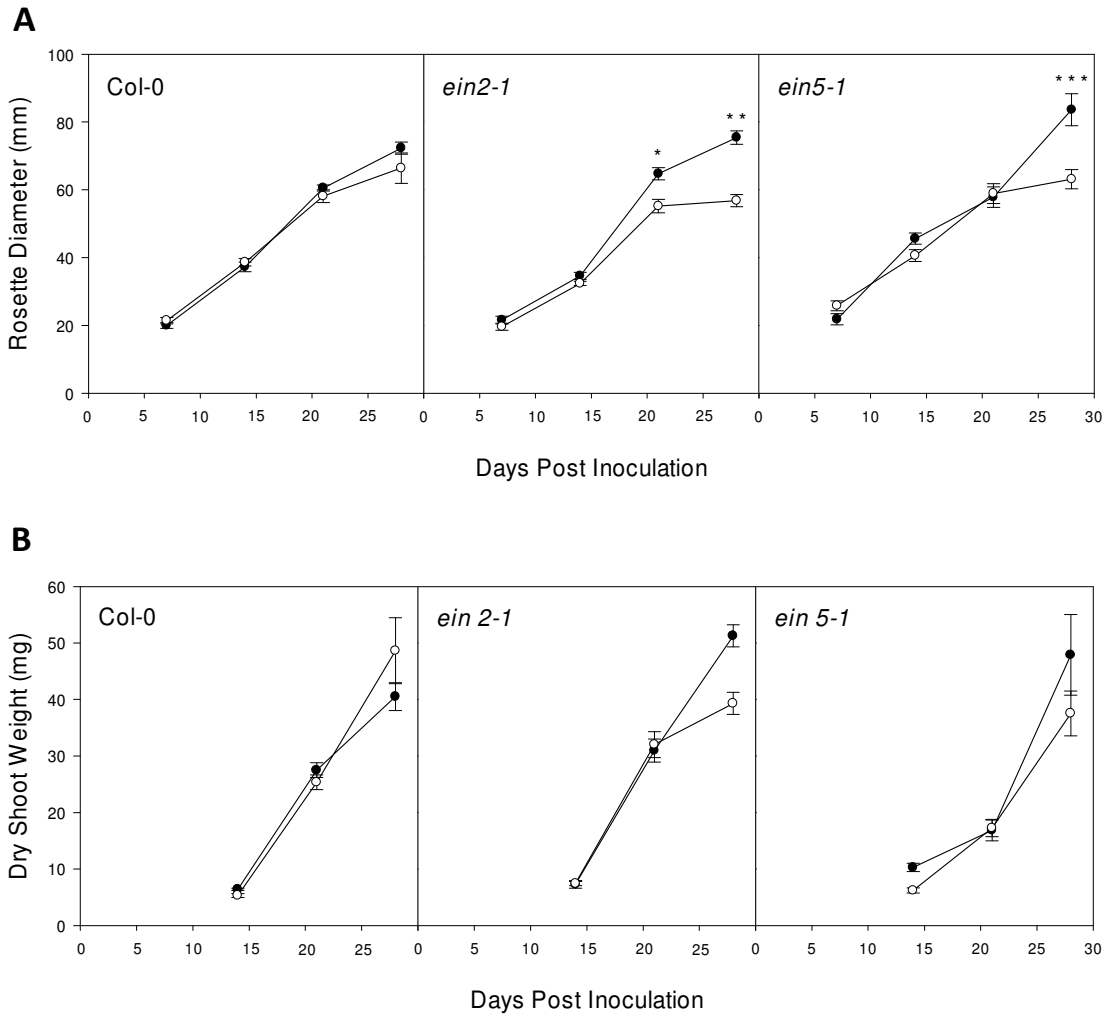

Figure 2.5. Impact of *P. brassicae* infection on the shoots of Col-0, *ein2-1* and *ein5-1*. The effect of *P. brassicae* infection on (**A**) the rosette diameter and (**B**) the dry shoot weight of *A. thaliana*. Uninfected controls (filled circles), *P. brassicae* infected plants (open circles). Results are means ± S.E. of 8-10 plants. (Tukey multi-comparison test *$p \leq 0.05$, ** $p \leq 0.01$, *** $p \leq 0.001$).

1.3 times smaller than those of uninfected plants, Figure 2.5. Infection had no significant effect on the dry shoot weight of Col-0, *ein2-1* or *ein5-1* plants, Figure 2.5.

Dry hypocotyl/root weight was used as a second measure of gall size, Figure 2.4. The hypocotyl/root consisted of the hypocotyl plus the uppermost 1cm of the root. Following infection a significant increase in the dry hypocotyl/root weight of Col-0 was observed from 21 DPI onwards with infected plants having a dry hypocotyl/root weight almost 6 times that of uninfected plants by 28 DPI. The dry weight data were also expressed as the percentage of biomass allocated to the hypocotyl/root, Figure 2.4. At 14DPI uninfected Col-0 plants allocated 3.5 % of their total biomass to the hypocotyl/root. This value declined during the course of the experiment to 1.7% at 28 DPI. Infection led to a significant increase in biomass allocation to the hypocotyl/root of Col-0 plants from 21DPI. By 28DPI Col-0 plants allocated 8.8 % of their biomass to hypocotyl/roots, 5 times that of uninfected plants.

The course of infection in *ein2-1* followed similar timing to that of infection in Col-0 plants, Figure 2.4. However, the increase in dry hypocotyl/root and percentage biomass allocated to the hypocotyl/root was somewhat smaller in *ein2-1* compared with Col-0. At 28DPI the dry hypocotyl/root weight of infected plants was 2.5 times that of uninfected plants. The percentage biomass allocated to the hypocotyl/root of infected *ein2-1* at 28DPI was 6.4 %, 3 times that of uninfected controls.

In the *ein5-1* mutant, *P. brassicae* induced gall formation was reduced and delayed, Figure 2.4. At 21DPI there was no significant difference between the hypocotyl/root weights and percentage of weight allocated to the hypocotyl/root of infected and uninfected *ein5-1* plants. At 28DPI the dry hypocotyl/root weight of infected plants was only 2 times that of uninfected controls and the percentage of biomass allocated to the hypocotyl/root was 5 %, just 2 times that of the uninfected controls.

2.3.2 Microscopic Analysis of Impact of *P. brassicae* Infection on *A. thaliana* Col-0, *ein2-1* and *ein5-1*

To examine the impact of clubroot infection at the cellular level cross sections of hypocotyls from infected and uninfected Col-0, *ein2-1* and *ein5-1* plants were taken at 7 day intervals following infection, until 28DPI. Toluidine blue was used to stain the cross sections, with xylem cells staining a light blue colour in contrast with other cells types which stained purple. The aim of this work was to understand the changes that occur following infection and place these in the context of the normal hypocotyl

developmental processes in Col-0 and then contrast these with changes occurring in *ein2-1* and *ein5-1*.

Initially the developmental processes occurring in the uninfected Col-0 hypocotyl were examined. Cross sections through hypocotyls of uninfected Col-0 plants from 7 to 28DPI are shown in Figure 2.6A. Secondary thickening occurs in the hypocotyl over this period resulting in an increase in girth. The activity of the VC leads to the production of xylem to the interior and phloem and phloem parenchyma to the exterior. The processes and re-organisation of tissue that occurs during this time are shown in more detail in Figure 2.7.

At 7DPI, Figure 2.7A, the structure of the hypocotyl consists of three outer cell layers the epidermis, cortex and endodermis which surround the central stele made up of pericycle, procambial and vascular cell types (i.e. xylem vessels and phloem bundles). A xylem axis exists horizontally across the centre of the cross section, with protoxlyem found at the periphery of the pole and metaxylem centrally. Phloem is present at two poles either side of and perpendicular to the xylem pole. The xylem axis is separated from the two phloem poles by procambium cells. By 14DPI, Figure 2.7C, a re-arrangement of the hypocotyl tissue has occurred; secondary thickening has begun to increase the girth of the hypocotyl. The VC has been established from the procambium. Cells of the VC form a ring of organised cell files, with xylem to the interior, phloem to the exterior and intervening parenchyma cells. At 21DPI, Figure 2.6A, VC activity has generated an increased number of xylem, phloem and parenchyma cells, leading to a wider hypocotyl. The three outer cell layers are shed between 14 and 21DPI, although the timing of this process is variable. At 28DPI, Figure 2.6A, these processes have continued to increase hypocotyl width.

Alterations occurring in the Col-0 hypocotyl as a consequence of infection were then examined. Cross sections through infected Col-0 hypocotyls from 7 to 28DPI are shown in Figure 2.6B. From 14 to 21DPI there is a large impact of clubroot on the morphology of the hypocotyl. At 21 and 28DPI infected hypocotyls are much wider than the equivalent uninfected hypocotyls. This increase in width is a consequence of hyperplasia and hypertrophy. Plasmodia are first visible in the hypocotyl 14DPI. Secondary plasmodia are first seen in the hypocotyl at 21DPI and are found throughout the hypocotyl by 28DPI.

At 7DPI, Figure 2.7B, there are no visible alterations in the hypocotyl occurring as a consequence of infection. By 14DPI, Figure 2.7D, plasmodia can be seen in the cells

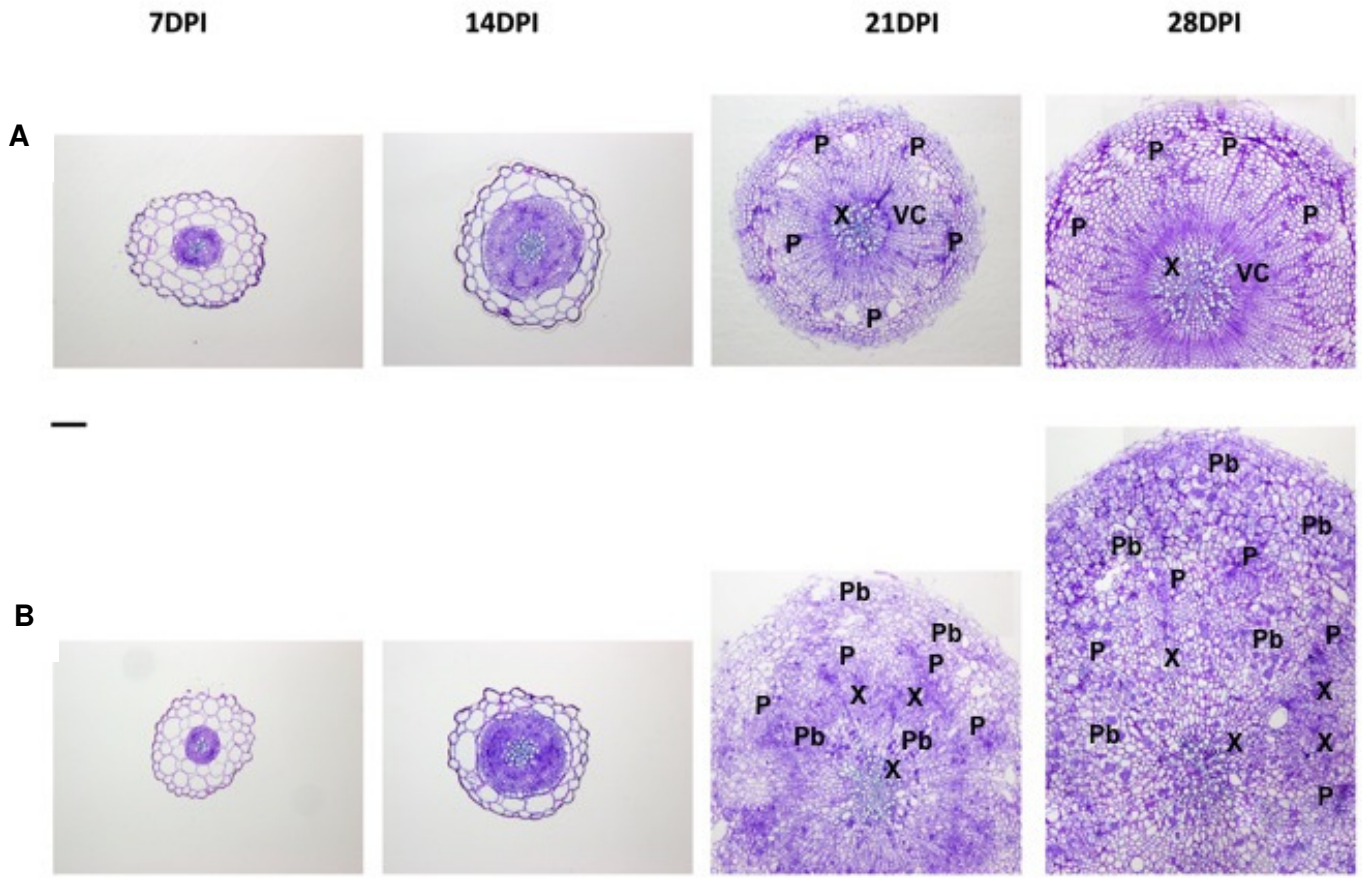

Figure 2.6. Alterations in *A. thaliana* Col-0 hypocotyl structure and morphology as a consequence of *P. brassicae* infection.
Cross sections were taken from (A) uninfected and (B) infected hypocotyls at 7 day intervals following infection. Uninfected plants were inoculated with water. X, xylem vessel; P, phloem bundles, Pb cells containing plasmodia; VC, vascular cambium. Scale bar = 100 µm

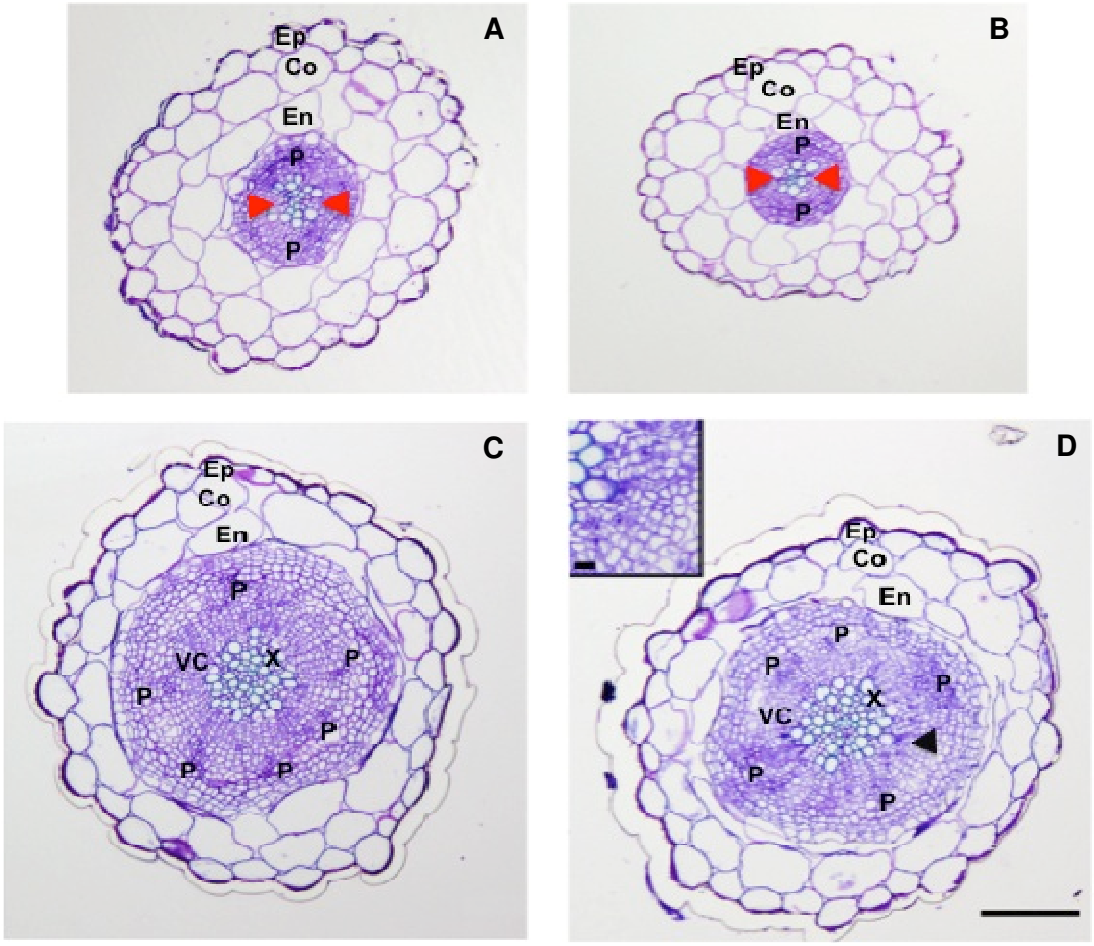

Figure 2.7. The early stages of hypocotyl development are not visibly affected by infection.

Cross sections of uninfected Col-0 hypocotyls (A) 7DPI and (C) 14DPI show the rearrangement of hypocotyl tissue that occurs as a consequence of secondary thickening. Cross sections from infected Col-0 hypocotyls (B) 7DPI and (D) 14DPI show that secondary thickening proceeds as normal. *P. brassicae* are seen 14DPI (D) in a ring around the xylem vessels. The insert in (D) shows a close up of cells containing plasmodia 14DPI. Ep, epidermis; Co, cortex; En, endodermis; X, xylem vessels; P, phloem bundles; VC, vascular cambium. Red arrow heads indicate the xylem axis. Black arrow indicates *P. brassicae* in cells. Main scale bar = 100 µm, Scale bar in insert = 10 µm.

surrounding the xylem vessels, however no other impact of infection is apparent. From 14DPI plasmodia spread outwards from the vicinity of the VC, so that by 21DPI secondary plasmodia are distributed across the hypocotyl, Figure 2.8. By 28DPI there are many more cells infected with secondary plasmodia and the number of plasmodia within cells has increased. Cells containing plasmodia are distributed right across the hypocotyl with many found at the edge of the hypocotyl.

At 21DPI there is a large increase in cell number across the hypocotyl compared with uninfected cross sections. By 28DPI the number of cells has increased even further in infected samples. At 21DPI cell expansion is mainly seen in the region of the VC, where cells are no longer differentiating into xylem. There are also expanded cells scattered throughout the hypocotyl. By 28DPI there is significant cell expansion throughout the hypocotyl. Expanded cells appear larger at 28DPI compared with 21DPI. At both 21 and 28DPI some of these expanded cells contain *P. brassicae*, Figure 2.8.

Infection leads to a reduction in cellular organisation in the hypocotyl. At 21DPI there is a cessation of xylogenesis (which is not seen in uninfected controls) and at 28DPI very few new xylem cells have been formed. At both 21 and 28DPI however, islands of xylem are formed away from the central xylem vessels, and their number increases from 21 to 28DPI, Figure 2.8. Phloem production is not halted at 21 or 28DPI, phloem bundles are common at both time points with their distribution appearing less organised than in uninfected cross sections, Figure 2.8.

Cross sections of hypocotyls from uninfected *ein5-1* from 7 to 28DPI are shown in Figure 2.9A. Development of the uninfected *ein5-1* hypocotyl is similar to that observed in Col-0. As in uninfected Col-0 sections there is a re-arrangement of hypocotyl structure, a consequence of secondary thickening, taking place over this period which leads to an increase in hypocotyl width. There are no distinguishable differences between Col-0 and *ein5-1* uninfected hypocotyls.

Cross sections of hypocotyls from infected *ein5-1* 7 to 28DPI are shown in Figure 2.9B. From 7 to 14DPI the progression of the disease occurs in a similar manner to infection in Col-0. However, by 21DPI there are some very apparent differences between infected *ein5*-1 and Col-0 hypocotyls. Infected *ein5-1* hypocotyls are much smaller than infected Col-0 hypocotyls, with a size similar to uninfected *ein5-1* hypocotyls at 21DPI, Figure 2.9 and 2.10.

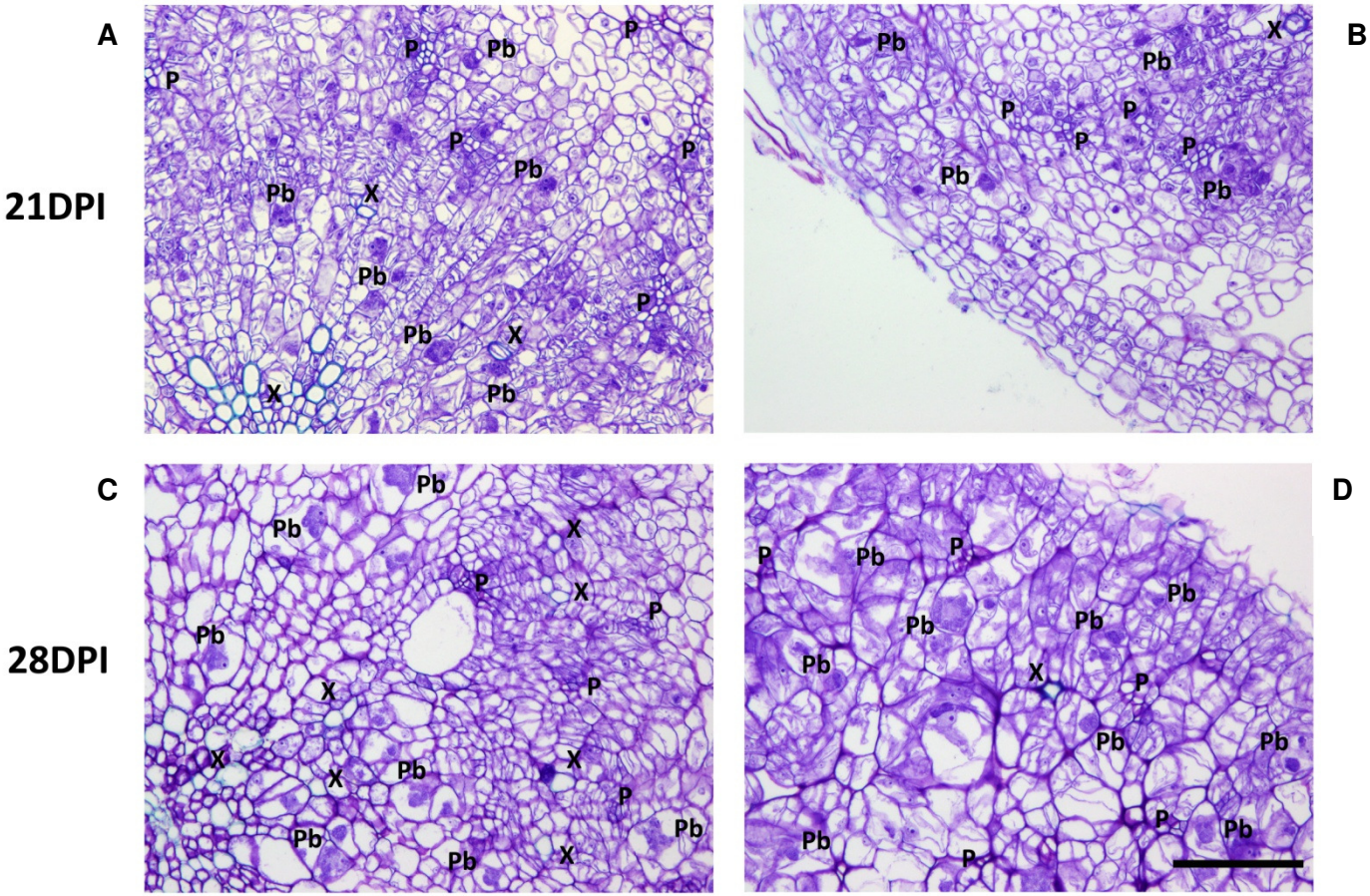

Figure 2.8. Changes in Col-0 hypocotyls occurring as a consequence of *P.brassicae* infection.
Secondary plasmodia are seen in the hypocotyl from 21DPI. They are distributed around the central xylem vessels (A) but can also be seen in cells at the edge of the hypocotyl (B). 28DPI the number of plasmodia has increased. Numerous cells at the periphery of the hypocotyl now containing plasmodia. Islands of xylem are seen in the hypocotyl from 21DPI (A, B) and their number increases by 28DPI (C,D). Phloem formation continues during infection. X, xylem vessels; P, phloem bundles; Pb, cells containing plasmodia. Scale bar = 100 µm.

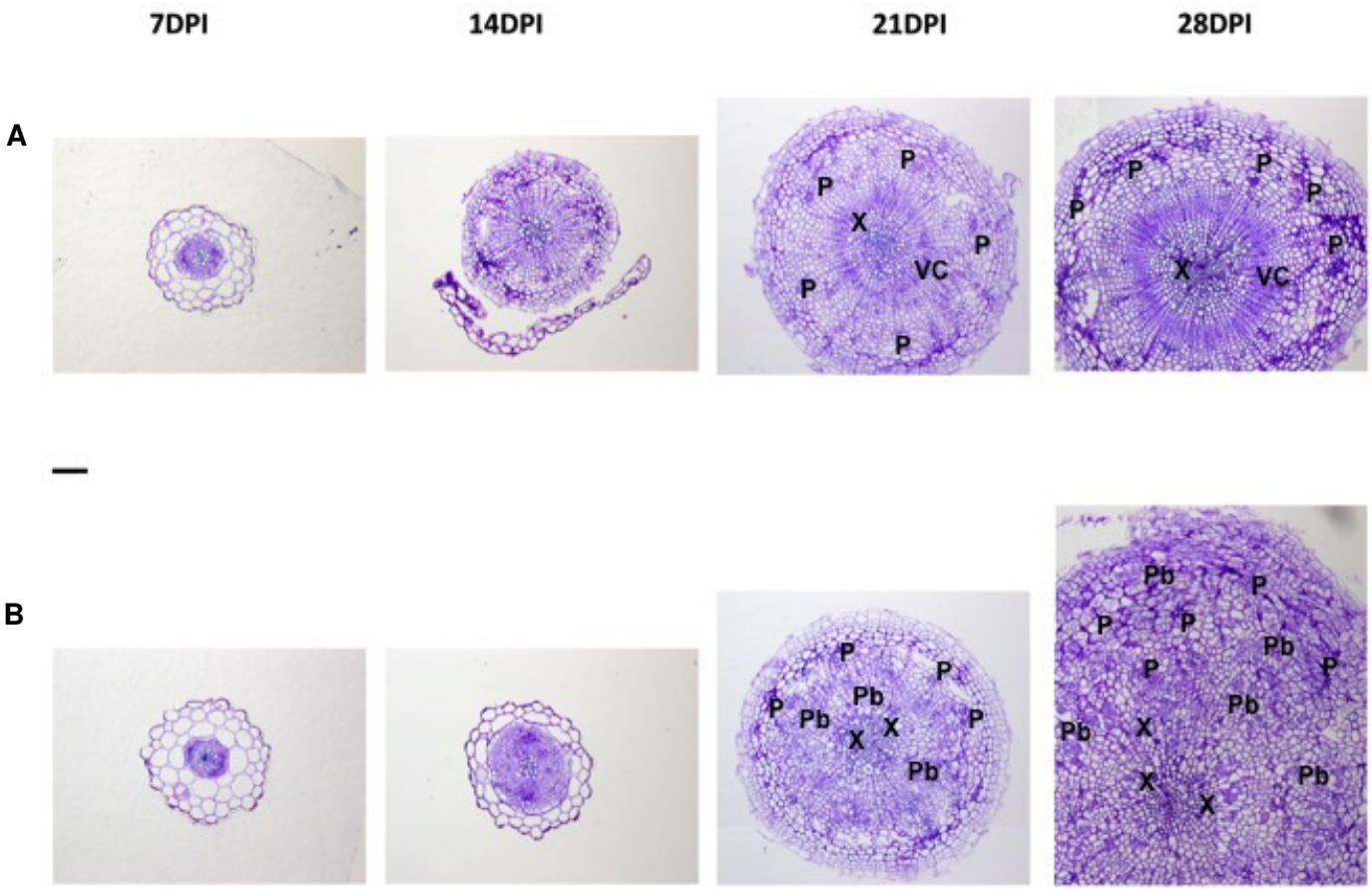

Figure 2.9. Alterations in *ein5-1* hypocotyl structure and morphology as a consequence of *P. brassicae* infection.

Cross sections were taken from (A) uninfected and (B) infected hypocotyls at 7 day intervals following infection. Uninfected plants were inoculated

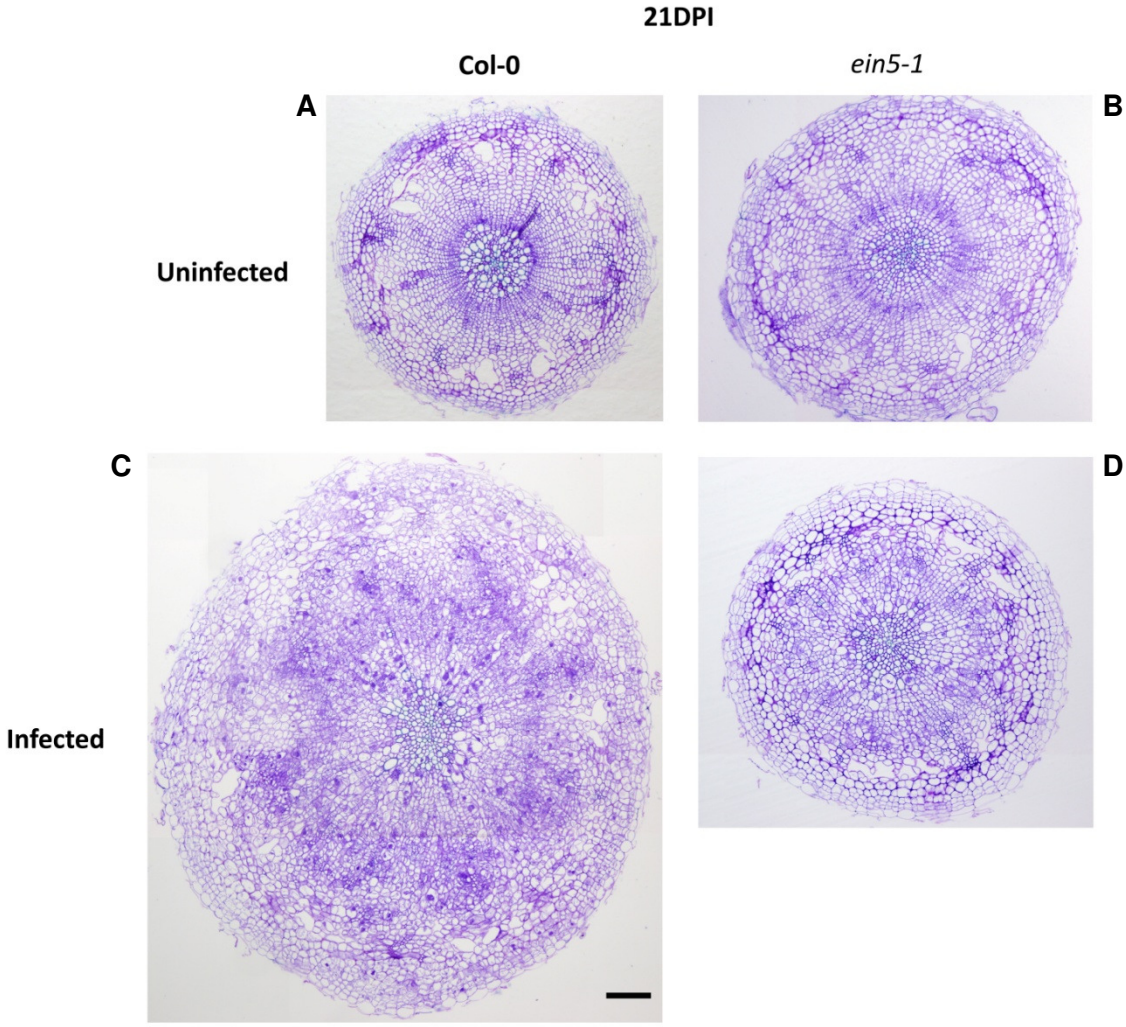

Figure 2.10. Alterations in the size and morphology of Col-0 and *ein5-1* hypocotyls 21DPI.
Cross sections of uninfected (A) Col-0 and (B) *ein5-1* hypocotyls and infected (C) Col-0 and (D) *ein5-1* hypocotyls 21DPI. Infected hypocotyls from *ein5-1* are smaller than infected Col-0 hypocotyls. The cellular organisation of *ein5-1* hypocotyls is much less disrupted following infection compared with Col-0 hypocotyls. Scale bar = 100 µm.

At 21DPI secondary plasmodia are present in infected *ein5-1* hypocotyls, however, their distribution differs from that seen in infected Col-0 hypocotyls, Figure 2.11. The migration of secondary plasmodia from around the central xylem vessels is slowed in infected *ein5-1* so that at 21DPI secondary plasmodia are not yet present at the edge of the hypocotyl. By 28DPI secondary plasmodia are distributed across the infected *ein5-1* hypocotyl and the number of cells infected has increased as has the number of plasmodia within cells, Figure 2.9.

By 28DPI there is an increase in the hypocotyl width of infected *ein5-1*; a consequence of *P. brassicae* induced cell division and expansion. Infected *ein5-1* hypocotyls are now wider compared to uninfected hypocotyls. Cell expansion seems to occur in a similar manner in *ein5-1* as in infected Col-0 hypocotyls. At 21DPI there is localised cell expansion occurring in the region interior to the VC where cells would normally be differentiating into xylem. There are also expanded cells present throughout the *ein5-1* hypocotyl. By 28DPI expanded cells are spread across the infected *ein5-1* hypocotyl and are larger than at 21DPI. As in infected Col-0 hypocotyls there is general cell expansion, with some expanded cells harbouring *P. brassicae*.

Infection in *ein5-1* does not lead to a loss of cellular organisation to the same extent as in Col-0. At 21DPI infected *ein5-1* hypocotyls appear much less disrupted by infection than Col-0 hypocotyls, and this is also the case at 28DPI. Xylogenesis in the centre of the infected *ein5-1* hypocotyl has ceased but no localised islands of xylem are seen in *ein5-1* 21DPI in contrast to Col-0, Figure 2.12. At 28DPI islands of xylem are present in infected *ein5-1* samples however, their numbers are much fewer than in Col-0 at the same time point, Figure 2.12. Phloem production is maintained in infected *ein5-1* and Col-0 in a similar manner.

Finally cross sections from uninfected and infected hypocotyls of *ein2*-1 were analysed, Figure 2.13. There were no notable differences in cross sections of uninfected *ein2-1* when compared with uninfected Col-0 or *ein5-1* hypocotyls. Infection in *ein2-1* 7-21DPI proceeded in a similar manner to infection in Col-0. At 28DPI infection appeared slightly more advanced in *ein2-1* with larger expanded cells containing many secondary plasmodia when compared with Col-0. However, the progression of infection can be variable. *ein2-1* was as susceptible (if not slightly more) to *P. brassicae* and its disrupting effects on cell division, expansion and differentiation as Col-0, in much contrast to *ein5-1* in which disease progression was slowed.

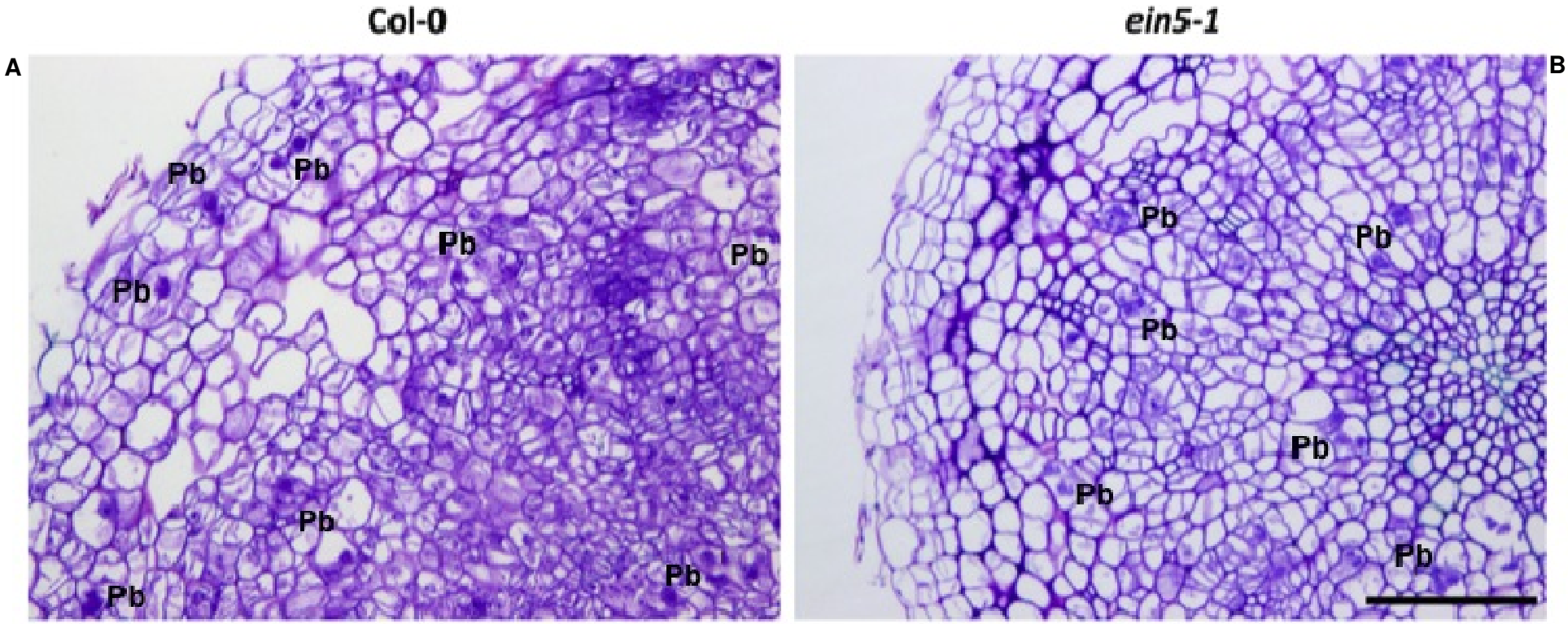

Figure 2.11. The migration of plasmodia is slowed in infected *ein5-1* hypocotyls compared with Col-0.
Cross sections of infected (A) Col-0 and (B) *ein5-1* hypocotyls 21DPI showing distribution of plasmodia. Plasmodia in *ein5-1* cross sections have not yet colonised to the edge of the hypocotyl, while in Col-0 cross sections plasmodia are present in cells at the periphery of the hypocotyl. Pb, plasmodia. Scale bar = 100 µm.

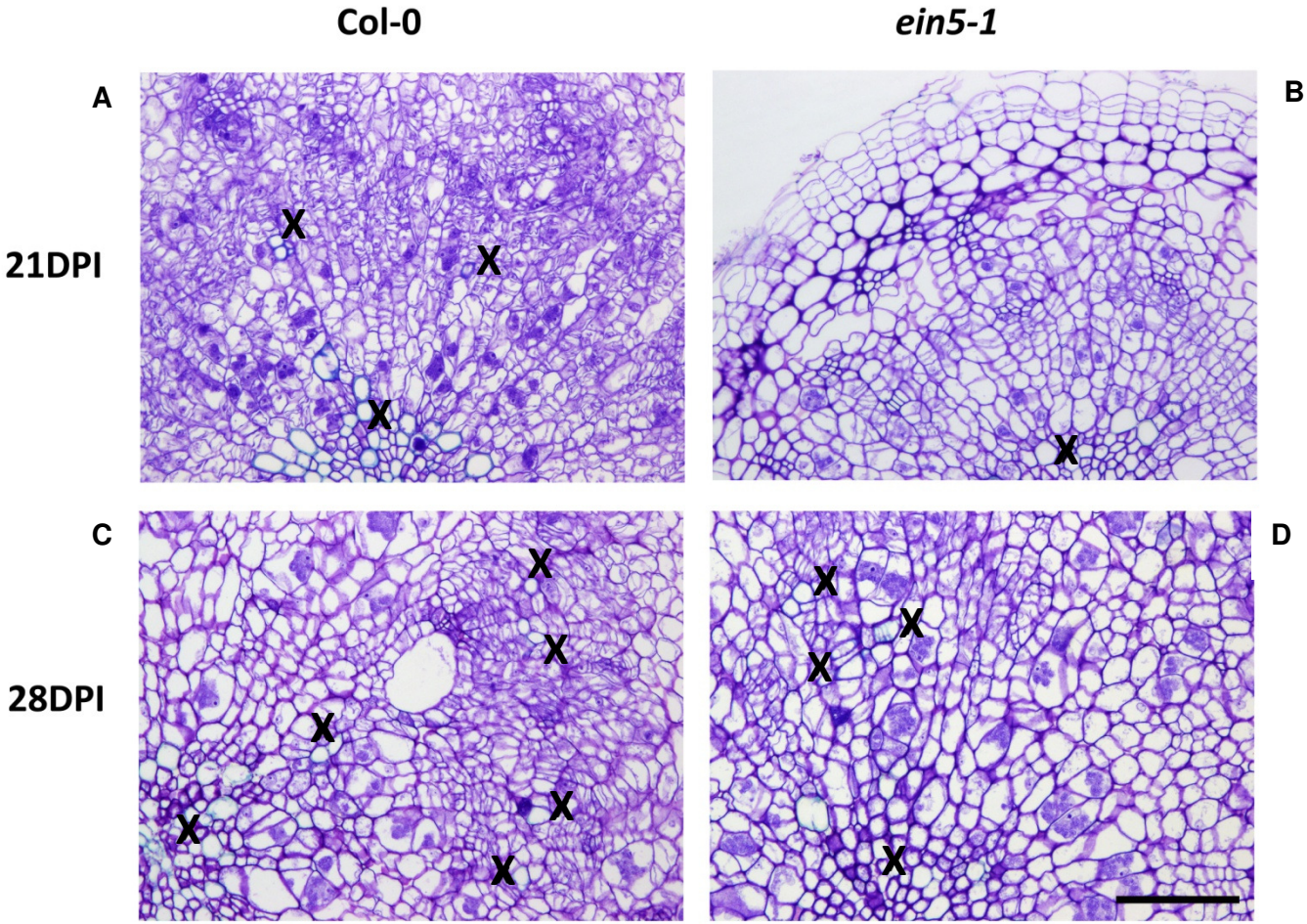

Figure 2.12. Alterations in xylem development in Col-0 and *ein5-1* hypocotyls as a consequence of infection with *P. brassicae* infection.
Islands of xylem form in the hypocotyl of infected Col-0 plants by 21DPI (A) but not in the hypocotyls of infected *ein5-1* (B). The number of these xylem islands increases at 28DPI in Col-0 (C) and develop in the hypocotyls of infected *ein5-1* plants by this time point (D). X, xylem vessel. Scale bar = 100 µm.

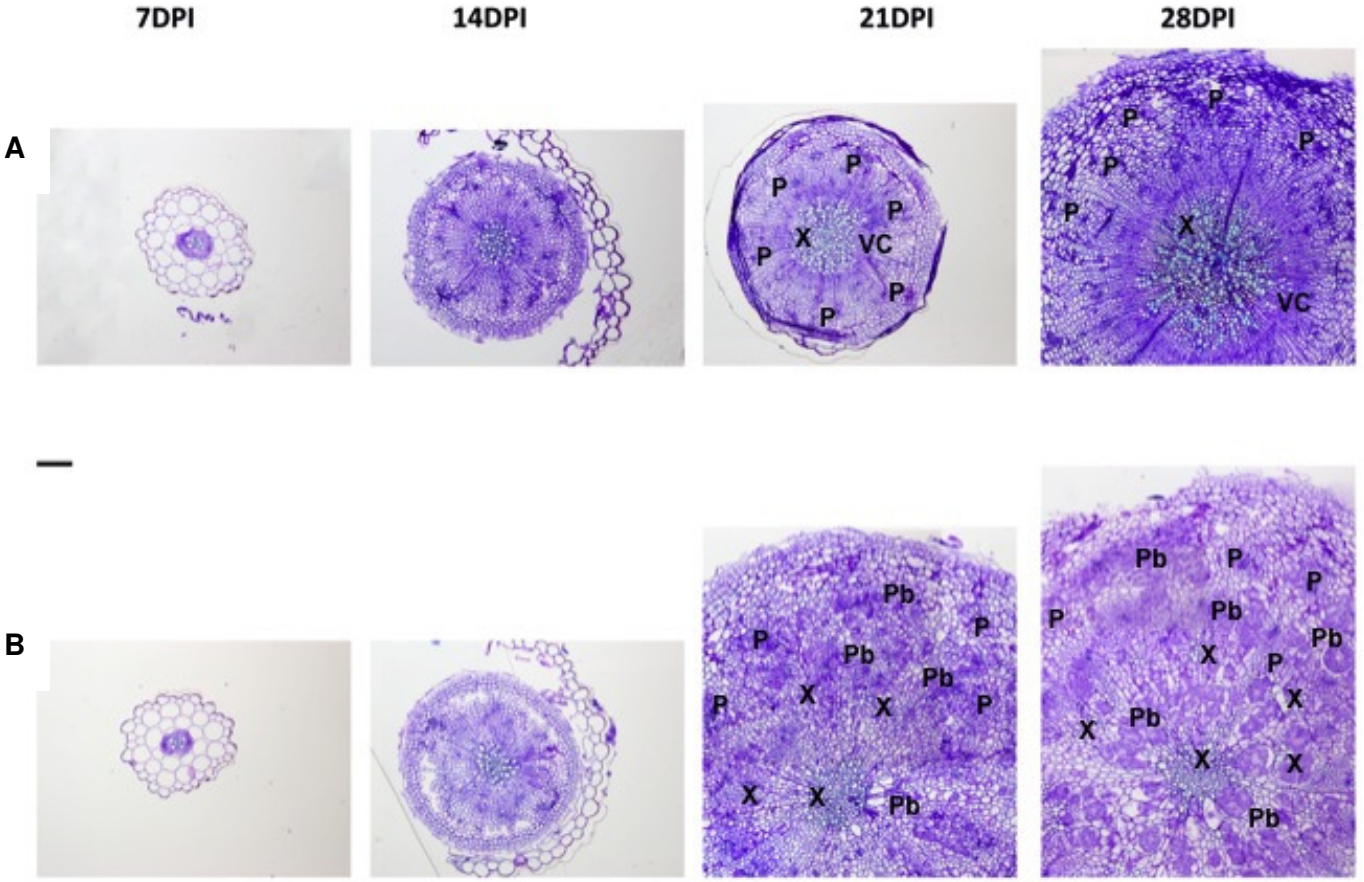

Figure 2.13. Alterations in *ein2-1* hypocotyl structure and morphology as a consequence of *P. brassicae* infection.

Cross sections were taken from (A) uninfected and (B) infected hypocotyls at 7 day intervals following infection. Uninfected plants were inoculated with water. X, xylem vessels; P, phloem bundles; Pb, cells containing plasmodia; VC, vascular cambium. Scale bar = 100 µm

2.4 Discussion

The aim of this chapter was to investigate whether an observation made several years ago in this laboratory, that *ein5-1* is tolerant to clubroot infection, was repeatable. Further to this the aim was to characterise, in much more detail than had been done previously, the response of *ein5-1* to infection and contrast this with that of *ein2-1* in order to examine whether ethylene signalling plays a role during infection.

At the time of the initial screen of PGR mutants little was known about the role EIN5 played in the ethylene signalling pathway or in the wider context of *A. thaliana* biology (Penny-Evans 2000). It has now been established that *EIN5* is allelic to *XRN4* which encodes a 5'-3' exoribonuclease (Olmedo et al. 2006; Potuschak et al. 2006). It has been shown that EIN5 is involved in the regulation of EBF1 and 2 which target EIN3 for degradation in the ethylene signalling pathway hence explaining the weakly ethylene insensitive phenotype of *ein5* mutants, see Figure 2.2 (Olmedo et al. 2006). In addition EIN5 has functions further reaching than the ethylene signalling pathway alone, playing a role in both the miRNA and siRNA-mediated decay pathways (Gazzani et al. 2004; Souret et al. 2004).

The response of *ein5-1* to clubroot can possibly be attributed to its involvement in pathways outside of ethylene signalling. In order to investigate whether perturbations in ethylene signalling are a factor in *ein5-1*'s response the analysis here included a second ethylene insensitive mutant *ein2-1.* EIN2 is a central component of the ethylene signalling pathway and the *ein2* mutation leads to complete ethylene insensitivity (Roman et al. 1995; Alonso et al. 1999). *ein5* on the other hand is one of the weaker of the ethylene signalling mutants (Roman et al. 1995). It was therefore hypothesised that if perturbations in ethylene signalling lead to the *ein5-1* mutant exhibiting a tolerance response then *ein2-1* mutants should also exhibit a response which would be expected to be more pronounced than that of *ein5-1*.

A series of measurements were carried out to indicate gall size and thus determine the extent of infection, Figures 2.4-2.5. These included measuring the hypocotyl width with digital callipers, taking the dry weight of the hypocotyl/root and also the percentage of dry biomass allocated to the hypocotyl/root. The latter is important as it takes into account the general growth condition of the plant, so is thought to be a more reliable measurement of the extent of the disease than dry weight measurements alone (Siemens et al. 2002). Researchers have used a variety of methods to measure gall formation. Mithen and Magrath (1992) for example used a method similar to that used

here; the relative dry weight of a 1 cm long section of hypocotyl tissue was their measure of gall size. A root index has also been used as a measure of gall formation i.e. the relation of root weights of infected plants to uninfected plants (R_i/R_{ni}), (Siemens et al. 2002; Siemens et al. 2006). Researchers have also made use of a subjective scale to grade the size of the gall which is then used to calculate a disease index (DI) (Klewer et al. 2001; Siemens et al. 2002; Siemens et al. 2006). DI is calculated using a formula after plants have been graded along a five point scale, with (0) = no symptoms and (4) = severe clubs in lateral, main root or rosette, fine roots completely destroyed, plant growth is affected.

No measure of gall formation can be completely reliable. There is a natural variation in the morphology of galls, some galls may occur as a consequence of radial swelling of the hypocotyl/root while others may occur as long and thin galls. Subjective measurements are hard to standardise between individual researchers making comparisons difficult. In some cases a small gall does not necessarily indicate that a plant is resistant or tolerant to infection; it may be that the disease has had such an impact on the plant that both growth and gall development has halted (Rausch et al. 1981). Also in the case of screening mutants' responses to infection it could be that the mutation has had an effect on the growth of the plant leading to galls not being evident, even when infection is proceeding. For example, in a recent analysis of infection in several *Arabidopsis* lines (pOpON:KRP1 and *cle41-1*) no visible galls were seen following infection, however, when a microscopic analysis was carried out plants were shown to be heavily infected and produced infective spores (Malinowski et al. 2012). A gall is essentially the end product of infection; a consequence of cell division, expansion and loss of cellular differentiation and organisation. The use of microscopy allows these changes to be visualised before a gall becomes apparent thus one can investigate the processes which lead to gall formation. Therefore, a survey of growth and biomass and a microscopic analysis were both used here to investigate responses to clubroot infection, allowing both the end point of infection and the changes occurring during infection to be examined.

2.4.1 Is *ein5-1* Tolerant to Clubroot Infection?

Gall formation was delayed by approximately 7 days in *ein5-1* compared with infection in Col-0. Galls formed on the hypocotyl/root of infected *ein5-1* were smaller than those formed on Col-0 21DPI. The infected hypocotyls of *ein5*-1 plants show a much more organised structure than that of infected Col-0 hypocotyls. A representative diagram of the cellular rearrangement occurring as a consequence of infection in *ein5-1* and Col-0

can be seen in Figure 2.14. The most striking difference between infection in *ein5-1* and Col-0 is that the hypocotyls of infected *ein5-1* plants are much smaller than those of infected Col-0. The hypocotyls of infected *ein5-1* hypocotyls at 21DPI were not significantly bigger than those of uninfected plants. The wild type increase in hypocotyl size that occurs as a consequence of infection is due to an increase in both cell expansion and division. Induction of cell expansion occurs in a similar manner in *ein5-1* and Col-0. However, cell number appears reduced in infected *ein5-1* compared with Col-0 and this could be a possible explanation for the reduced hypocotyl size of infected *ein5-1*. Mithen and Magrath (1992) reported that during the early stages of infection they first saw enlarged cells followed by an increase in cell division at later stages. Clubroot induced cell expansion is seen in *ein5-1* sections 21DPI with little apparent increase in cell number, which could suggest that the disease progression is slowed in *ein5-1*.

Another line of evidence pointing to the slowing down of disease progression in *ein5-1* is the delay in pathogen migration. In *ein5-1* 21DPI plasmodia are yet to reach the outer cell layers of the hypocotyl, while in Col-0 at the same time point plasmodia are present in cells right at the edge of the hypocotyl. Following infection of the root hairs plasmodia migrate inwards towards the cortical cells of the root where the secondary stage of their life cycle takes place (Ingram and Tommerup 1972). It appears that plasmodia then move upwards into the hypocotyl, as in the 14DPI cross sections presented here, where plasmodia are seen in a ring around the central vascular tissue. Plasmodia then proceed to move outwards, so that in Col-0 cross sections 21DPI cells at the edge of the hypocotyl are seen to contain plasmodia.

The process by which plasmodia move through the root/hypocotyl is a point of contention in the literature with two hypotheses presented. Firstly, researchers have indicated that plasmodia are spread from cell to cell when the cell undergoes cell division (Buczacki 1983). Plasmodia were said to cluster at the point where an infected cell was dividing to become two new daughter cells, thus dividing the plasmodia into two cells also. This theory was updated by Asano and Kageyama (2006) who used turnip suspension-culture cells to visualise the growth and movement of *P. brassicae*. It was shown that plasmodia moved across host cells via cytoplasmic streaming and that this movement was accompanied by division of the host cell. The authors suggested that this active movement of plasmodia via cytoplasmic streaming would increase the number of infected host cells following division (Asano and Kageyama 2006). The second hypothesis proposed by Mithen and Magrath (1992) suggested that plasmodia actively moved via a myxamoebae life stage from cell to cell via breakages in cell walls.

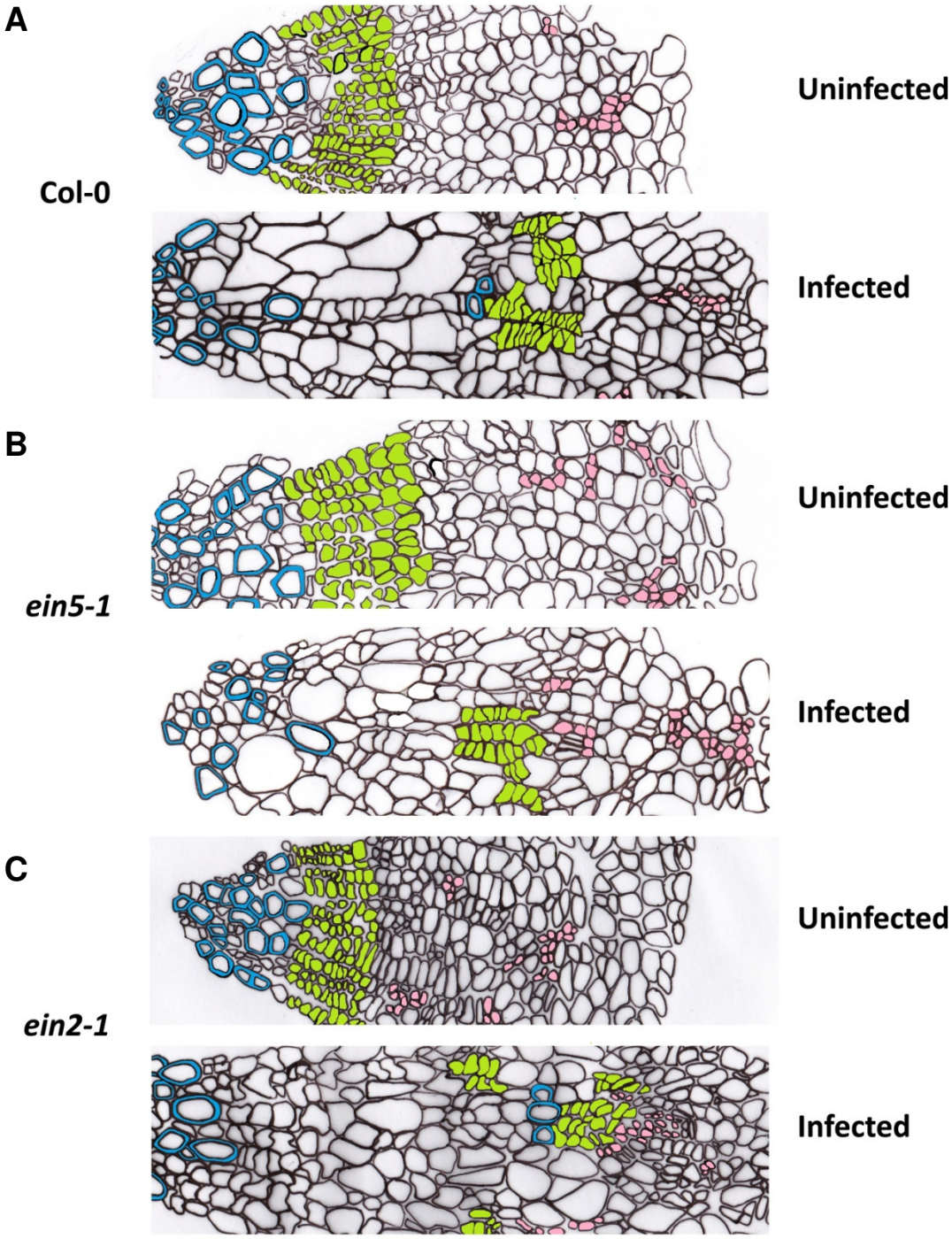

Figure 2.14 Representative diagrams showing changes that occur following infection with *P. brassicae.*
The line diagrams give a representation of cellular arrangement of uninfected and infected hypocotyls from Col-0 (A), *ein5-1* (B) and *ein2-1* (C). Different cell types are colour coded; blue = xylem cells, green = cells of the vascular cambium and pink = phloem cells.

They observed myxamoebae in infected *A. thaliana* frequently associated with breaks in cell walls, as well as large cells containing cell wall stubs and occasionally containing two nuclei; suggesting the coming together of two cells via the loss of cell walls. These cell wall breakages were not seen in uninfected tissue. It was further suggested that plasmodia may produce enzymes that are able to digest cell wall components which would enable pathogen migration (Mithen and Magrath 1992). Cell wall breakage was also reported by Kobelt *et al* (2000). During a susceptible reaction in *A. thaliana* ecotype Cvi-0 they observed enlarged cells containing multiple nuclei. It has been speculated that this myaxamoebae phase of *P. brassicae* may only be occurring during infection of *A. thaliana*. However, cell wall breakages as well as an amoeboid life stage have been shown to occur in infection of both susceptible and resistant *Brassica oleracea* (Donald et al. 2008), indicating this life stage is not just confined to infection of *A. thaliana.* It is certain that plasmodia are able to migrate large distances as they are seen in the hypocotyl which is distant from the root hairs; the point of infection.

Initially it was thought that plasmodia-induced cell division was occurring in the root/hypocotyl as a consequence of *de novo* meristem formation (Devos et al. 2006). This would make the spread of plasmodia throughout the tissue via host cell division a plausible hypothesis, as cell divisions occurring as a consequence of infection across the hypocotyl/root would spread the pathogen throughout the same area. However, recent work has now established that gall development occurs as a consequence of the amplification of the existing root/hypocotyl meristems (Malinowski et al. 2012). The CYCB1::GUS and ANT::GUS constructs were used as markers of cell division and meristematic activity respectively. The authors noted that infection takes place in areas wh ere secondary thickening (when cells of the VC form a secondary meristem to increase the girth of the tissue) is occurring, the hypocotyl and upper root. The CYCB1:GUS marker showed that cell division was increased in the vicinity of the VC during infection which was consistent with the proliferation of existing meristems during gall formation rather than *de novo* meristem formation. ANT activity overlapped with that of CYCB1 in the VC again in-line with the notion of existing rather than *de novo* meristematic activity. The authors concluded that *P. brassicae* hijacks the process of secondary thickening (existing meristem) to provide a pool of dividing cells which drives gall formation as opposed to the previously thought *de novo* meristem. In terms of divisions of host cells these are mainly occurring in the region of the vascular cambium. The idea of plasmodia spreading throughout the whole of the host tissue solely via host cell divisions is therefore less likely as cell divisions simply aren't occurring across the hypocotyl. It seems reasonable to suggest that at least some active movement of plasmodia must be occurring. However, there is no reason to suggest that both

movement via host cell division and active movement by plasmodia can't both occur, and this has been suggested by other researchers (Asano and Kageyama 2006).

Cook and Schwartz reported that in older infected roots xylem vessels appear as small isolated areas surrounded by diseased tissue (1930). Malinowski *et al* also reported small fragments of xylem associated with islands of cambial activity, forming away from the central xylem vessels (2012). These islands of xylem were seen to form here in hypocotyl cross-sections of Col-0 21DPI. In *ein5-1* they were not seen to be forming until 28DPI, this is another indicator that the disease progression is slowed in *ein5-1* and perhaps suggests that the normal functions of the hypocotyl development are maintained for longer during infection in *ein5-1*. Formation of new xylem vessels at the centre of the hypocotyl seem to be affected in the same manner as in Col-0.

The results here strongly indicate that *ein5-1* is tolerant to clubroot infection confirming and expanding on the work of Penny-Evans (2000). It appears that the disease is delayed and galls are smaller on *ein5-1* as a consequence of a slowing down of the disease progression.

2.4.2 Do Perturbations in Ethylene Signalling Lead to Tolerance to Clubroot Infection?

It would be expected that if the tolerance response exhibited by *ein5-1* was a consequence of its role in the ethylene signalling pathway then *ein2-1* would exhibit a more pronounced tolerance response, as *ein5-1* has only a weak ethylene insensitive phenotype while *ein2-1* presents a strong phenotype with knock out mutants being completely insensitive to ethylene (Roman et al. 1995; Alonso et al. 1999).

The growth analysis of infected *ein2-1* plants indicated that infection did not differ significantly from infection in Col-0, and thus was different from infection in *ein5-1*. This is in line with what Penny-Evans (2000) found in her initial screen of ethylene insensitive mutants. However, the work did not include a microscopic analysis of infection in *ein2-1* which was carried out here. It appears that infection in *ein2-1* proceeded in the same manner as in Col-0 7-21DPI. At 21DPI the cellular arrangement of infected *ein2-1* hypocotyls is comparable with those of Col-0; see Figure 2.12 for a representative diagram of cell arrangement. At 28DPI however, *ein2-1* presented slightly more advanced symptoms than Col-0. In cross sections of infected *ein2-1* 28DPI cells of the hypocotyl appear larger than those of Col-0 at the same time point and the number of secondary plasmodia also appears increased.

Recently Knaust and Ludwig-Müller (2012) have indicated that ethylene signalling is required to restrict gall size during infection. Data from a previous microarray using clubroot infected tissue was re-examined and indicated that a large amount of ethylene related genes were up-regulated during an early time point whereas at a late time point many ethylene signalling genes were down-regulated (Siemens et al. 2006). Inspection of the original Siemens *et al* (2006) data indicated that Knaust and Ludwig-Müller (2012) had based their analysis on raw data that had not been normalised or subjected to statistical analysis, making the conclusions drawn subject to doubt. They also found that ACC (an ethylene precursor) levels were down-regulated at early time points of infection, but could not conclude whether this was due to increased or decreased ethylene production. An ACC oxidase gene (*ACO2*) was found to be up-regulated by semi-quantitative RT-PCR but other ethylene biosynthesis genes were not found to be consistently regulated during infection. Finally an analysis of selected ethylene signalling mutants at different inoculation densities indicated that at low inoculation densities wild type plants are less susceptible to infection than the ethylene signalling mutants tested, including an *ein2* mutant. This increased susceptibility was variable however, and was only seen at certain inoculation densities. Knaust and Ludwig-Müller (2012) concluded that ethylene was not a major regulator of defence against clubroot infection.

The evidence both from this analysis and that of Knaust and Ludwig-Müller (2012) does not present strong enough evidence to state categorically that *ein2-1* is more susceptible to clubroot infection than Col-0. However, the aim of the analysis here was to investigate whether *ein5-1*'s response is due to perturbations of ethylene signalling and as the response is different to that of both *ein2-1* and mutants tested by Knaust and Ludwig-Müller (2012) it can be concluded that *ein5-1* exhibits a tolerance response when subjected to clubroot infection and this is not a consequence of perturbations in ethylene signalling.

2.5 Conclusion

ein5-1 was found to be tolerant to clubroot infection, with gall formation being delayed when compared to that of Col-0. Microscopic examination of hypocotyl galls from *ein5-1* showed that the progression of disease was delayed in terms of impact on the host and development/migration of the pathogen. *ein2-1* was examined for its response to clubroot infection and was found to respond in a manner that was not significantly different from that of Col-0. As EIN2 plays an irreplaceable role in ethylene signalling and does not show a response to infection altered from that of wild type it was

concluded that ethylene does not play a major role in infection. Thus perturbations in ethylene signalling do not account for the tolerance response of *ein5-1*. The other roles of EIN5/XRN4 must now be explored in order to begin to unravel the factors contributing to *ein5-1*'s tolerance to clubroot. As EIN5/XRN4 has been implicated in small RNA-mediated gene silencing the next chapter will look to explore whether the tolerance response of *ein5-1* can attributed to perturbations in these pathways.

Chapter 3: Investigating the Effect of *P. brassicae* Infection on Growth and Morphology of Small RNA Biogenesis Mutants

3.1 Introduction

In Chapter 2 it was shown that the *ein2* and *ein5* mutants responded differently to *P. brassicae* infection. EIN2 and EIN5 are both components of the ethylene signalling pathway; mutations in EIN2 lead to a strong ethylene insensitive phenotype while loss of EIN5 leads to a much weaker phenotype. These differing responses to clubroot seem difficult to resolve as the mutant with the weaker phenotype appears to be displaying the much stronger response to infection. It has become apparent however, that EIN5 has functions outside of the ethylene signalling pathway. Firstly, EIN5 and EIN2 were found to have distinct roles in *A. thaliana* response to bacterial harpin (Dong et al. 2004). This was supported by the observation that *ein5* plants display a serrated leaf margin phenotype which is not seen in any of the other ethylene insensitive mutants (Olmedo et al. 2006). Interestingly, a mutation in the *SERRATE* gene was found to lead to a similar phenotype; SERRATE was later found to be involved in miRNA biogenesis (Prigge and Wagner 2013; Lobbes et al. 2006; Yang et al. 2006).

EIN5 has now been shown to be allelic to *XRN4*; a 5'→ 3' exoribonuclease which is known to have functions in mRNA degradation and RNA interference (Gazzani et al. 2004; Souret et al. 2004; Olmedo et al. 2006; Potuschak et al. 2003). Within the ethylene pathway EIN5 was found to be responsible for indirectly negatively regulating the levels of *EBF1* and *EBF2* mRNAs (Olmedo et al. 2006; Potuschak et al. 2003). Reduction in these two mRNAs leads to their repression of the EIN3 protein being lifted and thus ethylene signalling can proceed through EIN3, see Section 2.1.1 (Olmedo et al. 2006; Potuschak et al. 2003).

Chapter 2 investigated the role of ethylene in clubroot infection. Due to the pivotal role played by EIN2 in ethylene signalling, it was concluded that ethylene signalling did not play an important role in clubroot infection and *ein5-1* was not exhibiting a tolerance response as a consequence of perturbations in ethylene signalling. Consequentially, it is now hypothesised that the response of *ein5-1* to clubroot infection is due to its role outside of ethylene signalling. This chapter therefore, aims to further investigate why *ein5-1* is tolerant to clubroot infection and to specifically examine the role of smRNA-mediated gene silencing in clubroot infection.

Mutations in xrn4/ein5 have been shown to affect both miRNA and siRNA-mediated decay. XRN4/EIN5 appears to perform differing tasks within these two pathways. Mutations in XRN4/EIN5 lead to an increase in post transcriptional gene silencing (PTGS) induced by siRNAs (Gazzani et al. 2004). Loss of *xrn4/ein5* leads to an increase in the number of uncapped RNAs which are potential substrates for RNA-dependent RNA polymerases (RdRPs); whereby they are used to form dsRNA which can be processed by DICER-like enzymes to form siRNAs. In the miRNA pathway XRN4/EIN5 acts to degrade selected 3' products produced as a result of miRNA-mediated cleavage (Souret et al. 2004).

3.1.1 Small RNA Induced Gene Silencing

Small RNAs (20-24 nt) are a group of regulatory molecules. They are divided into two major classes in *Arabidopsis*: microRNAs (miRNAs) and small-interfering RNAs (siRNA). These two classes of small RNA can affect gene expression through mRNA cleavage, translational repression and DNA/chromatin remodelling. Loss of EIN5/XRN4 has been shown to affect both miRNA and siRNA-mediated decay (Gazzani et al. 2004; Souret et al. 2004). A schematic of those RNA silencing pathways that XRN4 has been implicated in is shown in Figure 3.1.

In general, small RNAs are processed from longer dsRNA transcripts by a family of RNase III-like enzymes. These enzymes are homologous to the RNase-III enzyme DICER first discovered in *Drosophilla* (Bernstein et al. 2001). In *Arabidopsis* there are four such enzymes, DICER-LIKE 1 (DCL1), DCL2, DCL3 and DCL4 (Schauer et al. 2002). The DCL enzymes process miRNAs from imperfect RNA hairpins and siRNAs from longer dsRNAs, to form miRNA/miRNA* and siRNA/siRNA* duplexes. Following processing small RNAs are methylated by a methyl transferase HUA ENHANCER 1 (HEN1). This is a universal step in the biogenesis of both siRNAs and miRNAs (Li et al. 2005; Yu et al. 2005; Yang et al. 2006). Once methylated, one member of the small RNA duplex is loaded into a RNA induced silencing complex (RISC) which contains an ARGONAUTE protein. The *strand is usually not incorporated and is subsequently degraded. In *Arabidopsis* there are 10 ARGONAUTE proteins (AGO1-10) (Mallory and Vaucheret 2010a). The small RNAs are complementary to a section of their target gene and guide the AGO containing RISC to target the gene for repression, through RNA-directed DNA methylation, mRNA cleavage or translational inhibition.

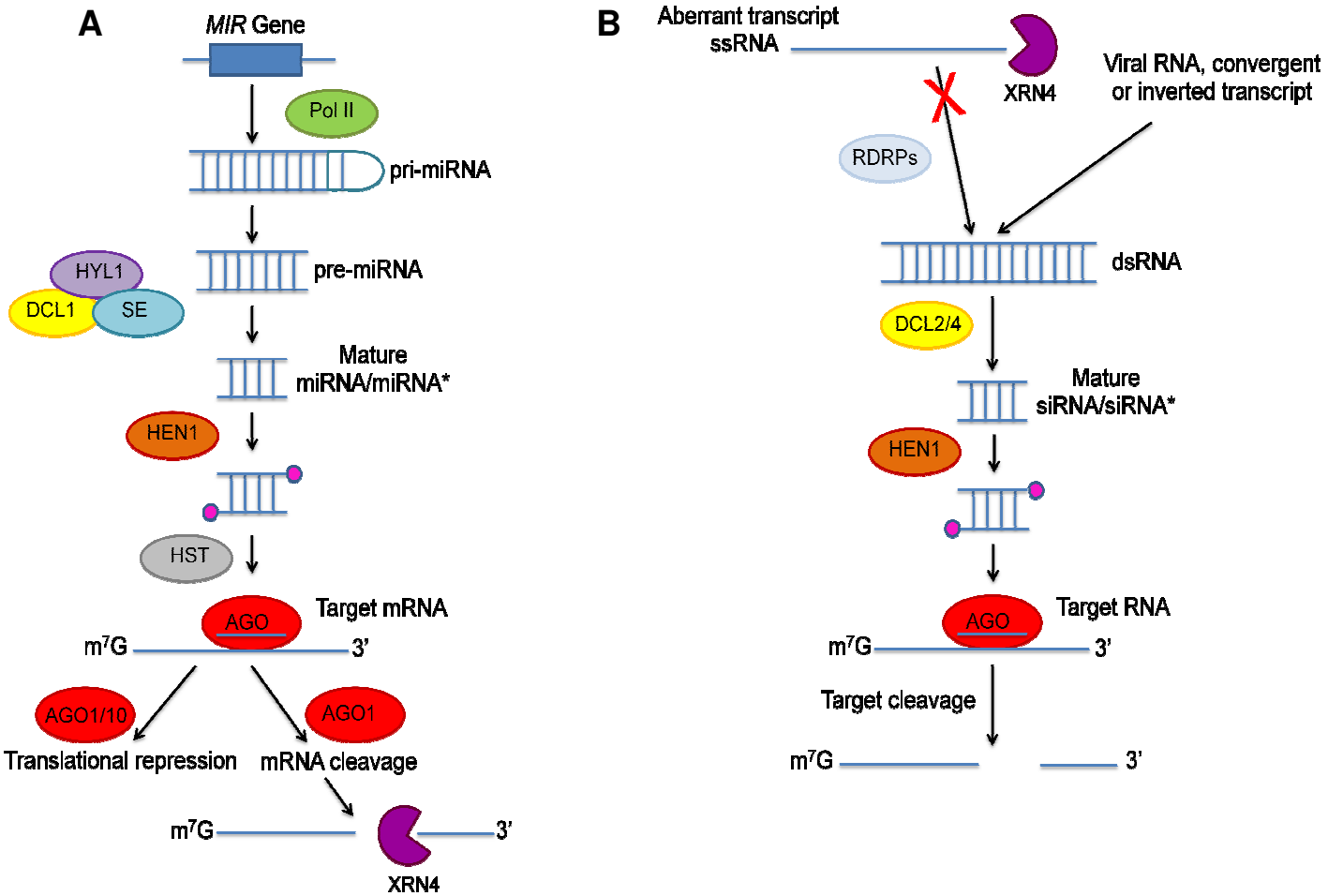

Figure 3.1 The small RNA pathways of *Arabidopsis* involving EIN5/XRN4.
Small RNAs in *Arabidopsis* fall into two categories the miRNAs and the siRNAs. The pathways depicted are (**A**) the miRNA-silencing pathway and (**B**) siRNA-mediated PTGS. The red cross indicates the pathway does not proceed if XRN4 degrades the ssRNA. Pink circles are methyl groups. See text for a more detailed description of each pathway.

3.1.3 miRNA-Mediated mRNA Decay

miRNAs have been implicated in the regulation of several developmental processes (Parent et al. 2012). miRNAs are predominately 21-nt small RNAs which are transcribed from *MIRNA* genes, found in intergenetic regions of the genome, by RNA Polymerase II to give rise to an initial primary transcript (pri-miRNA) (Kurihara and Watanabe 2004; Xie et al. 2005; Xie and Qi 2008). This pri-miRNA is first processed to a pre-miRNA and then to a mature miRNA/miRNA* by an RNAse III-like enzyme, DCL1 (Kurihara and Watanabe 2004). HYPONASTY LEAVES 1, HYL1, a dsRNA binding protein, has been shown to be involved in the processing of miRNAs (Han et al. 2004; Vazquez et al. 2004). HYL1 was found to form a complex with DCL1, an increase in pri-miRNA and a reduction in pre-miRNA and mature miRNAs was seen in *hyl1* mutants indicating that HYL1 functions to assist DCL1 in its processing of pri-miRNAs to mature miRNAs (Kurihara et al. 2006). In addition, SE, a zinc finger protein, was found to interact with HYL1 and DCL1 and is involved in the processing of pri-miRNAs to mature miRNAs (Prigge and Wagner 2001; Lobbes et al. 2006; Yang et al. 2006). Additional accessory proteins are also involved in these processing steps. Following processing by DCL1, both strands of the miRNA/miRNA* duplex are methylated by HEN1; methylation takes place at the 3' end of the nucleotide (Li et al. 2005; Yu et al. 2005; Yang et al. 2006). This methylation prevents uridylation of the 3' end of the miRNA/miRNA* and protects from 3'-to-5' exonuclease activity and other enzymatic activity; avoiding premature degradation (Li et al. 2005; Yang et al. 2006). These initial processing steps take place in the nucleus (Park et al. 2002; Kurihara and Watanabe 2004; Lobbes et al. 2006). HASTY (HST), a homolog of the nuclear receptor protein Exportin 5, is thought to be involved in transporting the miRNA/miRNA* into the cytoplasm (Park et al. 2005). One of the miRNA/miRNA* strands is incorporated into the AGO-containing RISC. The less stable of the two strands is incorporated into the RISC as the guide strand; this is usually the miRNA strand and the miRNA* is degraded. AGO1 is the main AGO involved in the miRNA-mediated gene silencing pathway. The miRNA guide strand allows the RISC to recognise the target mRNA. AGO1 has intrinsic slicer activity and is responsible for the cleavage of the target mRNA, cleavage of the mRNA occurs between the 10^{th} and 11^{th} nucleotide of the target region complementary to the miRNA (Baumberger and Baulcombe 2005; Pashkovskiy and Ryazansky 2013). Following cleavage by AGO a subset of the 3' cleavage products are degraded by EIN5/XRN4, meaning that these 3' cleavage products accumulate in *ein5*/*xrn4* mutants (Souret et al. 2004). AGO1 and AGO10 have also been shown to be required for miRNA-mediated translational repression (Brodersen et al. 2008). As an emerging field, components of the miRNA pathway are

continually being discovered and their functions in the pathway are beginning to be unravelled.

3.1.4 Post Transcriptional Gene Silencing Mediated by siRNAs

PTGS mediated by siRNA is used as a defence strategy by plants to combat invading molecular parasites like viruses and to degraded aberrant transcripts from endogenous genes or transgenes (Pattanayak et al. 2012). dsRNA from invading viruses, exongenously introduced RNA, inverted repeats and convergent transcription can act as templates from which 21-22 nt siRNAs are produced (Pattanayak et al. 2012). Alternatively aberrant ssRNA is transformed into dsRNA, by the action of RDRPs, which can then act as a precursor for siRNA production (Parent et al. 2012). Both DCL2 and DCL4 have been shown to process dsRNAs to form siRNA duplexes (Garcia-Ruiz et al. 2010). As detailed above, the siRNA/siRNA* is then methylated by HEN1 to protect it from degradation (Li et al. 2005; Yang et al. 2006). The strand that is least stable is recognised as the guide strand and is loaded into the AGO containing RISC (Pattanayak et al. 2012). The siRNA then guides the RISC to target mRNA, which an AGO protein cleaves at the centre of the siRNA-mRNA complementary region, between the 10^{th} and 11^{th} residues of the siRNA (Pattanayak et al. 2012). AGO1, 4, 6 and 7 has been implicated in siRNA-mediated cleavage (Pattanayak et al. 2012). XRN4 has been shown to degrade uncapped RNAs that would be targets for RDRP6, thus preventing them becoming dsRNA precursors for siRNA biosynthesis (Gazzani et al. 2004). Therefore, loss of XRN4 leads to a reduction in siRNA mediated PTGS.

3.1.5 Hypothesis, Aims, Objectives and Rationale

EIN5/XRN4 was found to degrade the 3' products of miRNA-mediated cleavage including the 3' ends of *SCARECROW-LIKE* transcripts which are cleaved via the action of miR171 (Llave et al. 2002; Souret et al. 2004). SCL transcription factors have been shown to function in the regulation of the radial patterning of the root (Di Laurenzio et al. 1996; Helariutta et al. 2000). Clubroot is thought to hijack the normal developmental processes in the root during gall formation. So, it is possible that disruptions to root patterning mechanisms could lead to alterations in response to clubroot. Therefore it was decided to explore the role of miRNA-mediated cleavage during infection. It was hypothesised that the tolerance response exhibited by *ein5-1* was a consequence of its role in miRNA-mediated mRNA decay. Further to this, it was hypothesised that if the tolerance response exhibited by *ein5-1* when infected with

clubroot was a consequence of alterations in the pathway then other mutants residing further upstream should exhibit a similar response.

In order to test this hypothesis, three mutants from the miRNA pathway were selected and screened for their response to clubroot. The three mutants represent the three major control points in the miRNA pathway; miRNA processing, methylation and loading into the RISC. Therefore, lines carrying mutations in AGO1, DCL1 and HEN1 were selected. miRNA-mediated gene control plays a pivotal role in many developmental processes, such that many of the miRNA biogenesis mutants present severe developmental abnormalities; many are completely sterile and some can be lethal at the embryo stage. Null mutations of *ago1* have severe developmental defects and are completely sterile; therefore a hypomorphic allele was selected: *ago1-27* which was shown to be impaired in silencing, with the silencing properties of this line not being distinguishable from null mutants (Morel et al. 2002). All of the *dcl1* alleles found in a Col-0 background are embryo lethal, therefore a partial loss-of-function mutant: *dcl1-9* found in the *Ler* background was used (Schauer et al. 2002). Plants carrying homozygote mutations of *dcl1-9* are sterile, although the heterozygote plants are fertile (Vazquez et al. 2004). Other researchers have used this allele for investigating RNA silencing and it has been shown that this mutant fails to accumulate miRNAs (Reinhart et al. 2002; Kurihara and Watanabe 2004). *hen1-5* plants were shown to maintain some level of fertility albeit much reduced and a reduction in the accumulation of miRNAs was reported in this mutant (Vazquez et al. 2004).

In order to establish the response of these mutants to clubroot infection a similar strategy was employed here as in Chapter 2. A growth analysis was carried out to assess the impact of infection on *ago1-27, dcl1-9* and *hen1-5*. In addition, a microscopic analysis was carried out to investigate the impact of infection at the cellular level. As stated previously, a combination of these two measures of disease is the best way to analyse the impact of clubroot disease on a plant.

The aims and objectives of this chapter were:

Aims

1. To examine the response of three miRNA biogenesis mutants; *dcl1-9*, *hen1-5* and *ago1-27* to clubroot infection, in order to examine whether the miRNA-mediated mRNA decay pathway plays a role during infection.

2. To contrast infection in the miRNA biogenesis mutants with infection in *ein5-1*, in order to establish whether perturbations in the miRNA-mediated mRNA decay pathway leads to the tolerance response exhibited by *ein5-1*.

Objectives

1. To conduct a growth analysis of infected and uninfected *dcl1-9*, *hen1-5* and *ago1-27*.

2. To undertake a microscopic analysis of infected and uninfected *dcl1-9*, *hen1-5* and *ago1-27*.

3. To contrast results from the growth and microscopic analysis from this chapter, with those from Chapter 2.

3.2 Materials and Methods

3.2.1 Plant Material

ago1-27 seeds were acquired from Hervé Vaucheret, Institut Jean-Pierre Bourgin. *dcl1-9* and *hen1-5* seeds were purchased from The Nottingham Arabidopsis Stock Centre (NASC). *Ler* seeds were provided by Marion Bauch, The University of Sheffield.

3.2.2 Genomic DNA Extraction

One leaf, approximately 2.5 cm in length, was removed from the plant and placed into an Eppendorf tube, which was immediately frozen in liquid nitrogen. The frozen leaf sample was then ground inside the Eppendorf tube using a micro-pestle. 200 µl of 'shorty' DNA extraction buffer (0.2 M TRIS-HCl pH 9, 0.4 M LiCl, 25 mM EDTA pH 8 and 1 % SDS) was added to the ground sample, which was further homogenised using the micro-pestle. Once homogenised a further 300 µl of 'shorty' buffer was added and the sample was mixed by inversion. The sample was centrifuged at 16438 g for 10 minutes. 350 µl of supernatant was transferred to a fresh Eppendorf tube containing 350 µl of isopropanol and mixed by inversion. Following mixing, the sample was centrifuged at 16438 g for 10 minutes. The supernatant was discarded and the remaining pellet was washed by adding 350 µl of 70 % ethanol and centrifuging at 16438 g for 10 minutes. The supernatant was removed and the pellet was allowed to air dry for approximately 20 minutes. Once dry, 200 µl of TE buffer (10 mM TRIS-HCl pH7.5 and 1mM EDTA) was added to the pellet, which was re-suspended overnight at

4 °C. To check that the extraction had worked 8 µl of sample was run out on an agarose gel, see Section 3.2.3. Extracted DNA was stored at -20 °C until needed.

3.2.3 Agarose Gel Electrophoresis

1 % (w/v) agarose was added to 1 x TAE buffer (40 mM TRIS-HCl pH8, 20mM acetic acid and 1 mM EDTA). The agarose was dissolved in the TAE buffer by heating in a microwave until the solution was clear. The solution was allowed to cool slightly and ethidium bromide added at a final concentration of 0.5 µg/ml before being poured into a gel casting tray with an appropriate comb. Once set, the gel was placed in an electrophoresis tank and covered with 1 x TAE buffer and the comb removed. DNA samples were mixed with 5 x bromophenol blue loading buffer (Bioline Reagents Limited, London) to give a final concentration of 1 x loading buffer. Samples were then loaded into the gel along with an appropriate DNA ladder. Electrophoresis was performed at 50 – 100 V depending on gel size, for approximately 30 – 60 minutes until DNA separation had occurred to an acceptable level. DNA was visualised in the gel using a UV transilluminator.

3.2.4 Polymerase Chain Reaction (PCR) Verification of Mutant Lines

A PCR mix was prepared in PCR tubes containing all the reagents required for a 25 µl PCR reaction (19.3 µl of nuclease free H_2O, 2.5 µl x10 NH_4 buffer, 1 µl 50 mM $MgCl_2$, 0.5 µl 10 mM dNTP mix, 0.25 µl 10 µM forward primer, 0.25 µl 10 µM reverse primer and 0.2 µl 5 u/µl Taq polymerase). 1 µl of genomic DNA, extracted as detailed in Section 3.2.3, was added to the PCR mix. The tubes were then placed in a thermocycler and the program specified below was run with alterations according to the primers being used in the reaction, see Sections 3.2.4.1 and 3.2.4.2 for details. Following PCR amplification 8 µl of sample was run out on an agarose gel, Section 3.2.3 and the results analysed as detailed in Sections 3.2.4.1 and 3.2.4.2.

PCR Program:

Initial denaturation	94 °C	5 minutes
---		
35 cycles of:		
Denaturation	94 °C	30 seconds
Annealing	X °C	30 seconds
Extension	72 °C	X seconds

Final extension	72 °C	5 minutes

See Sections 3.2.4.1 and 3.2.4.2 for values of X. The value of X was selected based on the melting temperature of both primers used in the reaction.

3.2.4.1 *dcl1-9* Verification

To distinguish between wild-type plants and plants heterozygous and homozygous for the *dcl1-9* mutation primers were used from the octopine synthase terminator sequence of the T-DNA insert, forward primer: CTCCGTTCAATTTACTGATTGTAC and reverse primer: TTGAATGGTGCCCGTAACTTTCG (Kurihara and Watanabe, 2004). The annealing temperature used was 60 °C and the extension time was 30 seconds. A PCR product would not be present in WT plants but would be seen in those plants carrying the *dcl1-9* mutation. To distinguish between plants heterozygous and homozygous for the *dcl1-9* mutation, primers were designed which were placed either side of the T-DNA insert; forward primer: AGCGGTGCCAGCAAACAAGC, reverse primer: ACACTCGGCATTGGCTCGCC, designed using Primer3, (http://bioinfo.ut.ee/primer3/). The annealing temperature used was 50 °C and the extension time was 30 seconds. A PCR product would not be seen in the *dcl1-9* homozygous plants as the T-DNA insert interrupts the primer pair, but a product would be seen in the plants carrying only one copy of the mutation or no mutation i.e. *dcl-9* heterozygotes and WT plants.

3.2.4.2 *hen1-5* Verification

The *hen1-5* mutant is a SALK line, therefore the T-DNA primer design tool was used to aid verification of this mutant; (http://signal.salk.edu/tdnaprimers.2.html). The primers used were left genomic primer (LP): TAGGGCATGGGTTTAGATGTG, right genomic primer (RP): CTCCATTCGTTCTTCTGATGG and left border primer (LB) b1.3: ATTTTGCCGATTTCGGAAC. The annealing temperature used for these primers was 55 °C and the extension temperature was 60 seconds. Two PCR reactions were set up for each plant to be verified LP + RP and RP + LBb1.3. The LP + RP reaction should produce a PCR for WT plants and plants heterozygous for *hen1-5* but no PCR product for plants homozygous for *hen1-5*. The RP + LBb1.3 reaction should yield a PCR product using DNA from plant heterozygous and homozygous for the *hen1-5* mutation but not for wild type plants.

3.2.5 Measurements of Growth and Biomass

The miRNA biogenesis mutants *ago1-27*, *hen1-5* and *dcl1-9* along with *Ler* were grown and infected with *P. brassicae* as described in Section 2.2.2.

Ten uninfected and ten infected *ago1-27* and *hen1*-5 plants were harvested 14, 21 and 28DPI. A series of measurements of plant growth and biomass were then undertaken as detailed in Section 2.2.3. In addition, measurements of *hen1-5* hypocotyl and root width were taken using images of the plants and the measure function of ImageJ, U. S. National Institutes of Health, Bethesda, Maryland, USA.

The F2 generation of *dcl1-9* plants were found not to segregate in a Mendelian fashion, i.e. homozygous for the mutation: heterozygous for the mutation: homozygous for the wild type gene at a ratio of 1:2:1. Plants containing the homozygous *dcl1-9* mutation appeared at a much lower frequency than 25% of the progeny. Therefore, large numbers of plants would have needed to be screened to gather enough *dcl1-9* homozygous for a full growth analysis. This was above the time, space and monetary constraints of the project. Therefore, it was decided that one time point would be selected for analysis. Based on the data from Chapter 2, it was decided that 21DPI would be the time point at which infection in *dcl1-9* would be investigated. This was due to this being the time point at which *ein5-1* displayed a tolerance response when compared with wild-type plants and other plant lines. The *dcl1-9* mutation is in the *Ler* background, so that line was used here as a wild-type, to which infection in *dcl1-9* could be compared. Therefore, ten uninfected and ten infected *dcl1-9* and *Ler* plants were harvested 21DPI, a series of measurements of plant grow and biomass followed as detailed in Section 2.2.3.

3.2.6 Statistical Analysis

Statistical analysis was carried out as detailed in Section 2.2.4.

3.2.7 Technovit Sectioning of Hypocotyl/Root Samples

ago1-27, *hen1-5*, *dcl1-9* and *Ler* were grown and infected as described in Section 2.2.2.

Three hypocotyl samples were taken from *ago1-27*, *dcl1-9* and *Ler* uninfected and infected plants 21DPI. These samples were then fixed, embedded and sectioned as described in Section 2.2.5.

Three hypocotyl and three upper root samples were taken from uninfected and infected *hen1-5* plants 21 and 31DPI. These were then processed as detailed in Section 2.2.5.

3.3 Results

Growth and microscopic analyses were conducted to examine the impact of clubroot infection on three small RNA biogenesis mutants, *agol-27*, *hen1-5* and *dcl1-9* and to investigate whether these plants displayed a tolerance response similar to that seen in *ein5-1*.

The *dcl1-9* mutation is in the *Ler* background and this was therefore used as a control. *ago1-27* and *hen1-5* are found in the Col-0 background, infection of which is described extensively in Chapter 2. Owing to the difficult nature of working with the *dcl1-9* line only one time-point following infection was examined, see Section 3.2.2. 21DPI was chosen, as data from the previous chapter suggests this is the time point when differences in infection in *ein5-1* are apparent compared with other *Arabidopsis* lines.

3.3.1 Investigating the Impact of Clubroot Infection on the Small RNA Biogenesis Mutants *ago1-27*, *hen1-5* and *dcl1-9*

As in Chapter 2, gall size and thus disease extent was measured by hypocotyl width, dry hypocotyl/root weight and % of dry biomass allocated to the dry hypocotyl/root.

3.3.1.1 The Impact of Infection on *ago1-27*

The hypocotyl/roots of *ago1*-27 are shown in Figure 3.2. Galls formed in the hypocotyl and upper root system in a manner similar to that seen in Col-0. The impact of infection on several growth parameters can be seen in Figure 3.3. As seen in the previous chapter, hypocotyl width, dry root weight and % of dry biomass allocated to the hypocotyl/root all increased upon infection. The hypocotyl width of infected *ago1-27* plants was significantly different from uninfected plants from 21DPI, and by 28DPI was 2.8 times that of uninfected *ago1-27* plants. The impact of clubroot infection on the dry root weight of *ago1-27* was evident from 14DPI, when infected roots were found to be significantly heavier than uninfected plants.

Figure 3.2. Hypocotyl/roots of uninfected and infected *ago1-27* 21DPI.
Hypocotyl/roots of (**A**) uninfected and (**B**) infected *ago1-27* plants 21DPI. Three representative hypocotyl/roots are shown for each condition. Scale bar = 2 mm.

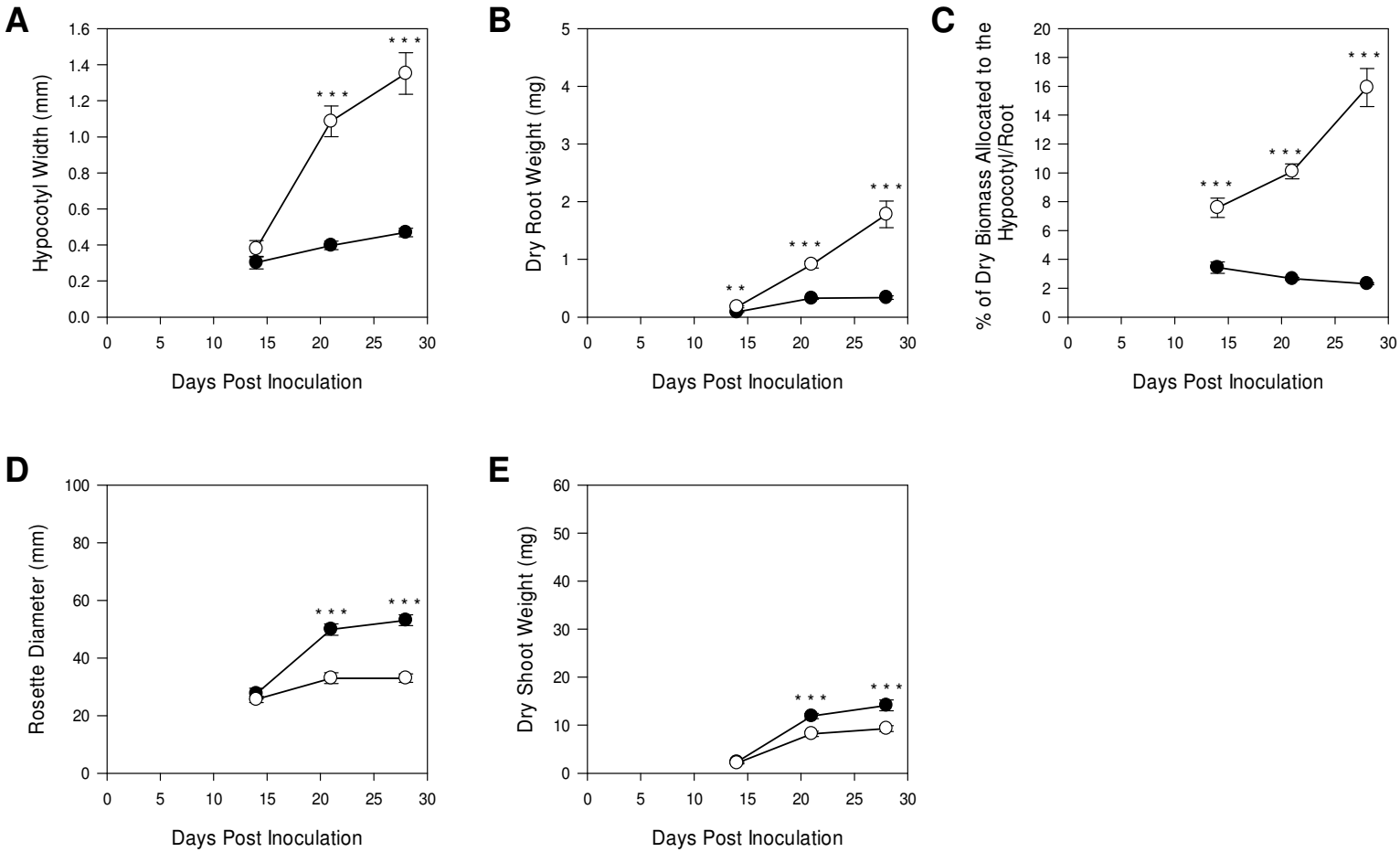

Figure 3.3. The impact of *P. brassicae* infection on the growth of the small RNA biogenesis mutant *ago1-27*.
The effect of *P. brassicae* infection on the (**A**) hypocotyl width (**B**) dry root weight (**C**) % dry biomass allocated to the hypocotyl/root (**D**) rosette diameter and (**E**) dry shoot weight of *ago1-27*. Uninfected controls (filled circles), *P. brassicae* infected plants (open circles). Results are means ± S.E. of 9-10 plants. (T-test *$p \leq 0.05$, ** $p \leq 0.01$, *** $p \leq 0.001$).

The dry root weight of infected plants continued to increase, and by 28DPI infected hypocotyl/roots were 5 times that of uninfected plants. From 14DPI there was a significant difference between the percent of dry biomass allocated to the hypocotyl/root of infected and uninfected *ago1-27* plants. At 14DPI uninfected *ago1-27* plants had 3.4 % of their dry biomass allocated to the hypocotyl/root, while infected plants had 7.5 %. This continued to increase throughout the course of the experiment, so that at 28DPI infected plants had 15.9 % of their biomass allocated to their hypocotyl/roots, 6.9 times that of their uninfected counterparts. Gall formation had a characteristic detrimental effect on shoot growth, with both rosette diameter and dry shoot weight of infected *ago1-27* being significantly smaller than uninfected plants from 21DPI. The initial growth analysis data indicates that *ago1-27* does not exhibit a tolerance response when infected with clubroot.

Data from the growth analysis indicated that infection in *ago1*-27 proceeded in a similar manner to those lines examined in Chapter 2. Therefore, it was decided that microscopic examination would be carried out at 21DPI only. It was shown in the previous chapter that this is the key time-point in terms of the tolerance response exhibited by *ein5-1*. *ago1-27* was examined at this time point in order to establish whether any tolerance to infection could be seen at the cellular level.

Representative cross sections of infected and uninfected *ago1-27* 21DPI are shown in Figure 3.4. Infection in *ago1-27* appears to be at an advanced stage which would be expected from 21DPI onwards. There is extensive cell division and expansion across the hypocotyl. Secondary plasmodia are present and numerous, some of which are found in expanded cells. Cellular organisation has been disrupted. The VC has become disjointed and dispersed. Xylem formation in the centre of the hypocotyl has ceased while phloem formation appears to continue. There are several islands of xylem forming away from the central xylem vessels. Examination of cross sections from infected *ago1-27* hypocotyl did not indicate *ago1-27* was exhibiting a tolerance response when infected with *P. brassicae*.

3.3.1.2 The Impact of Infection on *hen1-5*

As has been reported previously, infection in *Arabidopsis* usually leads to a large gall forming on the hypocotyl and some galling on the root system. It was noted during this work that some *hen1-5* plants did not display a typical hypocotyl gall, but rather galls were restricted to the root system, see Figure 3.5.

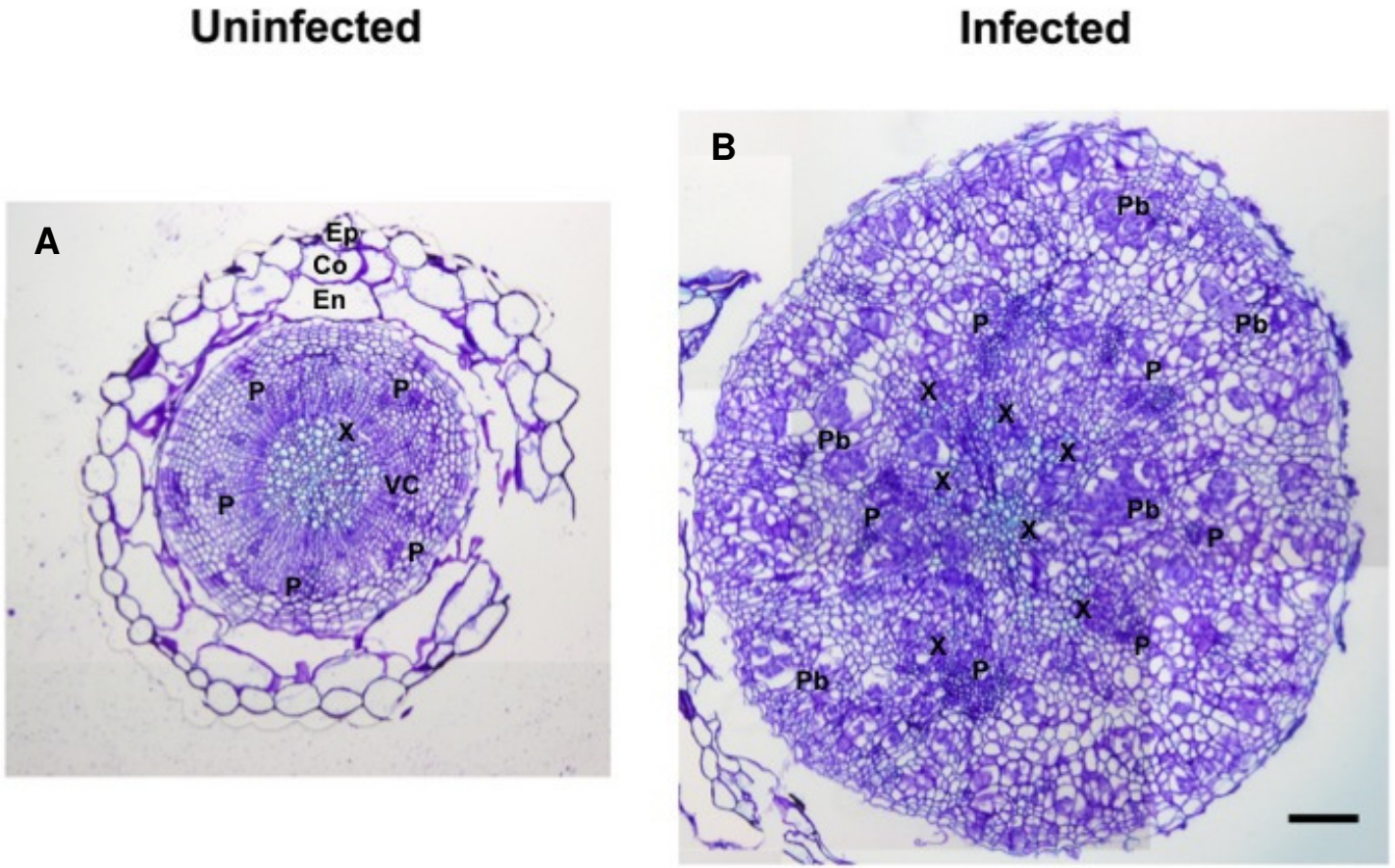

Figure 3.4. Alterations in *ago1-27* hypocotyls as a consequence of *P. brassicae* infection.

Cross sections of (**A**) uninfected and (**B**) infected hypocotyls 21DPI. X, xylem vessel; P, phloem; Pb, cells containing plasmodia; VC, vascular

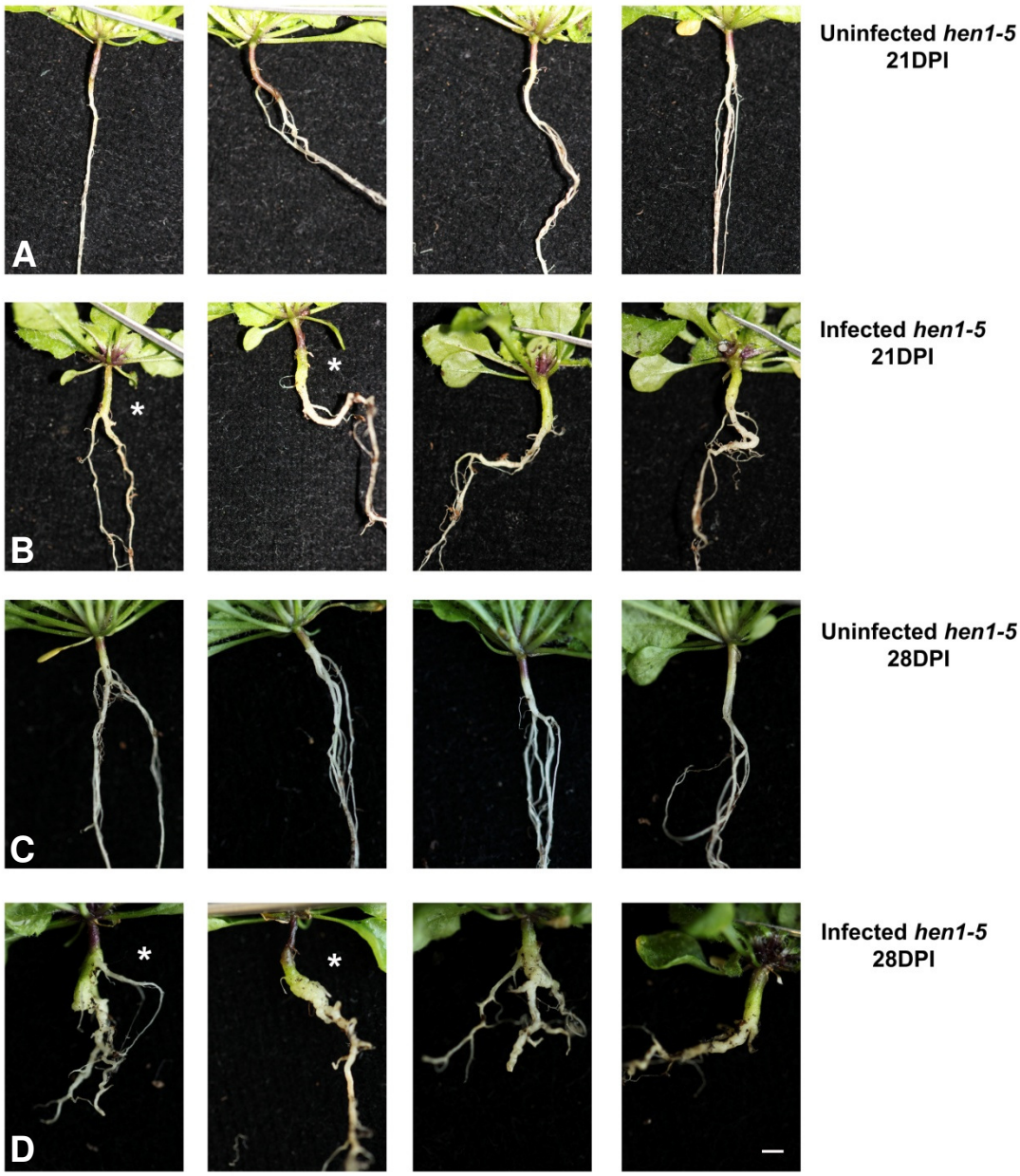

Figure 3.5. Hypocotyl/roots of uninfected and infected *hen1-5* 21 and 28DPI. Hypocotyl/roots of (**A**) uninfected *hen1-5* and (**B**) infected *hen1-5* plants 21DPI, (**C**) uninfected *hen1-5* and (**D**) infected *hen1-5* plants 28DPI. Four representative hypocotyl/roots are shown for each condition. * indicates those plants which have galls forming on the roots rather than on the hypocotyl/upper root. Scale bar = 2 mm.

The typical galls seen on *Arabidopsis* plants were termed type A galls, while galls restricted to the root system were termed type B galls. Differences in galls were seen at 21DPI but were even more apparent 28DPI. At 21DPI type B galls were seen in approximately 3 out of 10 plants examined, 5 out of 10 plants exhibited type A galls and the remaining plants seemed to be exhibiting an intermediate type gall. At 28DPI 4 out of 10 plants examined displayed type A galls, 4 out of 10 plants displayed type B galls and 2 out of 10 exhibited an intermediate gall.

The impact of infection on the growth of *hen1-5* plants can be seen in Figure 3.6. Despite the altered gall morphology, overall infected *hen1*-5 plants displayed a typical response to infection. An inhibition of shoot growth was seen in infected *hen1-5* plants, with both the rosette diameter and dry shoot weight of infected plants being significantly smaller than those of uninfected plants from 21DPI onwards. The dry root weight of infected *hen1-5* plants was significantly larger than uninfected plants from 14DPI, and by 28DPI was 3.5 times that of uninfected *hen1-5* plants. In line with this, the percentage of dry biomass allocated to the root/hypocotyl of infected *hen1-5* was significantly higher than that of uninfected plants from 14DPI. The percentage of biomass allocated to the hypocotyl/root of infected *hen1-5* continued to increase throughout the experiment, so that at 28DPI it was 15.4 %; 5.7 times that of uninfected *hen1-5*. There was a significant difference in the size of hypocotyls of uninfected and infected *hen1-5* plants 21DPI, with infected plants having hypocotyls which were 1.8 times wider than uninfected plants. At 28DPI hypocotyls of infected *hen1*-5 plants were larger than those of uninfected plants, however this was not found to be a significant difference; this is probably a consequence of the variability seen in the gall morphology at this time point.

In order to further investigate the differences in gall morphology, individual plots of the widths of hypocotyls and roots of uninfected and infected *hen1-5* plants were created, Figure 3.7. At both 21 and 28DPI the hypocotyl and root widths of uninfected *hen1-5* grouped tightly. The hypocotyl widths of infected plants however, were seen to separate into two distinct groups; those with larger hypocotyl width representing type A galls and those with smaller hypocotyls indicating type B galls. There was a slight overlap where those plants with intermediate gall morphologies lie. The root widths are reasonably tightly grouped at 21DPI but were seen to be spread at 28DPI. The data strongly suggests that a subset of *hen1-5* plants show altered gall morphology, compared to Col-0, when infected with clubroot. However, the data analysis did not strongly suggest any alterations in the impact of disease on *hen1-5* plants.

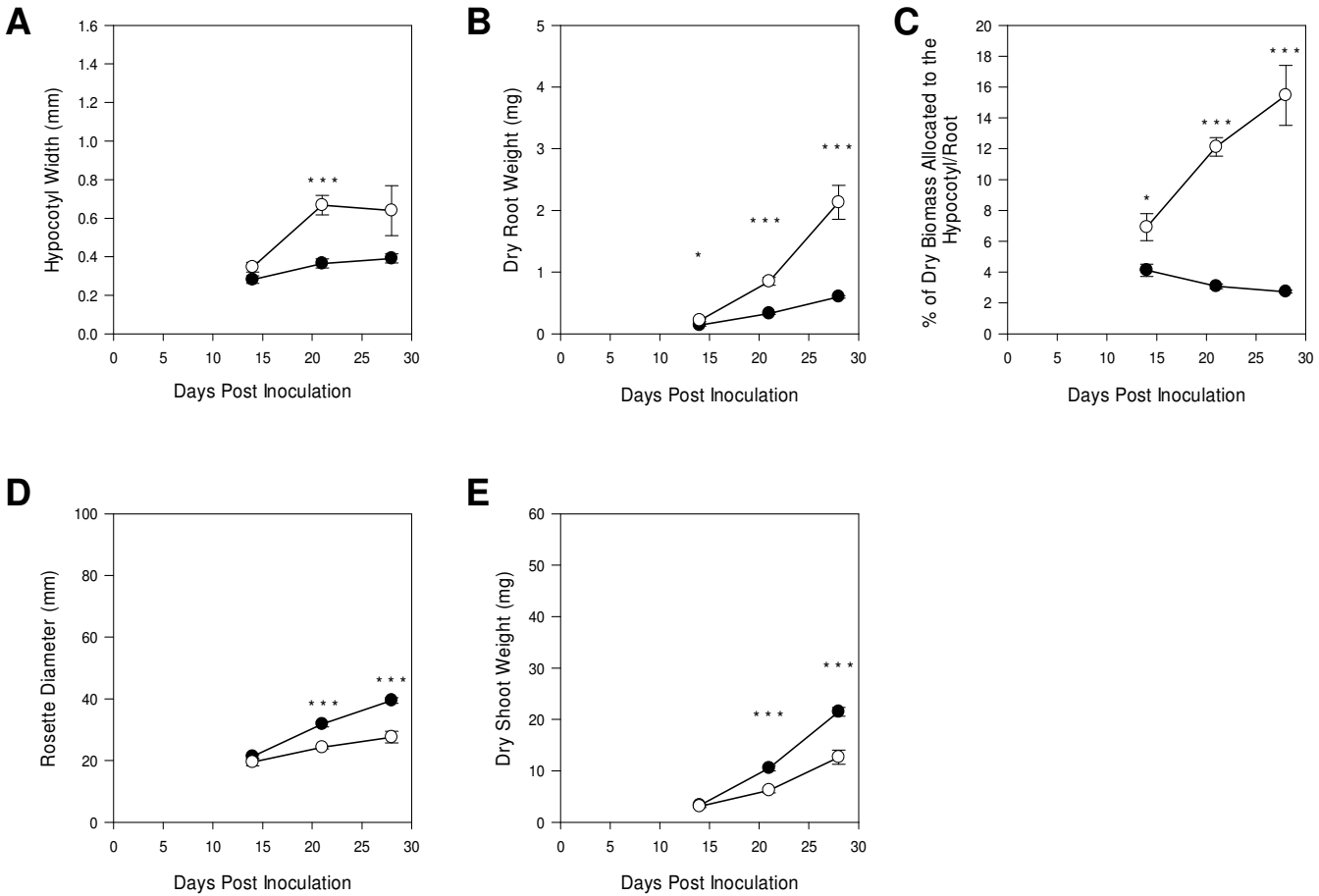

Figure 3.6. The impact of *P. brassicae* infection on the growth of the small RNA biogenesis mutant *hen1-5*.
The effect of *P. brassicae* infection on the (**A**) hypocotyl width (**B**) dry root weight (**C**) % dry biomass allocated to the hypocotyl/root (**D**) rosette diameter and (**E**) dry shoot weight of *hen1-5*. Uninfected controls (filled circles), *P. brassicae* infected plants (open circles). Results are means ± S.E. of 10 plants. (T-test *$p \leq 0.05$, ** $p \leq 0.01$, *** $p \leq 0.001$).

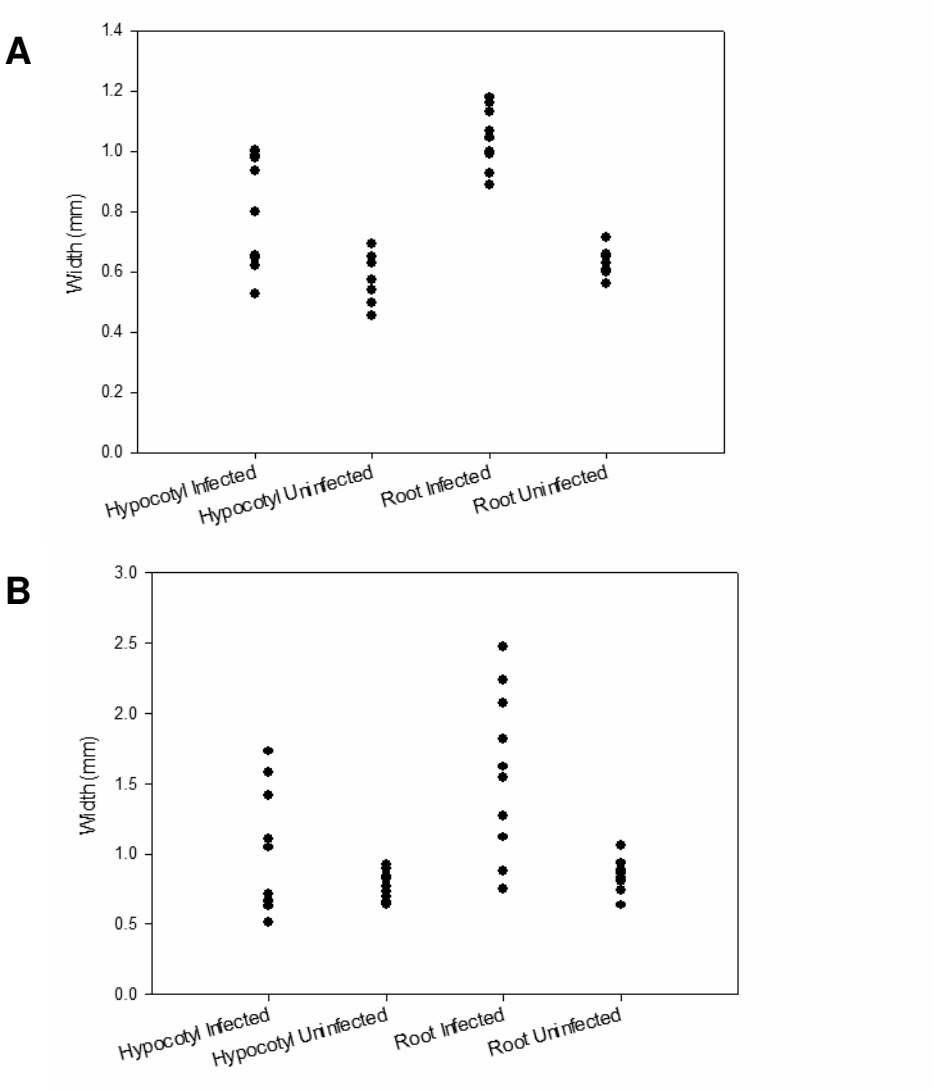

Figure 3.7 Hypocotyl and root widths of infected and uninfected *hen1-5* plants 21 and 28DPI.
The individual measurements of hypocotyl and root width from 10 uninfected and 10 infected *hen1-5* plants 21 (**A**) and 28DPI (**B**) are plotted. Widths were measured from photographs of galls, with the root width being measured at the widest point.

Growth analysis data alone is not a strong enough indicator of a plants response to clubroot infection. Therefore in order to further examine the altered gall morphology of *hen1-5*, cross sections were taken of hypocotyls/roots from plants displaying type A and B galls (Figures 3.8 and 3.9). In *hen1-5* plants displaying type A galls infection had proceeded to a level which would be expected 21DPI. Secondary plasmodia were numerous and present in cells across the hypocotyl. Cell division and expansion had occurred extensively. Some of the expanded cells were seen to contain plasmodia. There was a cessation of xylogenesis in the centre of the hypocotyl, while phloem production continued uninterrupted. Cellular organisation had been lost; the VC had become disjointed and xylem islands formed away from the central xylem vessels. In those *hen1-5* plants which did not display hypocotyl galls, disease was still present however, it was not advanced, see Figures 3.8.C and 3.9.B. A few cells appeared to contain secondary plasmodia, but they were not found right across the hypocotyl. They seemed to be mainly concentrated around the central xylem vessels. Disruption of the VC occurred in some places but it remained more intact than in type A plants. Little evidence of pathogen-induced cell expansion and division was seen. Few if any islands of xylem were noted. The disease progression appeared to be delayed in the hypocotyl of these *hen1-5* plants.

Cross sections through roots of *hen1-5* plants showed that at 21DPI plants with both type A and B galls were very heavily infected with secondary plasmodia (Figures 3.8 and 3.9). Extensive cell expansion and division had occurred but the latter was perhaps not as widespread in those plants with type B galls. This indicated that disease progression was slowed in plants with type B galls. A loss of organisation and differentiation was seen in both root examples. The VC had become disjointed and xylem formation in the centre of the root had ceased. Several islands of xylem were seen.

In order to examine how the disease progressed in *hen1-5* plants cross sections from the hypocotyls/roots of plants with both type A and B galls were taken 31DPI (Figures 3.10 and 3.11). In the hypocotyls of type A plants there was extensive cell division and expansion. Cellular organisation had been lost and the VC had become disrupted and disjointed. There were numerous islands of many xylem cells forming away from the central vessels and these appeared to be associated with many phloem cells. Secondary plasmodia were seen throughout the hypocotyl and some cells were seen to contain resting spores, the final life stage of *P. brassicae*. Infection was in a very advanced stage in these hypocotyls. Again in cross sections through type B galls, there appears to be a delay in the progression of the disease when compared to type A galls.

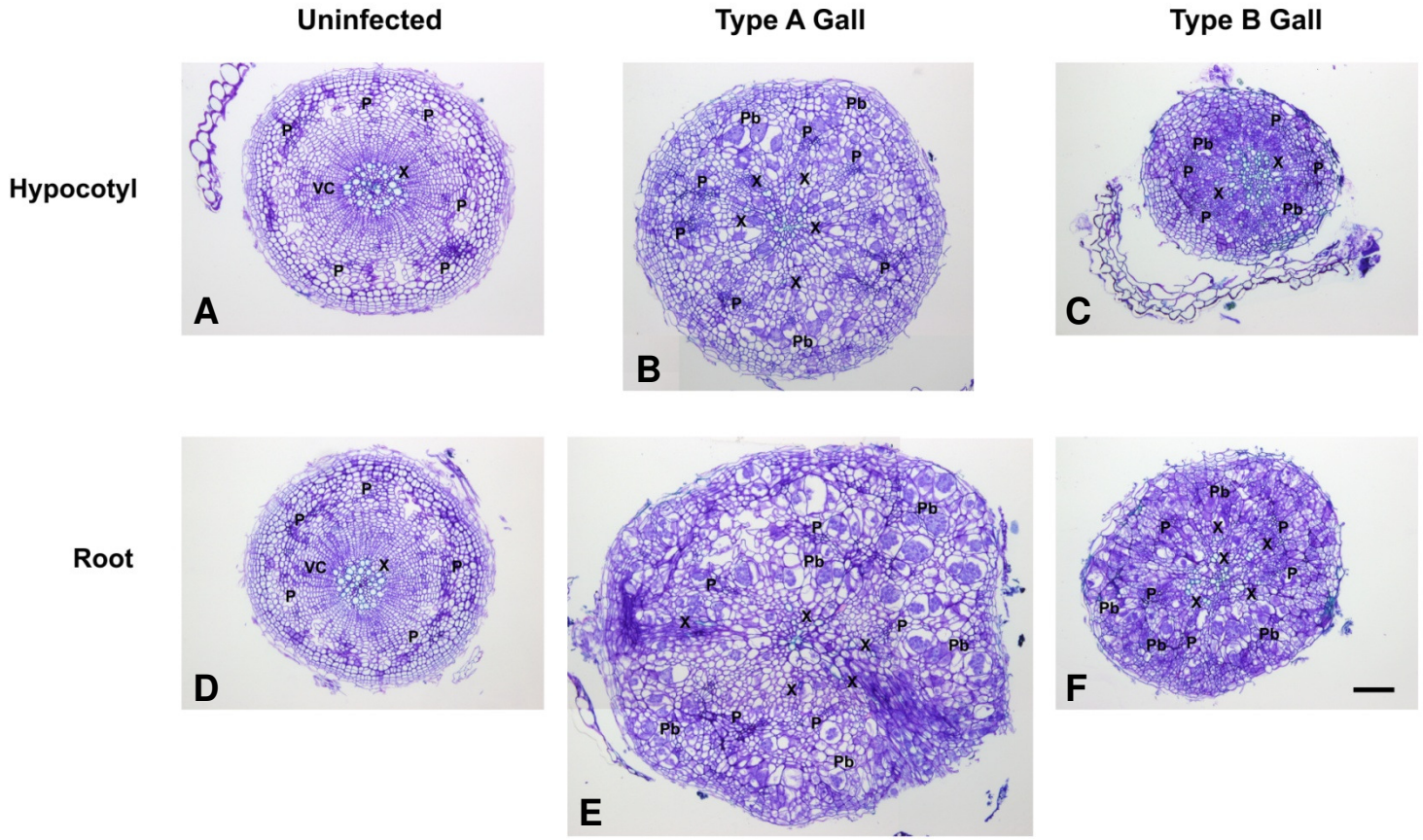

Figure 3.8. Alterations in *hen1-5* hypocotyls/roots as a consequence of *P. brassicae* infection 21DPI.
Cross sections of (**A**) uninfected and infected hypocotyls that had (**B**) galls on the hypocotyl/root and (**C**) galls on the root only, 21DPI. Corresponding cross sections from the roots of these plants 21DPI are shown in (**D**, **E** and **F**). X, xylem vessel; P, phloem; Pb, cells containing plasmodia; VC, vascular cambium. Scale bar = 100 µm

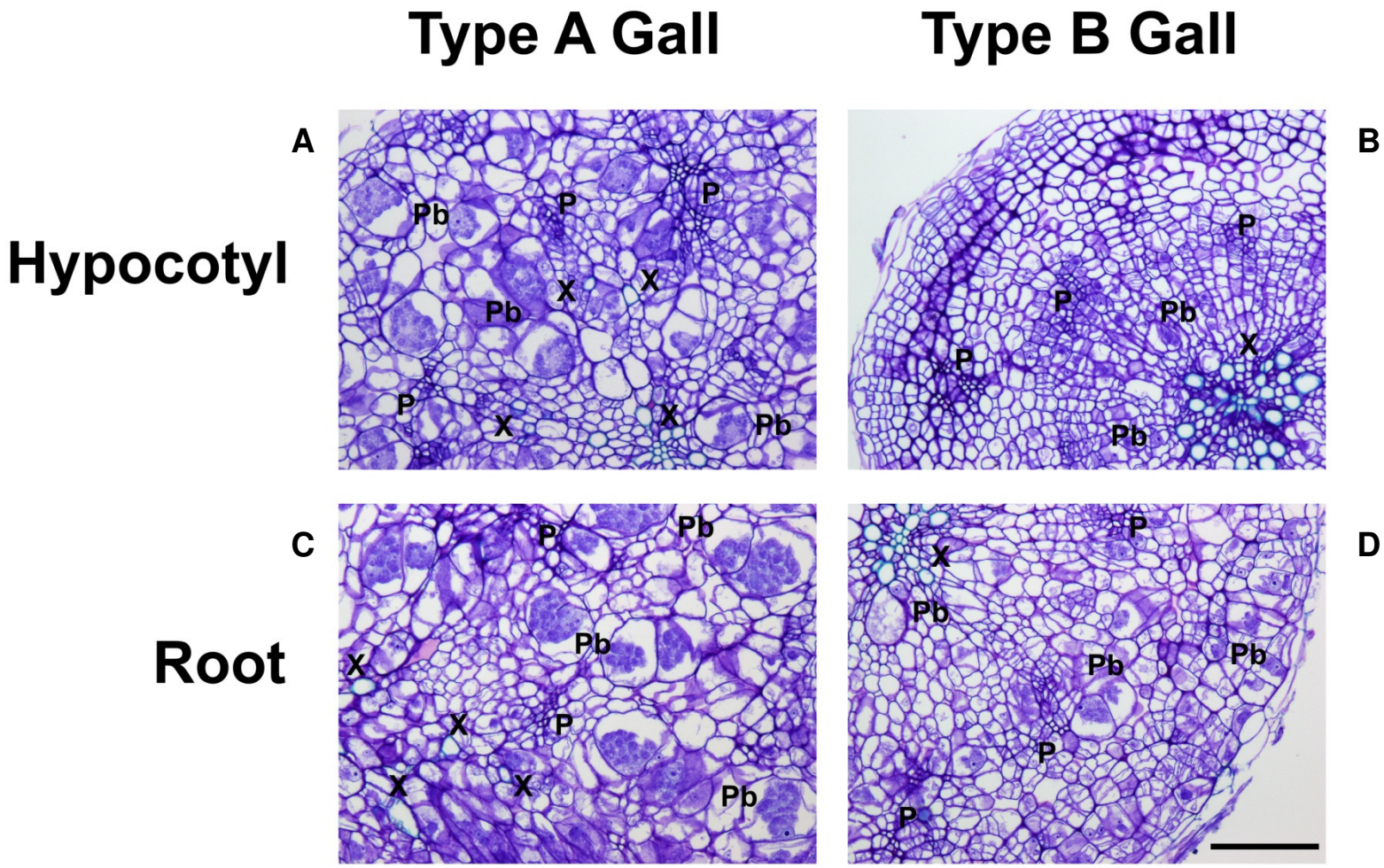

Figure 3.9. Changes occurring in *hen1-5* hypocotyl/roots as a consequence of *P. brassicae* infection 21DPI.
Cross sections through the hypocotyls of type A (**A**) and type B (**B**) galls and through roots of type A (**C**) and type B (**D**) galls from *hen1-5* plants 21DPI. X, xylem vessel; P, phloem; Pb, cells containing plasmodia; VC, vascular cambium. Scale bar = 100 µm.

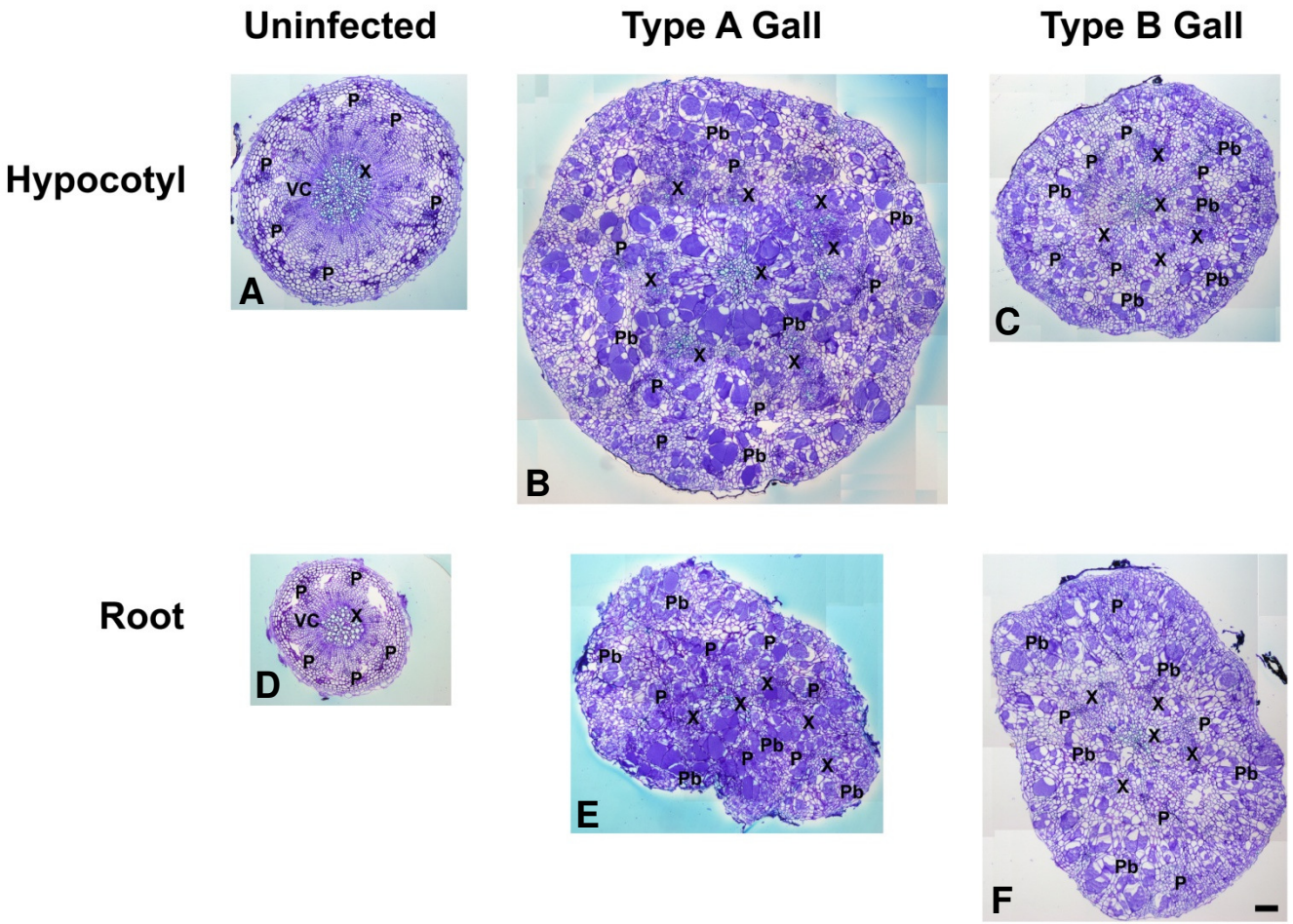

Figure 3.10. Alterations in *hen1-5* hypocotyls/roots as a consequence of *P. brassicae* infection 31DPI.
Cross sections of uninfected (**A**) and infected hypocotyls that had galls on the hypocotyl/root (**B**) and galls on the root only (**C**), 31DPI. Corresponding cross sections from the roots of these plants 31DPI are shown in (**D**, **E** and **F**). X, xylem vessel; P, phloem; Pb, cells containing plasmodia; VC, vascular cambium. Scale bar = 100 µm.

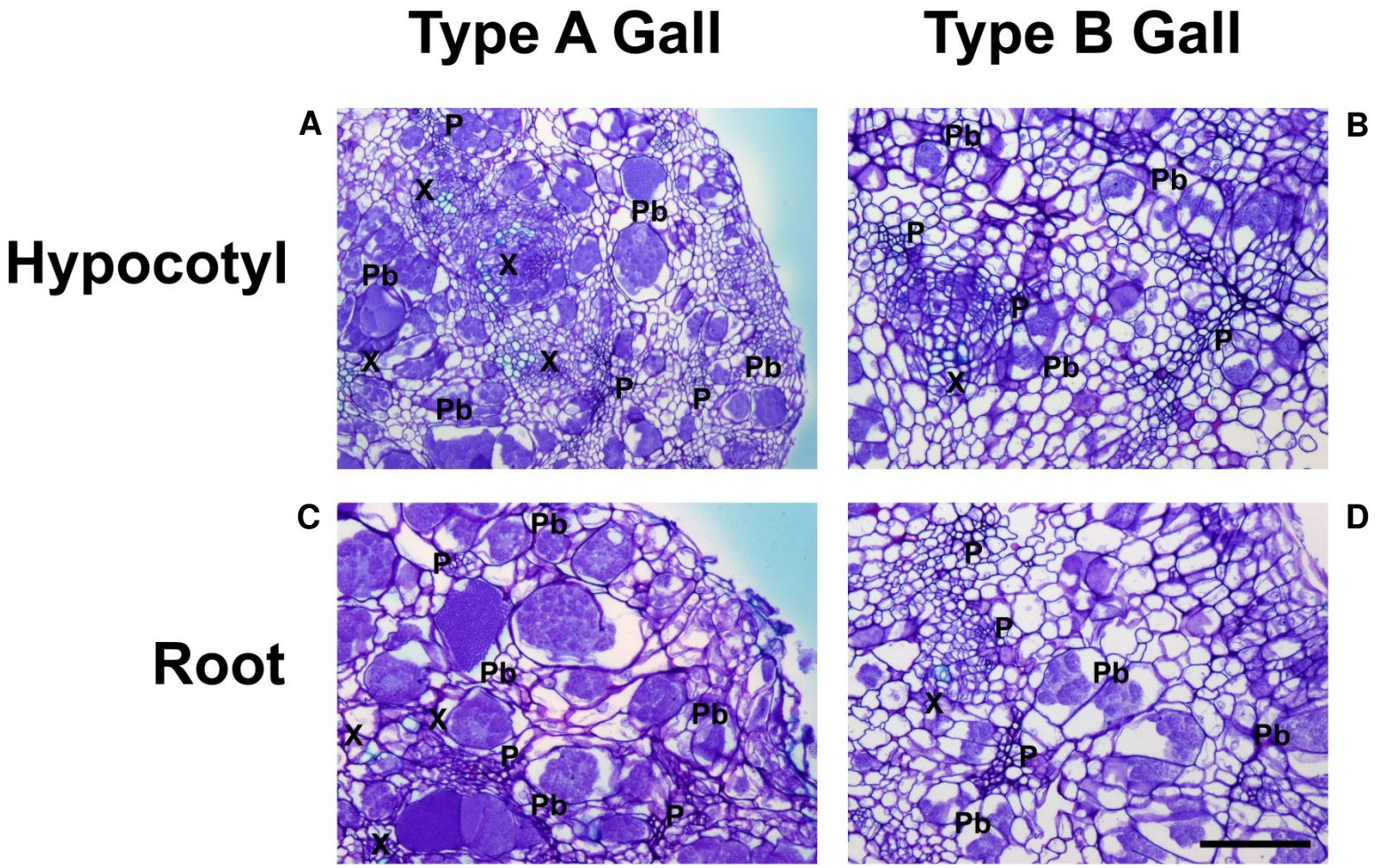

Figure 3.11. Changes occurring in *hen1-5* hypocotyl/roots as a consequence of *P. brassicae* infection 31DPI.
Cross sections through the hypocotyls of type A (**A**) and type B (**B**) galls and through roots of type A (**C**) and type B (**D**) galls from *hen1-5* plants 31DPI. X, xylem vessel; P, phloem; Pb, cells containing plasmodia; VC, vascular cambium. Scale bar = 100 µm.

Although *P. brassicae* induced cell division and expansion was seen, it was not to the extent seen in type A galls. Cell organisation was disrupted although again not to the level seen in type B galls and certainly not to a level which would be expected 31DPI. Type B hypocotyls were retaining some level of organisation. The VC was disjointed but remained organised in some areas. Secondary plasmodia were seen throughout the hypocotyl, but no resting spores were seen. Xylem can be seen forming in islands away from the central vessels, but not to the extent seen in type A hypocotyls. Phloem production had continued and phloem was widespread. Cross sections from the roots of type A and B galls paint a similar picture, the disease appears more advanced in type A galls compared to type B (Figures 3.10 and 3.11).

3.3.1.3 The Impact of Infection of *Ler* and *dcl1-9*

Representative hypocotyls of infected and uninfected *Ler* plants 21DPI can be seen in Figure 3.12. Infection in *Ler* led to swelling/galling of the hypocotyl/root 21DPI but not to the extent seen in *Arabidopsis* Col-0 lines. The impact of the disease on several growth parameters of *Ler* are shown in Figure 3.13. The hypocotyl width of infected plants was increased on infection, however at 21DPI it was not significantly different to that of uninfected *Ler* plants. The dry root weight of infected plants was significantly larger at 21DPI, being 2.9 times that of uninfected plants. The percentage of dry biomass allocated to the hypocotyl/root was also significantly different between infected and uninfected *Ler* 21DPI. Infected *Ler* plants had 5.9 percent of their biomass allocated to their hypocotyl/roots at this time point, which was 3.4 times the percent of biomass allocated by uninfected plants. Shoot development was detrimentally impacted by infection, with uninfected plants having significantly larger rosette diameters than infected plants 21DPI. Infected plants had a smaller dry shoot weight than uninfected plants, although the difference was not significant. The results suggest that infection in *Ler* is delayed compared with Col-0. This is in agreement with Malinowski *et al* who recently indicated that infection in *Ler* is delayed by approximately 10 days (2012).

Infection in *dcl1-9* plants appeared more advanced than observed in *Ler*. Large galls were formed on the hypocotyl/upper root of infected *dcl1-9* plants, see Figure 3.12. The impact of infection on *dcl1-9* growth can be seen in Figure 3.13. Infection impacted on the hypocotyl/roots of *dcl1*-9 as expected. The hypocotyl width, dry hypocotyl/root weight and percentage of biomass allocated to the hypocotyl/root all increased on infection. The hypocotyl width of infected *dcl1-9* was significantly larger than that of uninfected plants 21DPI, being 1.9 times that of uninfected plants.

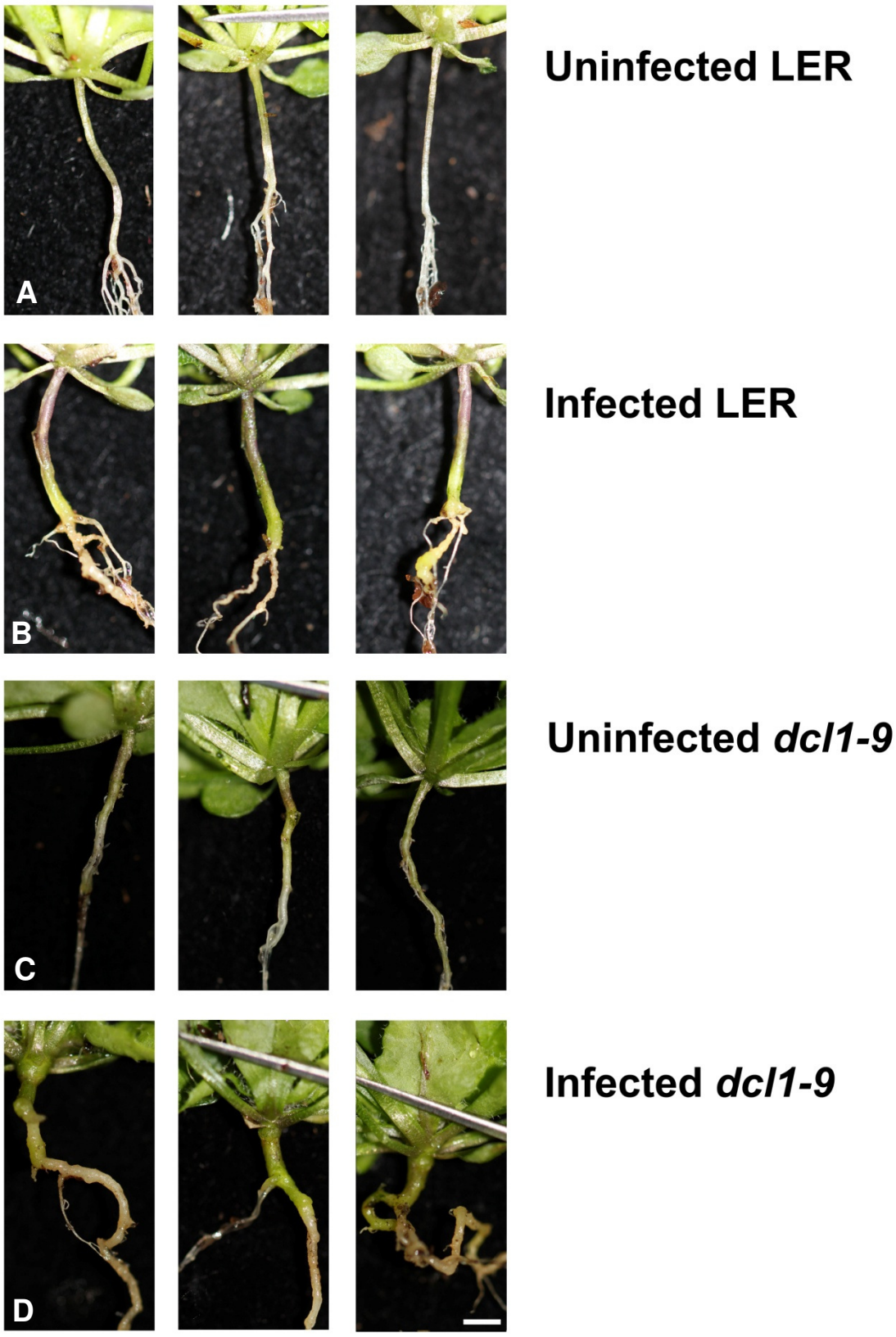

Figure 3.12. Hypocotyl/roots of uninfected and infected *Ler* and *dcl1-9* 21DPI. Hypocotyl/roots of (**A**) uninfected *Ler*, (**B**) infected *Ler*, (**C**) uninfected *dcl1-9* and (**D**) infected *dcl1-9* plants 21DPI. Three representative hypocotyl/roots are shown for each condition. Scale bar = 2 mm.

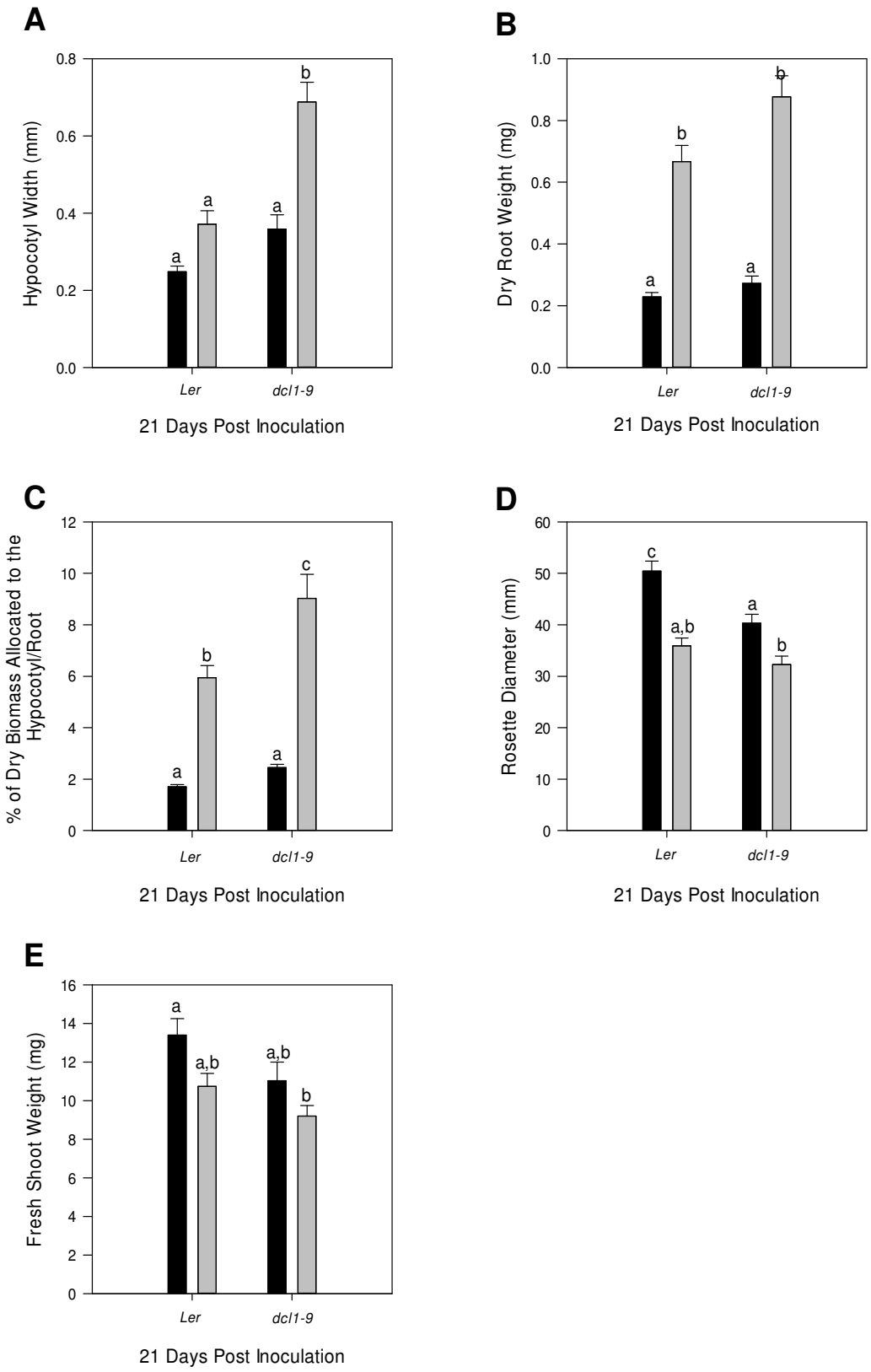

Figure 3.13. Impact of clubroot infection on the hypocotyl/root of *A. thaliana Ler* and *dcl1-9*.

The effect of *P. brassicae* infection on (**A**) hypocotyl width, (**B**) the dry hypocotyl/root weight, (**C**) % dry biomass allocated to the hypocotyl/root, (**D**) rosette diameter and (**E**) dry shoot weight of *A. thaliana*. Uninfected controls (black bars), *P. brassicae* infected plants (grey bars). Results are means ± S.E. of 10 plants. Data were (**B**) natural log and (**C**) arcsine square root transformed prior to statistical analysis. Bars showing same letter are not significantly different according to a Tukey multi-comparison test.

The dry root weight of infected *dcl1-9* 21DPI was also significantly larger than uninfected plants at 3.2 times that of uninfected *dcl1-9*. The percentage of biomass allocated hypocotyl/root 21DPI was again significantly higher in infected plants, being 9 % compared with 2.45 % for uninfected plants. The development of the shoot was also affected as expected, with uninfected *dcl1-9* plants having a significantly larger rosette diameter than infected plants. While the dry shoot weight of infected plants was smaller than that of uninfected plants, the difference was not significant. Data from the growth analysis did not indicate that *dcl1-9* displayed a tolerance response when infected with clubroot. The data of Malinowski *et al* and the data here suggest that as *dcl1-9* is in the *Ler* background effectively an earlier time point was examined compared to lines in a Col-0 background (2012). Still, there is no sign of a delay in infection in *dcl1-9* with the impact of infection being comparable to that of Col-0. Therefore the data strongly suggests that *dcl1-9* does not exhibit tolerance to clubroot infection.

As noted previously, it can be seen from cross sections of infected *Ler* hypocotyls 21DPI that infection in these plants is delayed, Figure 3.14. Plasmodia were seen in the hypocotyl but were mainly positioned around the central xylem cells, with few cells across the hypocotyl containing plasmodia. Cell division as a consequence of infection appeared to have occurred, although there was little *P. brassicae* induced cell expansion. Those cells which were expanded were found around the vicinity of the central xylem vessels. Cellular organisation seemed to be fairly well maintained. There were no islands of xylem forming away from the central xylem.

In contrast with infection in *Ler*, cross sections through infected *dcl1-9* hypocotyls show that at 21DPI infection is well advanced, Figure 3.14. The extent of infection did appear to be variable in cross sections of *dcl1-9* but was always at a much advanced stage than in *Ler* plants. Both cell division and expansion had occurred extensively. The cellular organisation of the hypocotyl was disrupted, the VC had become completely disjointed and central xylem formation had ceased. Numerous islands of xylem had formed across the hypocotyl. Phloem production was still occurring throughout the hypocotyl. Secondary plasmodia were numerous and found throughout the hypocotyl. These data in combination with the growth analysis data do not indicate that *dcl1-9* is tolerant to clubroot infection.

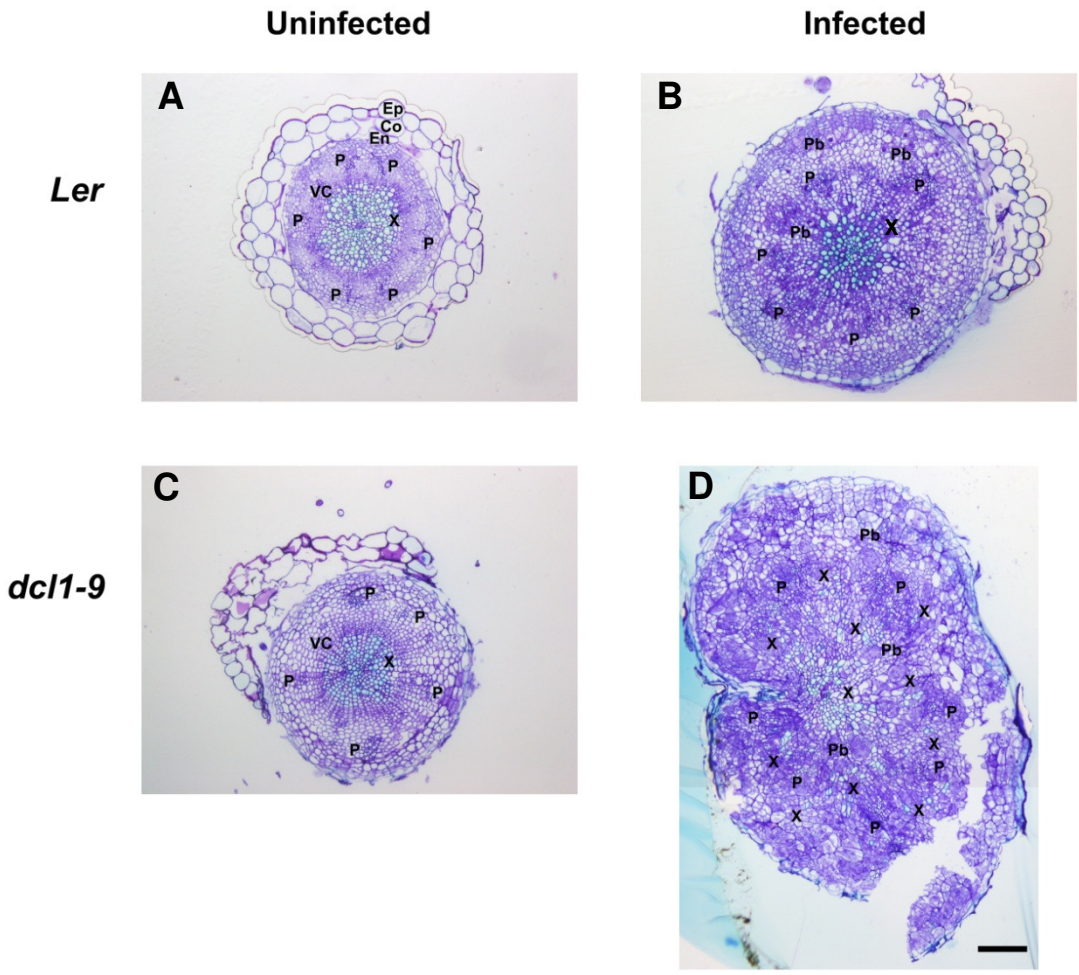

Figure 3.14. Alterations in *Ler* and *dcl1-9* hypocotyls/roots as a consequence of *P. brassicae* infection 21DPI.
Cross sections of (**A**) uninfected *Ler*, (**B**) infected *Ler* and (**C**) uninfected *dcl1-9*, (**D**) infected *dcl1-9* hypocotyls 21DPI. X, xylem vessel; P, phloem; Pb, cells containing plasmodia; VC, vascular cambium. Scale bar = 100 µm.

3.4 Discussion

In Chapter 2 it was established that the weak ethylene insensitive mutant *ein5-1* was displaying a tolerance response when infected with clubroot. With the use of *ein2-1*, a strong ethylene insensitive mutant, it was established that ethylene signalling did not play a critical role during infection. This chapter looked to investigate alternative explanations for the tolerance response of *ein5-1*. As EIN5/XRN4 has been shown to be involved in miRNA-induced silencing, it was hypothesised that perturbations to this pathway may result in tolerance to clubroot infection. Three miRNA biogenesis mutants were screened for their response to clubroot infection; in order to examine whether the tolerance response of *ein5-1* was a consequence of the role EIN5 plays in the miRNA-mediated mRNA decay pathway. A growth analysis and microscopic examination of the three miRNA biogenesis mutants was carried out to investigate the impact of disease on these lines.

The growth analysis data from *ago1-27* plants showed signs of gall formation from 14DPI. Galls were present from 21DPI onwards when all the parameters of growth measured were significantly different to those of uninfected plants. The growth analysis suggested that gall formation was in no way delayed in infected *ago1-27* plants. Cross sections through infected *ago1-27* plants at 21DPI showed that extensive pathogen induced cell division and expansion had taken place. Secondary plasmodia were numerous and seen throughout the hypocotyl. The VC had become disrupted and central xylem formation had ceased. Islands of xylem were seen to form away from the central vessels, while phloem production appeared unaffected. Together these results show that infection in *ago1-27* was approximate to that in Col-0: gall formation was not delayed and no tolerance response to the disease was displayed.

Examination of infection in *dcl1-9* provided no evidence to suggest that infection was delayed in these plants. During the course of this work it was reported that the disease progression in the *Ler* background is delayed by 10 days (Malinowski et al. 2012). A delay in disease progression was also seen here. The 21DPI time point was initially selected for investigation based on the data from Chapter 2 which showed this was the point at which differences between *ein5-1* and other Col-0 lines became apparent. As *dcl1-9* is in the *Ler* background 21DPI was in effect an earlier time point. Even so disease in *dcl1-9* was well advanced at this stage, although the cross-sections did show an amount of variability in terms of the extent of the disease. Therefore, *dcl1-9* certainly does not exhibit a tolerance response when infected with clubroot, and there is no delay in gall formation in these plants.

3.4.1 How is the Disease Phenotype Altered in *hen1-5* Plants?

dcl1-9 and *ago1-27* did not display a tolerance response when infected with clubroot. *hen1-5* plants however, did display an altered disease phenotype when infected with clubroot. At both 21 and 28DPI a subset of the infected *hen1-5* plants (approximately half) displayed galls that were restricted to the root system as opposed to being localised mainly in the hypocotyl. Growth analysis data did not indicate that *hen1-5* was delayed in gall formation or was exhibiting a tolerance response. However, as detailed in Chapter 2 it is always important that measurements of gall size are used in conjunction with microscopic analysis to gain an effective insight into what impact the disease is having on the plant. While gall size gives a measure of the end point of the disease, microscopic analysis allows the changes occurring at the cellular level that lead to gall formation to be examined.

Microscopic analysis of infected *hen1-5* plants revealed that those plants with altered gall morphology (type B galls) also had a quite different morphology at the cellular level when compared to wild-type and plants with 'normal' type A galls. At 21DPI these differences were seen both in the impact of the disease on the plant and in terms of the pathogen development and movement. The disease did not appear to be affecting the plant as would be expected 21DPI and pathogen development and movement were delayed. At 31DPI the plants with type B galls still appeared to maintain cellular organisation above the level expected although the disease had progressed significantly

This maintenance of cellular organisation and apparent delay in infection progress seen in *hen1-5* plants with type B galls was certainly reminiscent of the phenotypes seen in infected *ein5-1* plants. Interestingly, even those *hen1-5* plants displaying 'normal' galls did appear to retain a level of cellular organisation which would not be seen in wild-type plants at the same time points. This would indicate that disease in both *hen1-5* and *ein5-1* is occurring in a very similar manner. Based on the evidence from Chapters 2 and 3, two hypothesises can be formed. One is that *hen1-5* and *ein5-1* display similar phenotypes because both HEN1 and EIN5 play similar roles in infection. When these proteins are absent it leads to a similar disease phenotype with infection being delayed/tolerated by the plant to some extent. This first hypothesis strongly supports the notion that the delay in disease seen in *ein5-1* is a consequence of perturbations in RNA-induced silencing, as both HEN1 and EIN5 are involved in these pathways. The second hypothesis is that the disease phenotypes are a consequence

of differing roles played by HEN1 and EIN5 during infection and that the similarities in these phenotypes are simply a coincidence.

3.4.2 Why do *hen1*-5 and *ein5-1* Exhibit Tolerance to Clubroot Infection?

EIN5/XRN4 has been shown to be involved in both miRNA-mediated gene silencing, degrading the 3' products produced via miRNA-guided mRNA cleavage and siRNA-mediated gene silencing, degrading uncapped mRNAs preventing them from becoming templates for siRNAs (Gazzani et al. 2004; Souret et al. 2004). Methylation of newly synthesised and processed miRNAs and siRNAs by HEN1, to prevent their degradation, has been shown to be a universal step in all small RNA biogenesis pathways (Li et al. 2005; Yu et al. 2005; Yang et al. 2006). Thus both HEN1 and EIN5/XRN4 are involved in miRNA and siRNA-induced gene silencing.

The differing phenotypes of *dcl1-9* and *ago1-27* compared with *hen1-5* could therefore be a consequence of DCL1 and AGO1 mainly being involved in the miRNA silencing pathway, while HEN1 and EIN5/XRN4 are implicated in both the miRNA and siRNA silencing pathways. A phenotype is possibly seen in *hen1-5* and *ein5-1* as perturbations in the siRNA-silencing pathway may lead to tolerance to clubroot infection. HEN1 plays the same role in siRNA biogenesis as it does in miRNA biogenesis (Li et al. 2005; Yang et al. 2006). Loss of HEN1 leads to a reduction in silencing. Loss of XRN4 however, has been shown to lead to an increase in siRNA-induced silencing. ssRNAs that would normally be degraded by EIN5/XRN4 are instead targets for RDR which uses them to synthesise dsRNAs, which are potential templates for siRNA biogenesis (Gazzani et al. 2004). In the siRNA-silencing pathway loss of HEN1 and EIN5/XRN4 does not result in similar consequences leading to opposing phenotypes, therefore it seems unlikely that interruptions to this pathway result in a tolerance to clubroot infection.

What seems more likely is that a phenotype is seen in *hen1-5* and *ein5*-1 because of their role in miRNA-induced silencing. Loss of HEN1 leads to a reduction in miRNA-induced silencing while loss of EIN5/XRN4 leads to an accumulation of miRNA-targeted mRNA 3' ends, therefore silencing is not carried through to absolute completion (Souret et al. 2004). Mutations in both HEN1 and EIN5/XRN4 alter the pathway in a similar direction, having a negative impact on silencing. This does not however, explain why a similar phenotype was not seen in *ago1-27* or *dcl1-9* as mutations in AGO1 and DCL1 also alter the miRNA pathway in a similar direction. A possible explanation for this is the redundancy that is seen in the AGO and DCL

proteins; *Arabidopsis* encodes 10 AGO and 4DCL proteins (Schauer et al. 2002; Mallory and Vaucheret 2010a). Is a phenotype seen when *hen1-5* and *ein5-1* are infected because they don't have homologs in miRNA biogenesis but no phenotype is seen when *ago1-27* and *dcl1-9* are infected because they do have homologs? It may be that when AGO1 and DCL1 are absent another AGO or DCL protein compensates for this deficiency, alternatively it could be that specific AGO and DCL protein act with specific miRNAs and it is these miRNAs that are important during clubroot infection. There is no reason why these two explanations need to be mutually exclusive. Evidence in the literature indicates that an alternative DCL to DCL1 may be involved in miRNA biogenesis (Sunkar and Zhu 2004). For example, DCL4 has been shown to be responsible for the generation of selected miRNAs (Rajagopalan et al. 2006). In addition DCL3 has been shown to process a family of long-miRNAs from *MIR* genes (Vazquez et al. 2008). The authors also showed that DCL redundancy does play a role in miRNA biogenesis (Vazquez et al. 2008). Redundancy has also been seen with AGO proteins with AGO5 being assumed to carry out similar functions to AGO1 (Thieme *et al*, 2012). Also AGO1 and AGO2 have shown to act redundantly in the regulation of some miRNAs (Maunoury and Vaucheret 2011) AGO3 has a high sequence similarity to AGO2 and they are proposed to carry out similar functions (Thieme *et al*, 2012). Therefore, it seems reasonable to suggest that the redundancy of DCL and AGO may be the reason why a phenotype is not seen in the DCL1 and AGO1 mutants infected with clubroot.

In order to further investigate whether redundancy of the AGO and DCL proteins is the reason why a phenotype is seen in *hen1*-5 plants but not *ago1-27* or *dcl1-9,* a large scale screen could be carried out to investigate the impact of clubroot infection on the other *ago* and *dcl* mutants. In addition other proteins involved in miRNA biogenesis, which were not examined here, such as HASTY, SERRATE and HYPONASTIC LEAVES 1 could also being examined to see whether mutations in these genes lead to some level of tolerance to infection. If a response similar to that seen in *hen1-5* or *ein5-1* was seen in these other miRNA biogenesis mutants it would add further support to the hypothesis that miRNAs play a role in clubroot infection and disruption of their biogenesis and perturbations to their activities leads to tolerance to the disease.

3.4.3 Has the "Type B" Gall Morphology Been Seen Before?

Type B galls seen on a subset of *hen1-5* plants have been recorded previously in an unpublished screen of auxin mutants (Penny-Evans 2000). The gain of function mutant *axr2* was shown to present this gall morphology, although it was found to be

susceptible to clubroot infection (Penny-Evans 2000). *axr2* displays a dwarfed phenotype and cellular examination indicated this was a consequence of defects in cell elongation and to a lesser extent cell number (Timpte et al. 1992). Penny-Evans suggested this as a possible explanation for the altered gall morphology of *axr2* (2000).

hen1 mutants also display a dwarfed phenotype. Cells in the leaves and petals were found to be smaller than in wild-type plants, which led to the suggestion that *HEN1* is a promoter of cell expansion (Chen et al. 2002). The defect in cell expansion could account for the similarities in gall morphology between *axr2* and *hen1-5*. During clubroot a gall is formed as a consequence of cell division and expansion. Cell division has been shown to play a large role during infection (Malinowski et al. 2012). When cell division was blocked in infected plants smaller galls were formed. Following microscopic examination the plants were found to be heavily infected with large expanded cells containing plasmodia which were able to complete their life cycle forming viable spores. This indicates that if cell division and expansion do not occur concurrently a smaller gall will be formed; this could also be the case with both *hen1-5* and *axr2* plants if cell division but not cell expansion is taking place. As there was no microscopic analysis of the infected *axr2* plants comparisons with this work become difficult. No strong conclusions about the nature of *hen1-5* disease phenotype in contrast to that of *axr2* can be drawn. Targeting cell expansion could be a possible strategy to reduce gall formation in infected plants, but this would need further exploration. This again highlights the need for a multi-faceted approach and a standard screen when analysing the impact of infection on a plant, so that cross-study comparisons can be easily made.

In one clubroot study, invertase was found to be up-regulated during infection (Siemens et al. 2006). They expressed an invertase inhibitor under the control of a root-specific promoter in *Arabidopsis* plants which were then infected (Siemens et al. 2011). Those lines over-expressing an invertase inhibitor root-specifically were shown to have altered gall morphology. Galls were seen in the hypocotyl as normal but were reduced in the root system. The work indicates that changes in gall morphology can arise as a consequence of altered expression patterns of key genes. Therefore the lack of gall in the hypocotyl of *hen1-5* could be due to differential expression in the hypocotyl and root. It is known however, that Hen1 is expressed throughout the plant (Chen et al. 2002). It could be that one or more of HEN1's targets are expressed tissue specifically which could account for the altered gall morphology we seen in these plants.

3.4.4 Why is Infection Delayed in *ein5-1* and *hen1-5* Plants?

The data gathered thus far, in Chapters 2 and 3, does not point to a clear reason to why the impact of clubroot on *ein5-1* and *hen1-5* is less than on wild-type plants and other lines investigated. Pathogen movement and development appeared delayed in both these lines. The impact on the plant also appears delayed. The onset of pathogen induced cell expansion and division is delayed and cellular organisation is maintained for much longer than expected. The overarching hypothesis of this work is that the pathogen acts to subvert the normal developmental processes of the plant and uses these for its own means. Specifically the pathogen is hypothesised to use the process of secondary thickening in order to cause disease within the plant. This hypothesis is supported by work of Malinowski *et al* (2012). It is possible that the delay in disease seen in these two lines could be a consequence of the host maintaining control over its own development processes for a longer period than normally seen during infection. Or that these lines in some way cause a delay in either pathogen movement or development. Of course these two theories do not have to be mutually exclusive.

It is known that the presence of secondary plasmodia is associated with the symptoms of clubroot disease: mass cell division and expansion leading to gall formation (Ingram and Tommerup, 1972). Therefore, the response of *ein5-1* and *hen1-5* could possibly be a consequence of delays in pathogen development. If the onset of secondary plasmodia formation is delayed then secondary plasmodia induced cell division and expansion would also be delayed, meaning there would be a reduced impact on the plant. In *ein5-1* and *hen1-5* a reduction in the levels of pathogen induced cell division and expansion is seen, so it is possible that these plants are tolerant because for some reason plasmodia development is slowed. One possible way to begin to unravel this would be to make use of work that looked to study the expression of several *P. brassicae* genes over the course of infection in order to find molecular markers for the distinct developmental stages of *P. brassicae*'s lifecycle (Siemens et al. 2009). For example genes were shown to be expressed over the whole infection process, some were associated with the later stages of the disease and another gene was shown to be expressed during resting spore formation (Ando et al. 2006). The authors themselves highlighted a use for pathogen gene expression as a further measure of gall development, to be used in conjunction with other measures of disease (Siemens et al. 2009). In the case of *ein5-1* and *hen1-5* it could be used to detect changes in pathogen development compared with that in wild-type plants and could possibly lead to some insight as to whether pathogen development is slowed in these lines.

Although *hen1-5* does present some level of delayed response to clubroot infection, the response is a variable one. It is not always seen in infected plants. It is possible therefore, that the reason behind the phenotype seen in *hen1-5* is due to an effect on the rate of some process involved in the disease. For example, the loss of HEN1 could lead to the rate of some unknown process being either slowed or quickened which then in turn acts negatively on the progression of the disease and pathogen. The phenotype seen in *hen1-5* infected plants does not seem to be a consequence of a process simply being switched on or off completely.

3.5. Conclusion

In conclusion, when examined for their response to clubroot infection two miRNA biogenesis mutants *ago1-27* and *dcl1-9* did not display a tolerance response. Infection was not delayed in these plants in contrast with infection in *ein5-1*. However, when *hen1-5* was examined it did present an altered disease phenotype in terms of gall morphology. A subset of infected plants had galls which were restricted to the root system as opposed to the hypocotyl. Growth analysis of these plants did not indicate that disease was slowed in these plants. Microscopic analysis revealed that the cellular organisation of these plants was maintained much more than would be expected at 21DPI, even in those plants with 'normal' gall morphology. Those plants with altered gall morphology had maintained cellular organisation, showed little disease induced cell division and expansion and a delay in pathogen movement and development. This phenotype was reminiscent of that seen in *ein5-1* although not quite to the same extent. These results indicated that both *hen1-5* and *ein5-1* are responding in a similar manner to infection, suggesting that they are involved in similar pathways which are important during clubroot infection. Both HEN1 and EIN5 are involved in miRNA-induced gene silencing and their roles in this pathway both have a similar impact on gene silencing. As the disease phenotypes of both *ein5-1* and *hen1-5* are comparable, the evidence seems likely to maintain and add evidence to support the hypothesis that *ein5-1* is tolerant to clubroot infection as a consequence of perturbations in miRNA-induced gene silencing.

Both Chapter 2 and 3 have used a directed approach to investigate the role of EIN5 in infection, looking specifically at those genes which are known to work with EIN5/XRN4 to carry out its functions. This approach has successfully yielded some clues as the role played by EIN5 during clubroot infection, ruling out a role for ethylene signalling and indicating a possible role for miRNA-induced gene silencing. A less directed approach i.e. gene expression analysis will be discussed in the next chapter in the

hope of building on the work of the previous two chapters and allowing further understanding of the role played by EIN5/XRN4 in infection and the reasoning behind the tolerance response displayed by *ein5-1*.

Chapter 4: Microarray Analysis of *ein5-1* and Col-0

4.1 Introduction

The work reported in Chapters 2 and 3 focussed on the use of a targeted approach to understanding clubroot infection in *Arabidopsis*. Mutant *Arabidopsis* lines were screened for their response to clubroot infection. Firstly two ethylene signalling mutants (*ein2-1* and *ein5-1*) were screened in order to verify and characterise the tolerance response exhibited by *ein5-1* plants and to investigate the role of ethylene during infection with the use of *ein2-1*. Chapter 3 looked to build on the previous chapter by exploring the response of several miRNA biogenesis mutants (*ago1-27*, *dcl1-9* and *hen1-5*) to infection, as EIN5/XRN4 has been shown to be involved in miRNA-mediated gene silencing. The results from Chapter 3 suggested that miRNA-mediated gene silencing may play a role during clubroot infection.

Using a targeted approach here has proved to be useful in examining tolerance to clubroot infection; identifying mutated genes which lead to altered response to infection. The genes investigated are based on circumstantial evidence which suggests they may be important during infection. However, as it is a directed approach it could lead to some genes which may be playing a role in clubroot disease being overlooked. A targeted approach does not give an overview of alterations in the transcriptome as a consequence of infection. Therefore this chapter looked to use a non-targeted approach to explore the role of EIN5 during infection, using microarray analysis to examine global changes in gene expression that occur as a consequence of infection.

Microarray analysis allows the measurement of the expression levels of thousands of genes in a single experiment. The array used here was an Affymetrix GeneChip®. Briefly, RNA is extracted from samples usually a control sample and an experimental sample. This is then used to create cDNA using reverse transcriptase and then biotin-labelled cRNA via *in vitro* transcription. The array contains probes, short oligonucleotide sequences, which are complementary to a small section of a specific gene; there are multiple different probes on the chip representing each gene. The fragmented cRNA is hybridised to the array, and binds to complementary probes on the chip. Un-bound cRNA is washed from the array and a fluorescent dye, phycorerythrin, bound to streptavidin is added to the array which stains the bound cRNA by binding to the biotin. The array is then “read” using a laser scanner. An expression value for each probe is produced, which correlates to gene expression. The higher the expression of a gene the more cRNA will be bound, thus more dye will be present giving a more

intense signal. The gene expression data from the control and experimental sample can then be compared in order to identify genes which are differentially expressed between the two samples. The Affymetrix microarray procedure is summarised in Figure 4.1.

The specific microarray chip used here was the GeneChip® Arabidopsis Gene 1.0 ST Array (Affymetrix Inc., USA). GeneChip® Gene 1.0 ST Arrays provide whole transcriptome coverage for selected model and applied research organisms, based on the most recent genomic annotation. Probes (25-mer oligonucleotides) on the chip cover the whole of the transcript as opposed to just the 3' end of the transcript offered by other arrays. There are up to 26 unique probes per transcript. The Arabidopsis Gene 1.0 ST Array is based on The Arabidopsis Information Resources' (http://www.arabidopsis.org) most recent annotation of the Arabidopsis genome, TAIR10, and covers 28,501 genes.

To date there have been only two microarray analyses carried out during clubroot infection of *A. thaliana* (Siemens et al. 2006; Agarwal et al. 2011). Both studies analysed changes in gene expression during infection only in wild-type plants. Agarwal *et al* examined changes in gene expression during the primary infection stage: 4, 7 and 10DPI (2011). Siemens *et al* examined gene expression at two time points; pre- (10DPI) and post- (23DPI) symptom development (2006). The analysis conducted here differed by including a plant exhibiting a tolerance response to infection, *ein5-1*, to investigate how gene expression is different in a wild-type response compared to a tolerant response. Both these studies made use of the GeneChip Arabidopsis ATH1 Genome Array (Affymetrix Inc., USA) which provides coverage of approximately 24,000 genes, meaning the array used here provided coverage of approximately 4500 more genes. In Chapter 2 it was found that gall formation in *ein5-1* is delayed by approximately 7 days. Gall formation is the end point of infection. It is hypothesised that changes in gene expression which precede gall formation impact the host causing symptom development. Therefore it was decided to examine changes in host gene expression 14DPI in the anticipation that it would give some indication of the reasons for the differing responses to infection in *ein5-1* and Col-0.

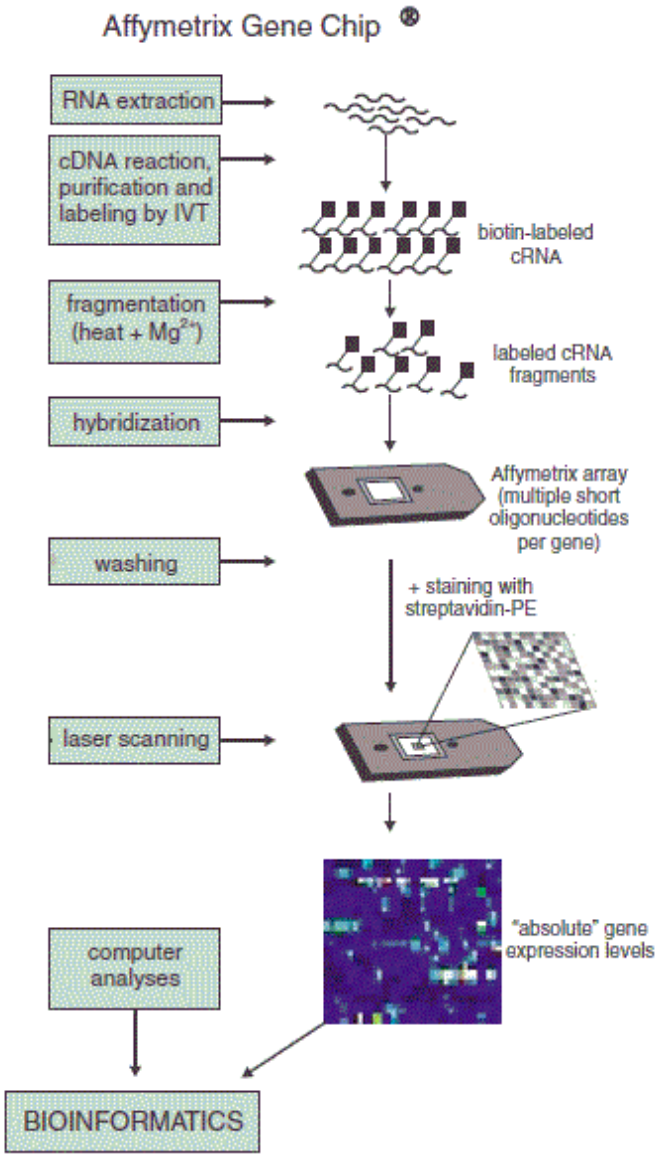

Figure 4.1 The Affymetrix microarray procedure.
RNA is extracted from the sample and used to produce cDNA and then cRNA. Fragmented cRNA is hybridised to the array. The cRNA binds to probes on the array, which represent genes. The array is washed to remove un-bound cRNA and then stained with a fluorescent dye. The array is then scanned using a laser and expression values for genes are produced based on the intensity of the fluorescence. Adapted from Stall et al (2003).

The aims and objectives of this chapter were:

Aims:

1. To examine the changes in host gene expression that proceed gall formation in *ein5-1* and contrast this with changes in gene expression in Col-0 in order to begin to unravel the mechanisms underlying *ein5-1*'s tolerance response

Objectives:

1. To conduct a microarray analysis of infected and uninfected Col-0 and *ein5-1* hypocotyl tissue 14DPI

2. To make use of bioinformatic tools to examine changes in gene expression in Col-0 and *ein5-1* during infection

3. To contrast gene expression data from Col-0 and *ein5-1* in order to investigate the cause of the tolerance response of *ein5-1*

4.2 Materials and Methods

4.2.1 Plant Material

Col-0 and *ein5-1* plants were grown and infected as described in Section 2.2.2. 14DPI plants were harvested for RNA extraction. Plants were carefully removed from the soil and the roots gently clean with water. Cleaned roots were placed on damp tissue until 20 plants had been collected. Very quickly the hypocotyl from each plant was removed using a clean scalpel and hypocotyls were transferred as a group to an eppendorf tube which was immediately frozen in liquid nitrogen. Each biological repeat consisted of the hypocotyls from 20 plants. Three biological repeats were collected for each treatment. The four treatments were Col-0 14DPI uninfected hypocotyl tissue, Col-0 14DPI infected hypocotyl tissue, *ein5-1* 14DPI uninfected hypocotyl tissue and *ein5-1* 14DPI infected hypocotyl tissue. This gave a total of 12 samples. Samples were stored at -70 ^{o}C until needed.

4.2.2 RNA Extraction

RNA was extracted from the hypocotyl tissue using TRIzol® reagent (Life Technologies Ltd, UK). Samples were removed from -70 °C storage and place immediately into liquid nitrogen. Samples were ground whilst still frozen using a pre-cooled micro pestle. 500 µl of TRIzol® reagent was then added to the sample which was homogenised using a micro pestle. A further 500 µl of TRIzol® reagent was added. The sample underwent further homogenisation until no large root fragments could be seen. Samples were kept on ice throughout the extraction procedure unless otherwise stated. Samples were incubated at 37 °C for 5 minutes and then centrifuged at 4 °C for 10 minutes at 14006 g. The supernatant was collected, taking care not to disturb the pellet, and transferred to a fresh ice-cold eppendorf tube. 200 µl of chloroform was added to the sample and mixed via inversion for 30 seconds. The sample was then centrifuged at 14006 g at 4 °C for 20 minutes. After centrifugation samples separated into a pink lower layer, an interphase and a clear upper layer; RNA is present in the upper layer. This was collected into a fresh ice-cold eppendorf, without disturbing the layers below. 10 µl of glycogen was added to the sample to aid RNA precipitation. 500 µl of isopropanol was also added to the samples which were then gently mixed and incubated for 10 minutes at room temperature. Samples were kept -20 °C overnight to allow precipitation of the RNA.

Following overnight incubation samples were centrifuge at 14006 g at 4 °C for 15 minutes to pellet the RNA. The supernatant was discarded and 1 ml of 80 % of ethanol was added to the pellet. The samples were centrifuged at 5471 g at 4 °C for 5 minutes. The ethanol was removed from the pellet. If the samples smelt of phenol or chloroform the ethanol wash was repeated. Pellets were air dried for 5 minutes. RNA was resuspended in 20 µl of nuclease-free water and heated at 55 °C for 3 minutes. RNA samples were stored at -70 °C until required.

4.2.3 Assessing RNA Quality

The concentration of the RNA and the 260 nm:280 nm ratio was assessed using a Thermo Scientific NanoDrop 8000. The 260:280 ratio is used to detect contamination of the RNA, a ratio between 1.6 and 2.2 was deemed acceptable.

To check that the RNA was not degraded a 1 % agarose gel was prepared as detailed in section 3.2.3. 1 µl of sample plus 7 µl of nuclease-free water and 2 µl of loading buffer were loaded. The gel was ran at 50 volts and visualised using a UV

transilluminator. Smearing of the RNA bands on the gel indicated that the RNA was degraded and could not be used further.

4.2.4 Microarray Analysis

Once RNA of an appropriate quality had been collected 20 µl of RNA was transported on dry ice to European Arabidopsis Stock Centre (NASC), Nottingham, UK. NASC carried out further quality control checks and processing of samples before hybridisation to Arabidopsis Gene 1.0 ST Arrays (Affymetrix Inc., USA). Array data was provided by NASC in the form of CEL files which were used in further analysis.

4.2.5 Analysis of Microarray Data

Data analysis was carried out using the open source software Bioconductor written in the R programming language. A series of Bioconductor packages were used in the analysis including “oligo” to pre-process the arrays, “arrayQualityMetrics” to test the quality of the arrays and “limma” to identify differentially expressed genes. Top tables of differentially expressed genes were imported into Microsoft Excel for further analysis. Annotation of differentially expressed genes was carried out with the aid of The Arabidopsis Information Resource (TAIR) database: http://www.arabidopsis.org/ GO analysis, to determine patterns in gene expression of differentially expressed genes (log2 Fold-change ≥ 1 and p-value ≤ 0.05), was carried out using the free web-based programmes: *GOrilla* http://cbl-gorilla.cs.technion.ac.il/ and REVIGO http://revigo.irb.hr/ SigmaPlot (Systat Software, San Jose, CA) was used to produce additional graphs. MAPMAN analysis was carried out to examine further patterns in gene expression. Log2 fold-changes were used in the analysis.

4.3 Results

4.3.1 Quality Control Checks and Data Normalisation

Microarray data is subject to variation from multiple sources including sample preparation, hybridisation of the samples to the arrays and quantification of signal intensities (Do and Choi 2006). Normalisation is carried out to minimise and standardise non-biological variation, so that arrays within the experiment can be compared. Robust multi-array analysis (RMA) was used to normalise the data using the “oligo” package (Irizarry 2003).

The “arrayQualityMetrics” package carries out a series of checks to assess the quality of the data at the array level. These checks examined: between array comparisons, array intensity distributions and individual array quality. The package runs the quality checks and produces a report showing the analyses and their output. Analyses included PCA plots of arrays, boxplots, density plots and MA plots. Both the output from this analysis and visual inspection of the individual arrays indicated that the data was of appropriate quality to be analysed further.

The “limma” package was used to identify differentially expressed genes. Four treatments were prepared (1) uninfected Col-0, (2) infected Col-0, (3) uninfected *ein5-1* and (4) infected *ein5-1*. All treatments were of hypocotyls 14DPI. “limma” allows pairs of treatments to be contrasted. The contrasts were (1) Col-0 infected vs. uninfected, (2) *ein5-1* infected vs. uninfected, (3) *ein5-1* vs. Col-0 uninfected and (4) *ein5-1* vs. Col-0 infected. “limma” provided a top table of differently expressed genes for each contrast, including the log fold change in gene expression. False discovery was corrected for using the Benjamini and Hochberg method, which gave rise to an adjusted P-value.

4.3.2 Principal Component Analysis

Principal component analysis (PCA) is carried out to extract the components from a data set that account for the variation within the data. These components can be plotted to show how samples in the data separate. Figure 4.2A shows the first component plotted against the second component. The first component separated uninfected treatments from infected treatments while the second component separated the uninfected treatments, Col-0 from *ein5-1*. The infected Col-0 and *ein5-1* treatments did not separate when only two components were plotted. A scree plot of the variance of each component shows that the first three components account for the majority of variation in the data (Figure 4.2B). A third component was therefore necessary to separate the Col-0 and *ein5-1* infected treatments. When a 3D PCA plot of the first three components was plotted treatments separated into the four treatments: uninfected Col-0, uninfected *ein5-1*, infected Col-0 and infected Col-0 (Figure 4.2C). The greatest level of variation therefore comes from uninfected versus infected treatments. The second largest amount of variation comes from Col-0 versus *ein5-1* treatments. Only when the third level of variation is included are infected treatments separated.

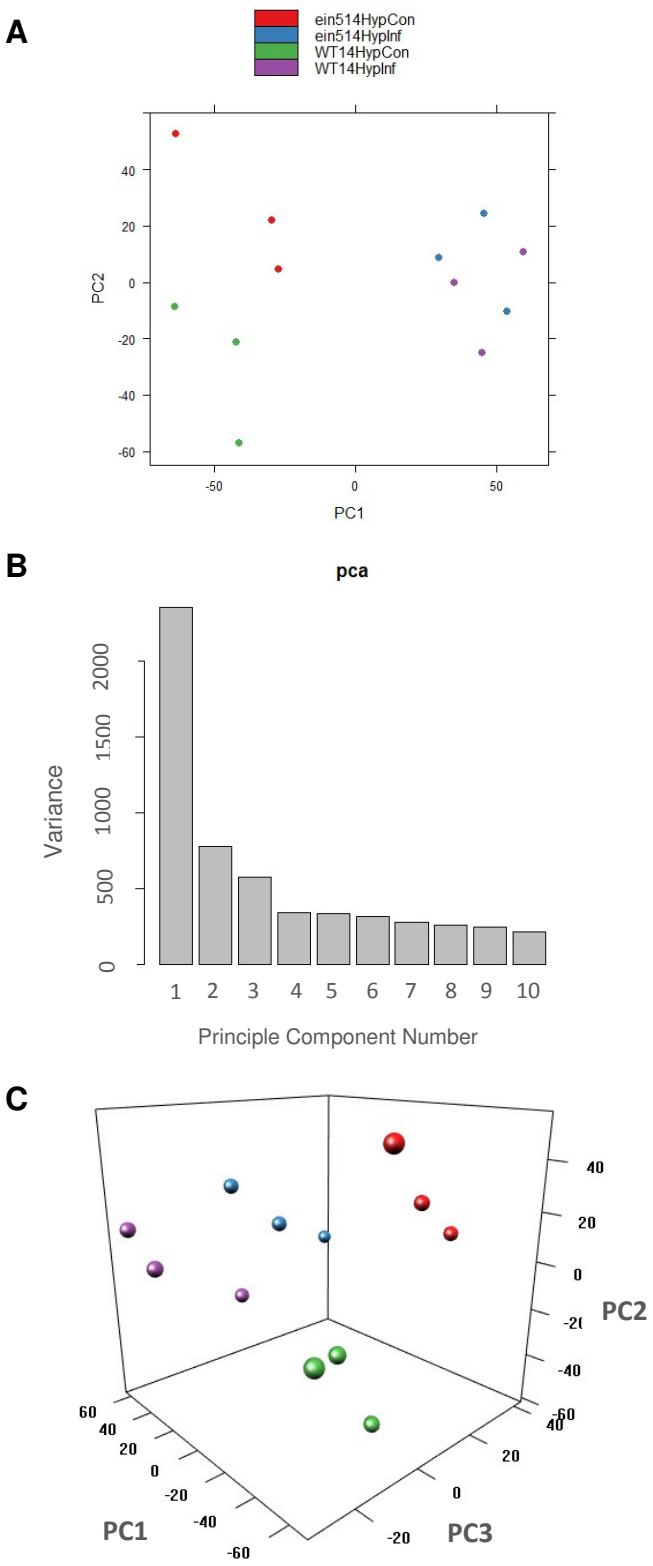

Figure 4.2. Principal component analysis of arrays.
PCA plot of the first and second components (A); separates the arrays into uninfected and infected clusters along the first component and Col-0 and *ein5-1* uninfected arrays along the second component. A scree plot (B) shows the variance of each component of the array data and indicates the first 3 components account for the variation in the data. A 3D PCA plot (C) with the first 3 components separates the arrays into their biological groupings: uninfected Col-0 (green), uninfected *ein5-1* (red), infected Col-0 (purple) and infected *ein5-1* (blue).

4.3.3 Differentially Expressed Genes

The microarray data was analysed at the gene level. Volcano plots were produced that showed the relationship between log2 fold-differences in gene expression and the statistical significance of these differences (adjusted P-value) (Figure 4.3). Genes that were differentially expressed in Col-0 infected versus uninfected hypocotyl 14DPI samples were plotted (Figure 4.3A). Those genes which were differentially expressed with a log2 fold-change in expression ≥ 1 and an adjusted P-value ≤ 0.05 were coloured blue. In total 1484 genes were differentially expressed within these parameters. 794 genes showed an increase in expression and 690 genes showed a decrease in expression. When differential gene expression was examined between infected *ein5-1* and uninfected *ein5-1* (Figure 4.3B), fewer genes were differentially expressed with a log2 fold-change ≥ 1 and an adjusted P-value ≤ 0.05. 857 genes in total fell within these parameters with 514 being up-regulated and 343 being down-regulated. Infection therefore leads to significant changes in gene expression in both Col-0 and *ein5-1*. Genes differentially expressed between *ein5-1* and Col-0 were then examined (Figures 4.3C and D). When differences between uninfected *ein5-1* and Col-0 were plotted, 140 genes were coloured blue (Figure 4.3C). Of those 55 genes showed increased expression and 85 genes showed decreased expression. The differences in gene expression between uninfected *ein5-1* and Col-0 are smaller than the differences between the infected and uninfected plant. When differences in infection in *ein5-1* and Col-0 were examined very few genes were differentially expressed (Figure 4.3D). 13 genes in total had a log2 fold-change ≥ 1 and an adjusted P-value ≤ 0.05; 7 of these genes are up-regulated and 5 are down-regulated. Infection therefore leads to the differences in gene expression between *ein5-1* and Col-0 becoming much smaller.

Venn diagrams show the shared differentially expressed genes (log2 fold-change ≥ 1 and P-value ≤ 0.05) from the Col-0 infected – Col-0 uninfected and *ein5-1* infected – *ein5-1* uninfected comparisons, Figure 4.4. 409 genes are up-regulated in both Col-0 and *ein5-1* when infected. 169 genes are down-regulated in both infected Col-0 and *ein5-1.*

The log2 fold-change of those differentially expressed genes from Col-0 infected – Col-0 uninfected and *ein5-1* infected – *ein5-1* uninfected (log2 fold-change ≥ 1 and P-value ≤ 0.05) were plotted (Figure 4.5). A line of regression was plotted through the graph (black) the R^2 value of this line was 0.83.

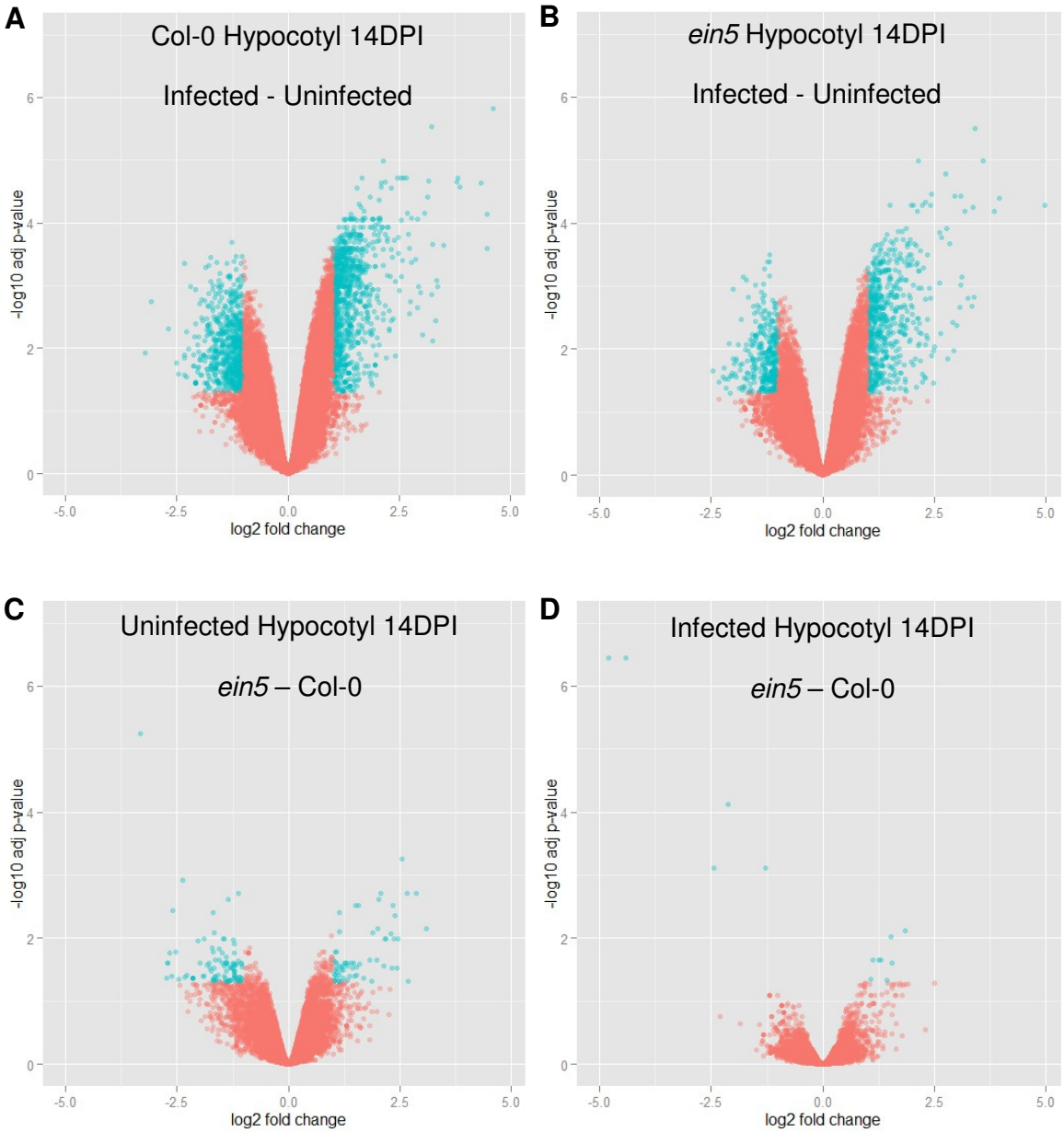

Figure 4.3. Volcano plots of differentially expressed genes.
Volcano plots of differentially expressed genes showing the relationship between log2 fold-change in expression and statistical significance. Points labelled in blue show log2 fold-change ≥ 1 and P-value ≤ 0.05 (Benjamini and Hochberg corrected).

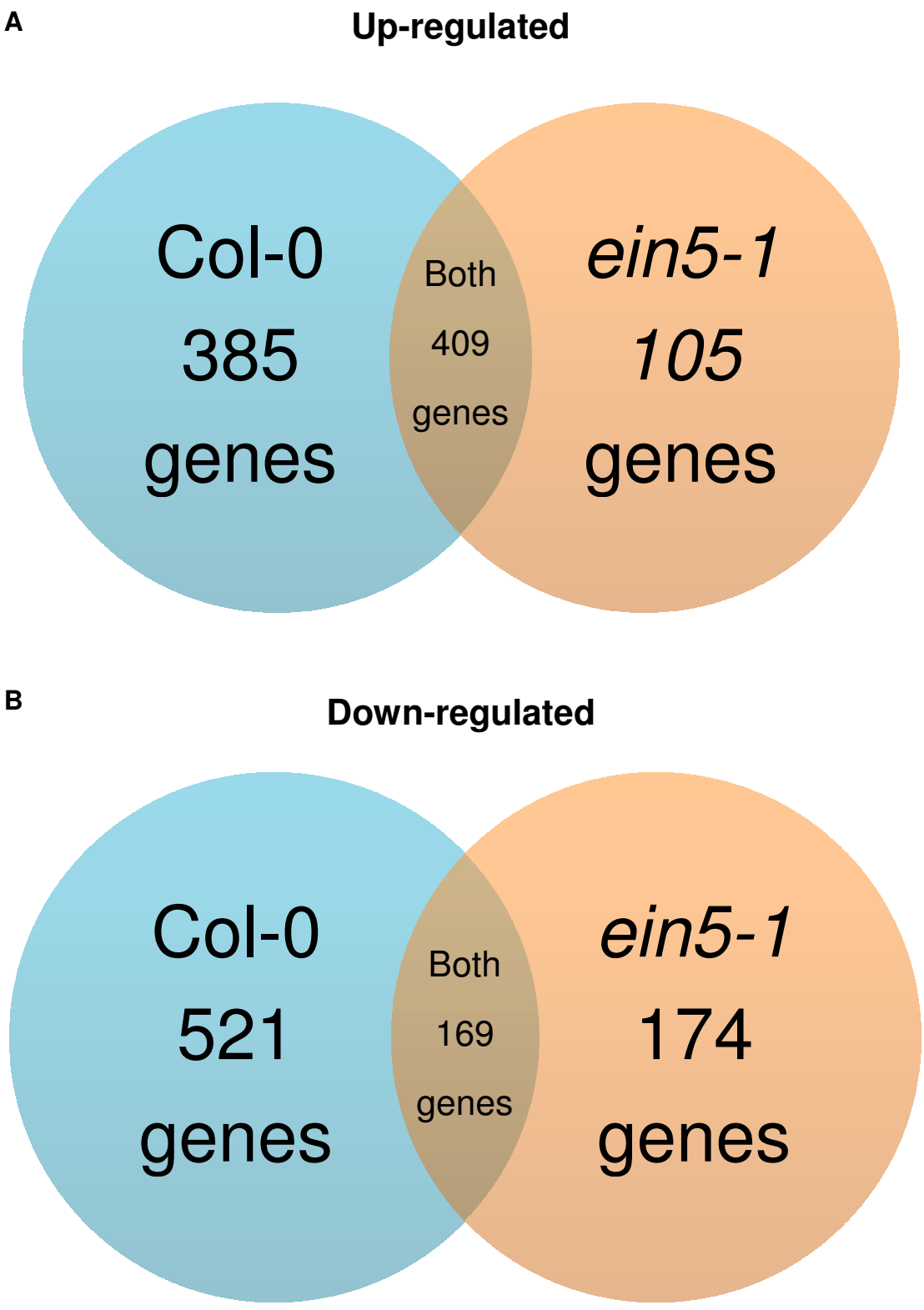

Figure 4.4 Venn diagrams of up and down-regulated genes.
Venn diagrams shown differentially up-regulated (A) and down-regulated (B) genes from Col-0 infected - Col-0 uninfected and *ein5-1* infected – *ein5-1* uninfected contrasts. Differentially expressed genes had a log2 fold-change ≥ 1 and P ≤ 0.05.

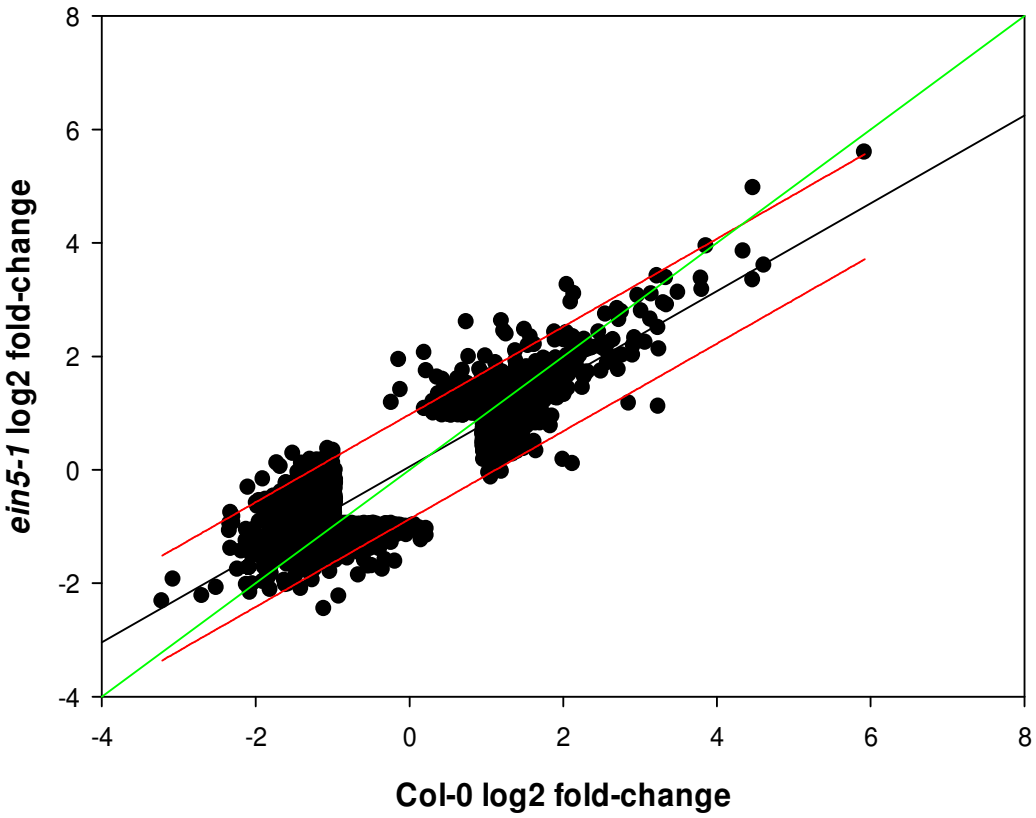

Figure 4.5 Fold-change of differentially expressed genes during infection. Differentially expressed genes were those that had a log2 fold-change ≥ 1 and a P-value ≤ 0.05. Black line is the regression plot for the data set R^2 value = 0.83, red lines indicate the 95 % confidence limits. The green line has a gradient of 1.

This indicates a strong relationship between the two data sets, genes that have a certain log2 fold change in the Col-0 comparison have a log2 fold-change that would be similar in the *ein5-1* comparisons. Infection is having a comparable impact on gene expression in both lines. 95 % confidence limits were added for the regression line, the vast majority of data points stayed within these limits. Log2 fold-changes falling outside of the 95 % confidence limits represent genes that may be of interest in terms of why *ein5-1* responds to infection differently to Col-0.

A second line (green) with a gradient of 1 was plotted, to indicate a perfect relationship between the two data sets, therefore this line shows were the regression line would lie if infection in Col-0 and *ein5-1* was exactly the same.

Heat maps were produced which show differentially expressed genes represented by coloured blocks (Figure 4.6). Rows represent differentially expressed genes while columns represent different samples. Genes are colour coded by a gradient depending on their expression value, those genes that have high expression are yellow and those that have low expression are red. The genes present on the heat maps are those which show differential expression in a specific comparison. Data for all treatments is shown for each biological repeat. Only those differentially expressed genes which were shown to be significantly different at the $P \leq 0.05$ level were included.

Comparisons between different biological samples were made which indicated the genes that should be shown in the heat map i.e. those genes that were differentially expressed in the comparison. Treatments cluster within the heat map based on similarity, with the closest groups lying adjacent. Differentially expressed genes from Col-0 infected tissue were compared to those from Col-0 uninfected tissue (Figure 4.6A). Samples clustered firstly into uninfected and infected groupings and then secondly into Col-0 and *ein5* samples. Generally those genes up-regulated in uninfected Col-0 samples were down-regulated in the infected Col-0 samples and *vice-versa*. Again generally, the *ein5* samples displayed a similar expression pattern to that of their respective Col-0 samples. Comparisons between differentially expressed genes from *ein5* infected tissue and *ein5* uninfected tissue were used to produce a heat map (Figure 4.6B). Although a different set of differentially expressed genes were present, a similar pattern to that described above was seen. Samples clustered into uninfected and infected samples and then *ein5* and Col-0 samples. Again when gene expression is up in *ein5* uninfected samples it is usually down in infected samples, with the inverse also being true. Col-0 samples show a similar pattern to those of *ein5* samples. Infection is the main factor driving differential gene expression in these to comparisons.

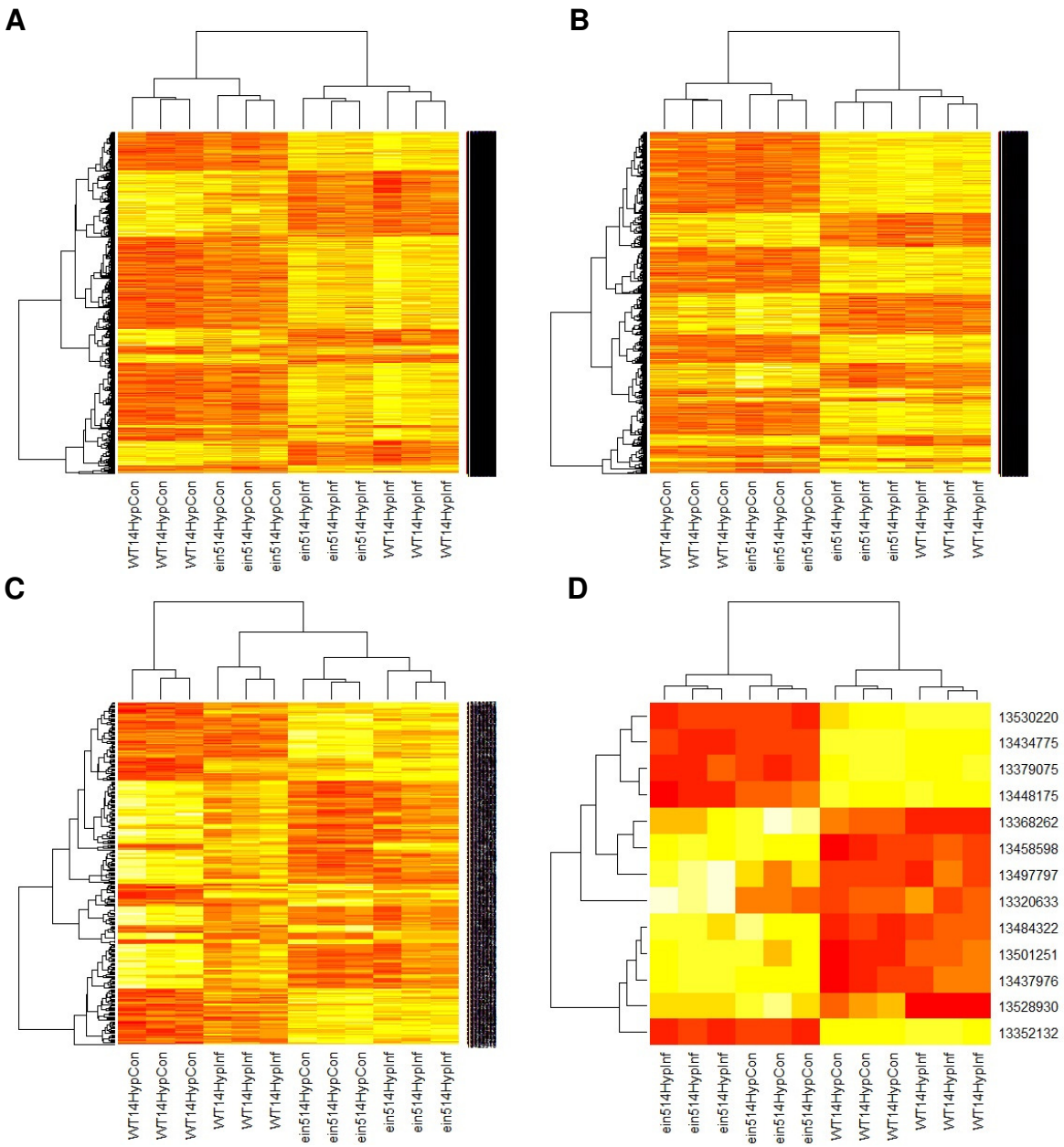

Figure 4.6 Heat maps of differentially expressed genes.
Heat maps are used to visualise the similarities/differences in gene expression between samples. The columns represent different samples and the rows differentially expressed genes. Genes with high expression are shown in yellow while those with low expression are shown in red. Only those genes that were significantly differentially expressed at the $P \leq 0.05$ are shown in the plots. The heat maps cluster samples so that the samples that are closest lie adjacent to one another. Each map is driven by a different comparison of differentially expressed genes: (A) Col-0 14DPI infected hypocotyl tissue compared to uninfected Col-0 tissue, (B) *ein5-1* 14DPI infected hypocotyl tissue compared to uninfected *ein5-1* tissue, (C) 14DPI uninfected hypocotyl tissue from *ein5-1* compared to Col-0 tissue and (D) 14DPI infected hypocotyl tissue from *ein5-1* compared to Col-0 tissue.

Only when Col-0 and *ein5* uninfected samples were compared were Col-0 and *ein5* samples separated in terms of differentially expressed genes. Col-0 samples both infected and uninfected clustered as did both sets of *ein5* samples (Figure 4.6C). When differential gene expression in infected *ein5* samples was compared to that in Col-0 infected samples only 13 genes were significantly different at the $P \leq 0.05$ level. One of which encodes EIN5/XRN4. Again samples clustered into *ein5* and Col-0 groupings and within these grouping into infected and uninfected treatments.

4.3.4 GO Analysis of Differentially Expressed Genes

The gene ontology (GO) project was devised to "produce a structured, precisely defined, common, controlled vocabulary for describing the roles of genes and gene products in any organism" (Ashburner et al. 2000). Three vocabularies were described and defined: biological process, molecular function and cellular components. Biological process refers to the biological objective to which a gene or gene product contributes to, for example "cell growth and maintenance". Molecular function is the biochemical activity of a gene product, for example "transporter". Cellular component describes where in a cell the gene product is active, for example "nuclear membrane".

A GO enrichment analysis allows the identification of GO terms that are significantly over-represented in a given set of genes. This allows functional characteristics of a gene set to be established. There are several programmes that carry out GO enrichment analysis; the one employed here was the web-based application *GOrilla* (Eden et al. 2009). *GOrilla* uses a list of target genes and compares these to a background gene list to identify GO terms that are enriched in the target gene list. Here the target gene list was a list of differentially expressed genes with a log2 fold-change ≥ 1 and an adjusted P-value ≤ 0.05. Lists of differentially expressed genes came from the four contrasts made previously. The analysis was carried out on both up-regulated gene sets and down-regulated gene sets. The background list was all of the genes found on the microarray chip.

Differentially expressed genes from the Col-0 infected vs uninfected comparison were used in the *GOrilla* analysis. When those genes that were up-regulated were used in the analysis 209 process GO terms were significantly enriched in the gene list, see Appendix. Many of the significant GO enriched terms were associated with gene expression indicating that infection leads to a whole range of changes in plant gene expression. The GO terms associated with transcriptional changes enriched for in the up-regulated gene set included: histone modification, gene silencing, chromatin

silencing by small RNA, transcription factor import into nucleus and regulation of gene expression, epigenetic. The most up-regulated gene is in fact AT1G12805 a nucleotide binding protein and several transcription factors are seen to be significantly up-regulated including WRKY, GRF and ERF/AP2 family members. The GO terms: response to hypoxia, response to decreased oxygen levels and response to oxygen levels were also enriched in the up-regulated gene set. Infection appears to leads to reduced oxygen levels which the plant is attempting to respond to. Other associated GO terms that are enriched in the target gene list are: regulation of hydrogen peroxide metabolic process and regulation of reactive oxygen species metabolic process. Genes that are found to be significantly up-regulated associated with these terms include a glutathione S-transferase, acireductone dioxygenase 3, thioredoxin H-type 8 and members of the peroxidase superfamily. Other terms significantly enriched in the up-regulated gene list included those associated with cell division including: cell proliferation, cell cycle, regulation of cell cycle, regulation of cell cycle phase transition, regulation of miotic cell cycle and cell cycle process. When the top table of differentially expressed genes was examined several genes associated with these GO terms were found to be significantly up-regulated genes in Col-0 infected tissue compared to uninfected tissue. These included cell cycle genes such as cyclin a2;1, cyclin B2;3 and mitotic-like cyclin 3B along with several other cell cycle regulated genes. See Table 4.1 for fold-changes of selected up-regulated genes.

REVIGO is a web based program that uses the lists of enriched GO terms from *Gorilla* which are usually quite large and have many redundant terms, and summarises these by clustering highly similar GO terms (Supek et al. 2011). This facilitates summarising and visualising the data and can make interpretation less difficult. REVIGO was therefore used here to produce treemaps of enriched GO terms. Treemaps shows clusters of GO terms as rectangle blocks which are then grouped into super-clusters of related terms shown in different colours. The treemap of GO enriched terms from the up-regulated gene set from the comparison Col-0 infected – uninfected can be seen in Figure 4.7. The GO terms cluster into two super-clusters: histone modification and ribonucleotide biosynthesis, again indicating the large changes in host gene expression that are occurring as a consequence of infection. Also several of the clustered terms are associated with metabolism indicating infection is leading to alterations in plant metabolism.

Table 4.1 Selected genes differentially regulated in Col-0 infected vs. Col-0 uninfected hypocotyls 14DPI.

Gene	Description	Log2 fold-change	Adjusted P-value
AT1G12805	nucleotide binding protein	5.92	$9.x10^{-5}$
AT5G01900	WRKY DNA-binding protein 62	3.31	$3x10^{-3}$
AT1G62300	WRKY6	2.47	$1x10^{-3}$
AT5G28650	WRKY DNA-binding protein 74	1.75	$1x10^{-3}$
AT2G22840	growth-regulating factor 1	2.67	$7.1x10^{-5}$
AT4G37740	growth-regulating factor 2	2.02	$2x10^{-4}$
AT5G13330	related to AP2 6l	4.47	$7.4x10^{-5}$
AT2G47520	Integrase-type DNA-binding superfamily protein: a member of the ERF superfamily	1.52	$1.7x10^{-3}$
AT5G25380	cyclin a2;1	3.14	$3.9x10^{-5}$
AT2G26400	acireductone dioxygenase 3	3.01	$6.1x10^{-3}$
AT1G69880	thioredoxin H-type 8	2.97	$1.3x10^{-3}$
AT1G17180	glutathione S-transferase TAU 25	3.86	$2.6x10^{-5}$
AT1G20610	Cyclin B2;3	2.18	$1.5x10^{-4}$
AT5G11300	mitotic-like cyclin 3B	2.05	$4.27x10^{-5}$

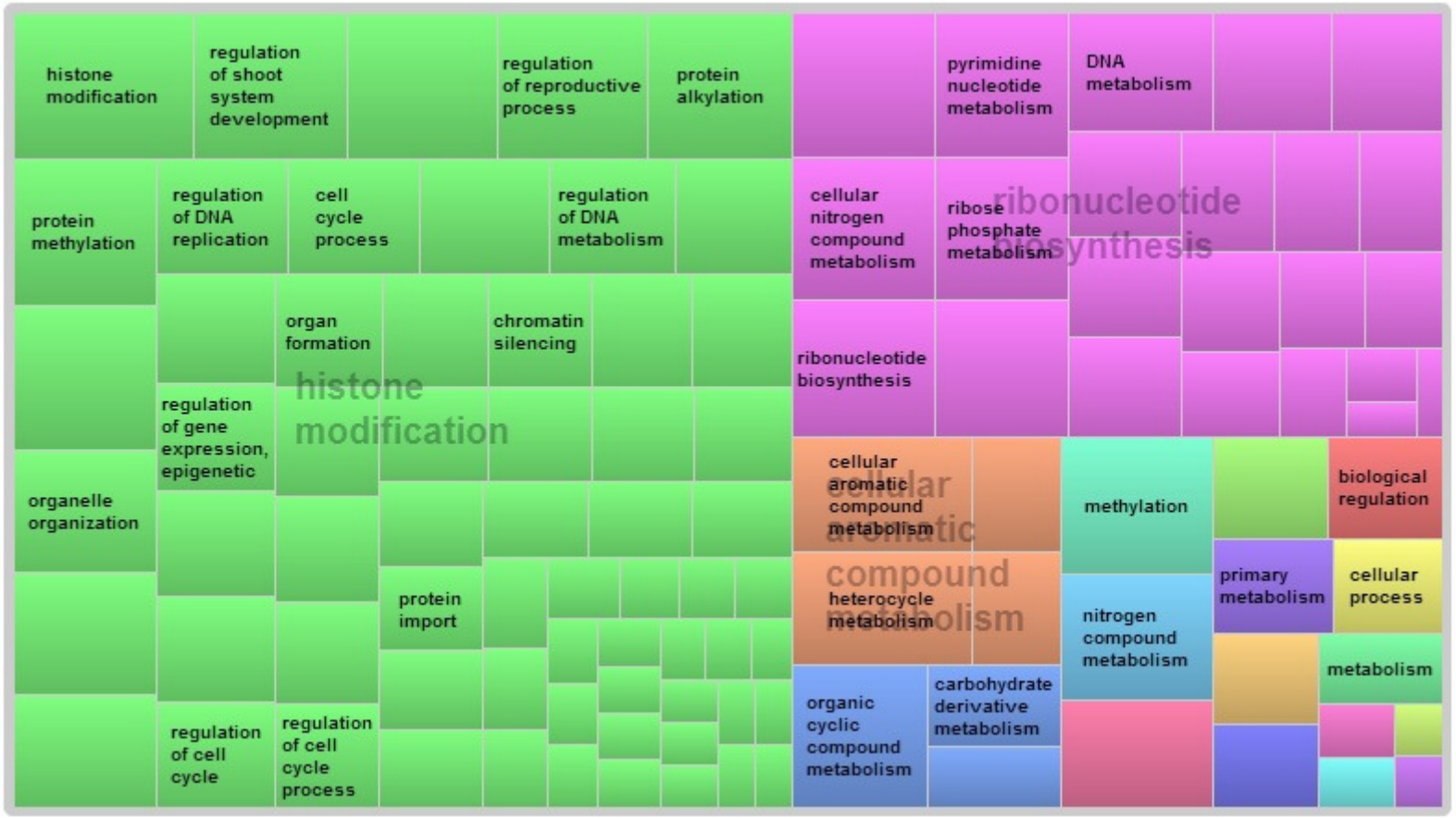

Figure 4.7. Treemap of enriched GO terms in up-regulated genes from the comparison Col-0 infected – uninfected hypocotyl 14DPI. REVIGO uses the enriched GO terms from the *Gorilla* analysis and removes redundant terms by clustering similar terms together. Treemap produced at http://revigo.irb.hr/

When the down-regulated genes for the Col-0 infected – uninfected comparison were used in the *Gorilla* analysis 38 GO terms were significantly enriched, see Appendix. Many of the GO terms enriched in the down-regulated gene list were associated with the plant response to some stimulus including: response to endogenous stimulus, response to chemical, response to wounding, response to stress and response to hormone. Also seen to be significantly enriched in the down-regulated genes are several terms associated with plant defence including: respiratory burst involved in defence response, regulation of immune response and regulation of plant-type hypersensitive response. Terms associated with the ethylene signalling pathway were enriched in the down-regulated list: ethylene mediated signalling pathway and cellular response to ethylene stimulus. Several terms related to flavonoid biosynthesis were also enriched in the down-regulated gene set: regulation of flavonoid biosynthetic process and positive regulation of flavonoid biosynthetic process. The REVIGO treemap shows how enriched GO terms for the down-regulated genes clustered, Figure 4.8. There are fewer clustered GO terms in the down-regulated gene set compared to the up-regulated gene set. Terms associated with response to endogenous stimulus form a large super-cluster. Also peptide transport forms a super-cluster. The respiratory burst and regulation of flavonoid biosynthesis are also seen on the treemap.

Up-regulated differentially expressed genes from the *ein5-1* infected - *ein5-1* uninfected comparison had 143 GO terms significantly enriched in the data, see Appendix. The majority of GO terms that were significantly enriched in the gene set were also significantly enriched in up-regulated gene list from the Col-0 infected – Col-0 uninfected comparison. Only 7 GO terms were exclusive to the *ein5-1* up-regulated list. Three of these terms were associated with salicylic acid: cellular response to salicylic acid stimulus, salicylic acid mediated signalling pathway and response to salicylic acid. The rest of the enriched terms were also enriched in the Col-0. This indicates the similarity of infection in both *ein5-1* and Col-0. Terms associated with changes in gene expression were significantly enriched as were those associated with cell division and response to hypoxia. When the top table of differentially expressed genes is examined for *ein5-1* infected vs *ein5-1* uninfected, it is seen that many of the genes that are up-regulated in Col-0 during infection are also up-regulated in *ein5-1* during infection; again indicating the similarity in response to infection in both lines. When REVIGO clustered the enriched terms many of the same clusters were seen as in the equivalent Col-0 treemap (Figure 4.7 and 4.9).

Figure 4.8. Treemap of enriched GO terms in down-regulated genes from the comparison Col-0 infected – uninfected hypocotyl 14DPI.

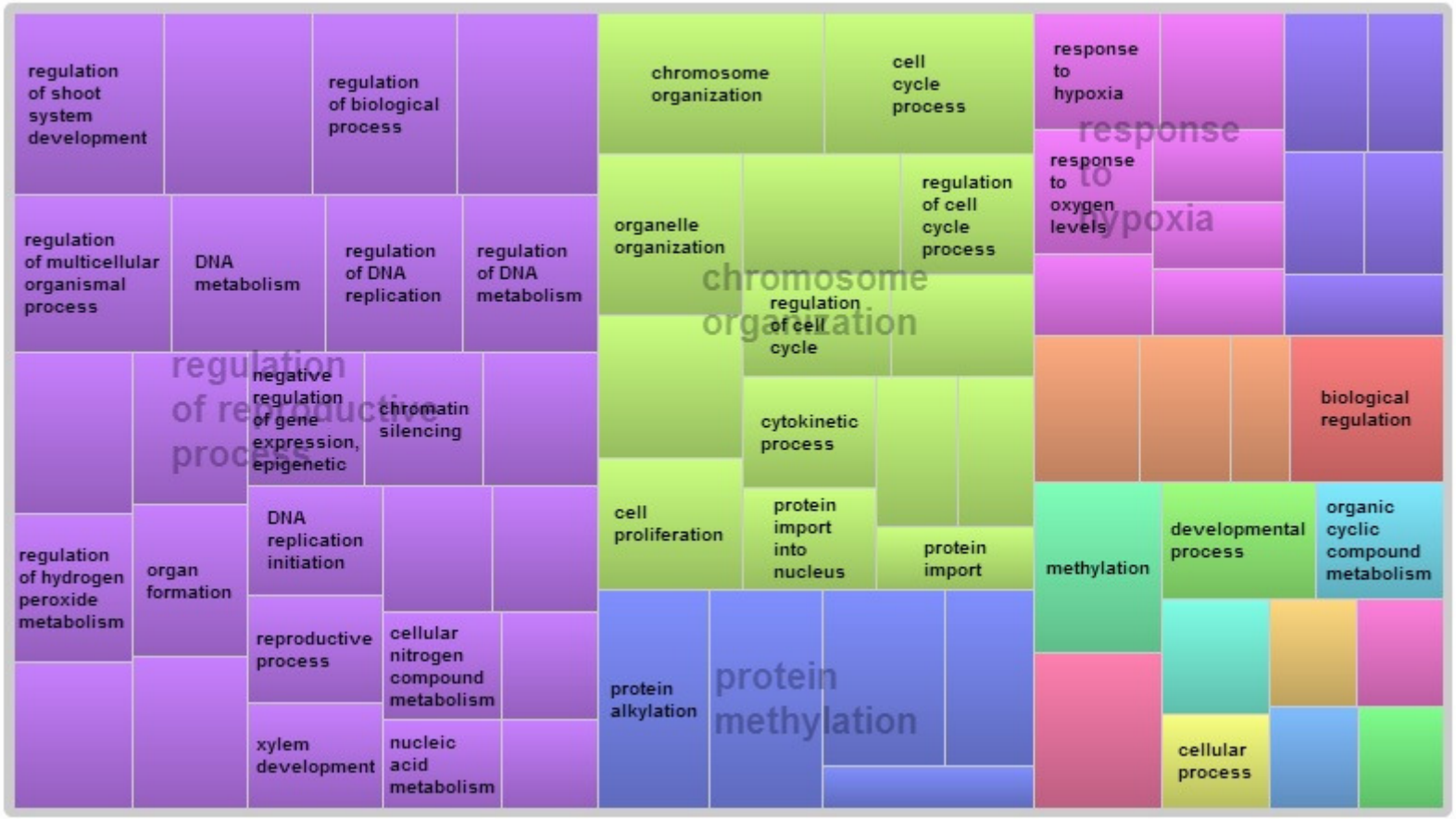

Figure 4.9. Treemap of enriched GO terms in up-regulated genes from the comparison *ein5* infected – uninfected hypocotyl 14DPI.

The down-regulated genes from *ein5* infected – *ein5* uninfected were significantly enriched for 32 GO terms, see Appendix. Only 6 of these terms were also in the down-regulated Col-0 uninfected – infected differentially expressed gene list. Indicating that the genes down-regulated in response to infection in *ein5* and Col-0 are quite different. GO terms enriched for included several terms associated with transport: metal ion transport, peptide transport and nitrate transport. Terms associated with the cell wall were also enriched in the down-regulated genes: cell wall polysaccharide metabolic process, cell wall macromolecule biosynthetic process and cell wall macromolecule metabolic process. The GO terms cellular response to auxin stimulus and auxin mediated signalling pathway were also significantly enriched. Down-regulated genes associated with enriched GO terms included: KNAT7 which regulates cell wall biosynthesis, several auxin responsive genes including some of the SAUR-like genes and transporter proteins including phosphate and EamA-like transporters. The REVIGO treemap shows the GO terms clustered into one large super-cluster termed cell wall macromolecule metabolism, which contained smaller clusters associated with the cell wall, transport and auxin signalling (Figure 4.10). The GO terms also clustered into groups associated with carbohydrate metabolism and biosynthesis.

When up-regulated differentially expressed genes from the uninfected 14DPI hypocotyl *ein5* – Col-0 contrast were used for *Gorilla* analysis no GO terms were significantly enriched in the gene list. When the down-regulated genes were analysed for enriched terms 20 GO terms were significantly enriched for that were down-regulated in uninfected *ein5* samples compared to uninfected Col-0 samples, see Appendix. Unsurprisingly several terms were associated with ethylene signalling: ethylene mediated signalling pathway, cellular response to ethylene stimulus, ethylene metabolic process and ethylene biosynthetic process. Associated down-regulated genes included several members of the ethylene response factor (ERF) transcription factor family. Also the gene encoding XRN4 is significantly down-regulated, as would be expected. Other GO terms enriched in this data set included many stress response associated terms: response to wounding, response to stimulus, response to stress and response to mechanical stimulus. The REVIGO output for these enriched terms is shown in Figure 4.11. The super clusters in this data set include response to stress, ethylene biosynthesis and response to stimulus.

7 genes were up-regulated and 5 were down-regulated (log2 fold-change ≥ 1 and P-value ≤ 0.05) when the infected *ein5* – Col-0 contrast was examined. As so few genes were differentially expressed GO analysis was not performed, instead the differentially expressed genes can be seen in Tables 4.2 and 4.3.

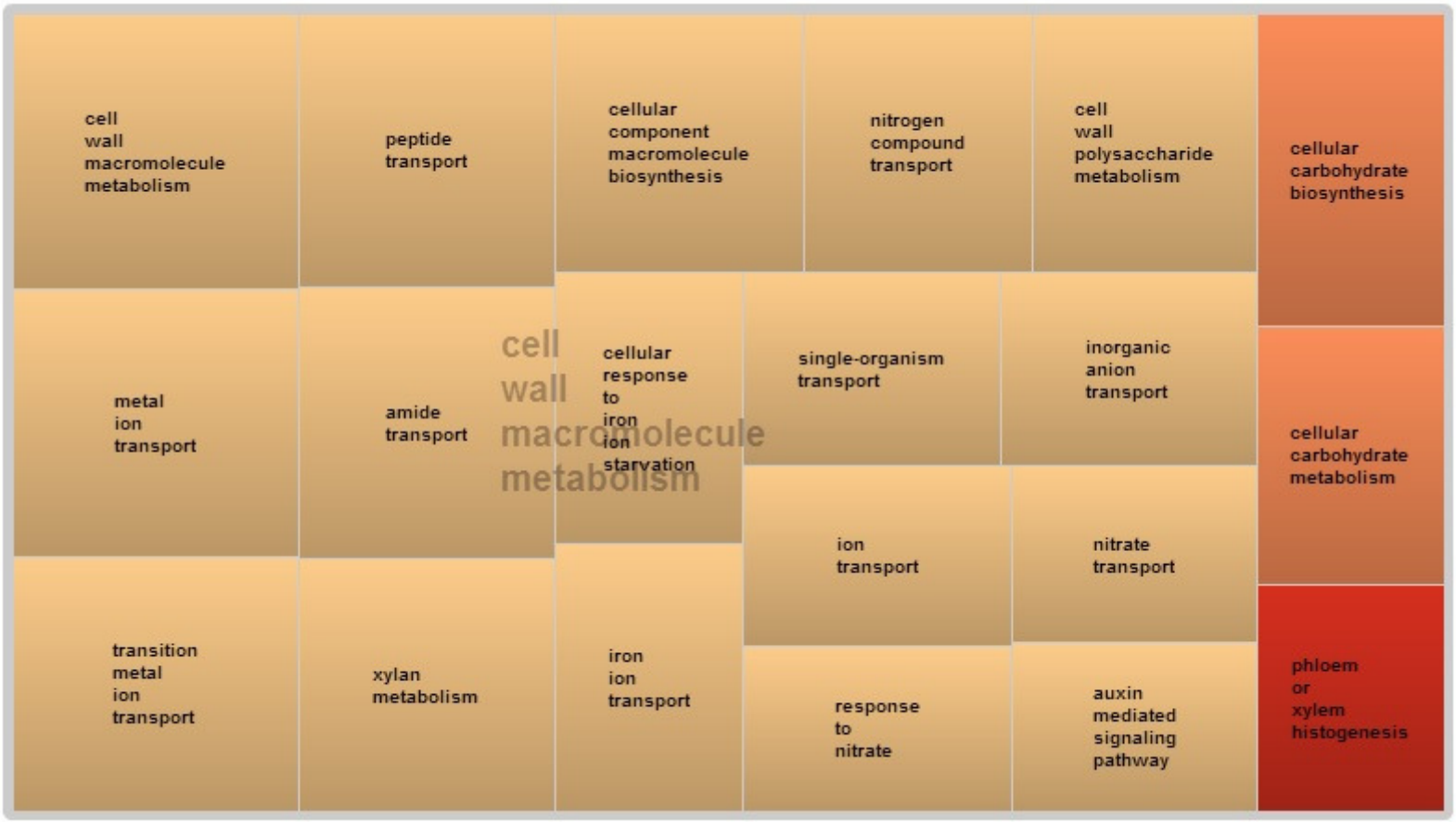

Figure 4.10. Treemap of enriched GO terms in down-regulated genes from the comparison *ein5* infected – uninfected hypocotyl 14DPI.

Figure 4.11. Treemap of enriched GO terms in down-regulated genes from the comparison *ein5* uninfected – Col-0 uninfected hypocotyl 14DPI.

Table 4.2. Up-regulated genes from the comparison *ein5* infected – Col-0 infected hypocotyl 14DPI.

Gene	Other Names	Description
AT4G14090		Encodes a anthocyanidin 5-O-glucosyltransferase specifically glucosylating the 5-position of the flavonoid A-ring.
AT3G51240	F3'H, F3H, FLAVANONE 3-HYDROXYLASE, TRANSPARENT TESTA 6, TT6	Encodes flavanone 3-hydroxylase that is coordinately expressed with chalcone synthase and chalcone isomerases. Regulates flavonoid biosynthesis. Not responsive to auxin or ethylene stimulus.
AT5G13930	ATCHS, CHALCONE SYNTHASE, CHS, TRANSPARENT TESTA 4, TT4	Encodes chalcone synthase (CHS), a key enzyme involved in the biosynthesis of flavonoids. Required for the accumulation of purple anthocyanins in leaves and stems. Also involved in the regulation of auxin transport and the modulation of root gravitropism.
AT1G15100	RHA2A, RING-H2 FINGER A2A	Encodes a putative RING-H2 finger protein RHA2a.
AT3G51238		Potential natural antisense gene, locus overlaps with AT3G51240
AT5G20885		RING/U-box superfamily protein
AT5G05270	ATCHIL, CHALCONE ISOMERASE LIKE, CHIL	Chalcone-flavanone isomerase family protein

Other Names and Descriptions taken from www.arabidopsis.org

Table 4.3. Down-regulated genes from the comparison *ein5* infected – Col-0 infected hypocotyl 14DPI.

Gene	Other Names	Description
AT1G54490	ATXRN4, EIN5, ETHYLENE INSENSITIVE 5, EXORIBONUCLEASE 4, XRN4, ACC INSENSITIVE 1, AIN1,	Involved in the ethylene response. Endogenous suppressor of posttranscriptional gene silencing.
AT3G12100	METAL TRANSPORT PROTEIN 5, MTP5	Cation efflux family protein
AT1G53480	ARABIDOPSIS MTO 1 RESPONDING DOWN 1, ATMRD1, MRD1, MTO 1 RESPONDING DOWN 1	Encodes MRD1 (mto 1 responding down). Down-regulated in mto1-1 mutant that over-accumulates soluble Methionine
AT5G24240		Phosphatidylinositol 3- and 4-kinase; Ubiquitin family protein
AT3G30720	QQS, QUA-QUINE STARCH	

Other Names and Descriptions taken from www.arabidopsis.org

Four of the up-regulated genes were associated with flavonoid biosynthesis; a flavone-3-hydroxylase, chalcone synthase, chalcone isomerase and anthocyanidin 5-O-glucosyltransferase. In the down-regulated gene set there appeared to be no functional groupings. As would be expected *Ein5*/*XRN4* is significantly down-regulated in *ein5* plants when compared to Col-0 plants.

4.3.5 Gene Expression Related to Secondary Metabolism

Interestingly two groups of secondary metabolites were highlighted during the GO analysis. GO terms associated with salicylic acid were found to be significantly enriched in the genes that were up-regulated in *ein5-1* during infection. Also four out of seven genes that were differentially up-regulated in infected *ein5-1* hypocotyls compared to infected Col-0 hypocotyls were associated with flavonoid biosynthesis.

In order to analyse the pathways associated with secondary metabolism MAPMAN software was used (Thimm et al. 2004). MAPMAN allows the visualisation of up- and down-regulated genes, which aids the discovery of general trends. MAPMAN was used to examine up- and down-regulated genes in Col-0 infected compared to Col-0 uninfected, *ein5-1* infected compared to *ein5-1* uninfected and *ein5-1* infected compared to Col-0 infected, Figures 4.12 to 4.14. Genes are arranged into functional categories and appear as squares which are colour coded on a scale based on their regulation; down-regulated genes are red and up-regulated genes are blue.

Secondary metabolism associated genes appeared to be altered in a similar manner in both Col-0 and *ein5-1*, Figures 4.12 and 4.13. This was in line with the findings of the GO and REVIGO analysis detailed above, that infection in Col-0 and *ein5-1* is comparable. The general trend appeared to be that infection in both Col-0 and *ein5-1* caused down-regulation of genes associated with secondary metabolism; including lignin and glucosinolate associated genes. Glucosinolate associated genes appeared to be particularly down-regulated during infection in *ein5-1*. When infection in *ein5-1* and Col-0 is compared it appears that several groups of secondary metabolite associated genes are up-regulated in *ein5-1*. These include glucosinolates, flavonoids, lignins and phenylpropanoids. This could indicate that secondary metabolism may play a role in *ein5-1*'s response to clubroot infection.

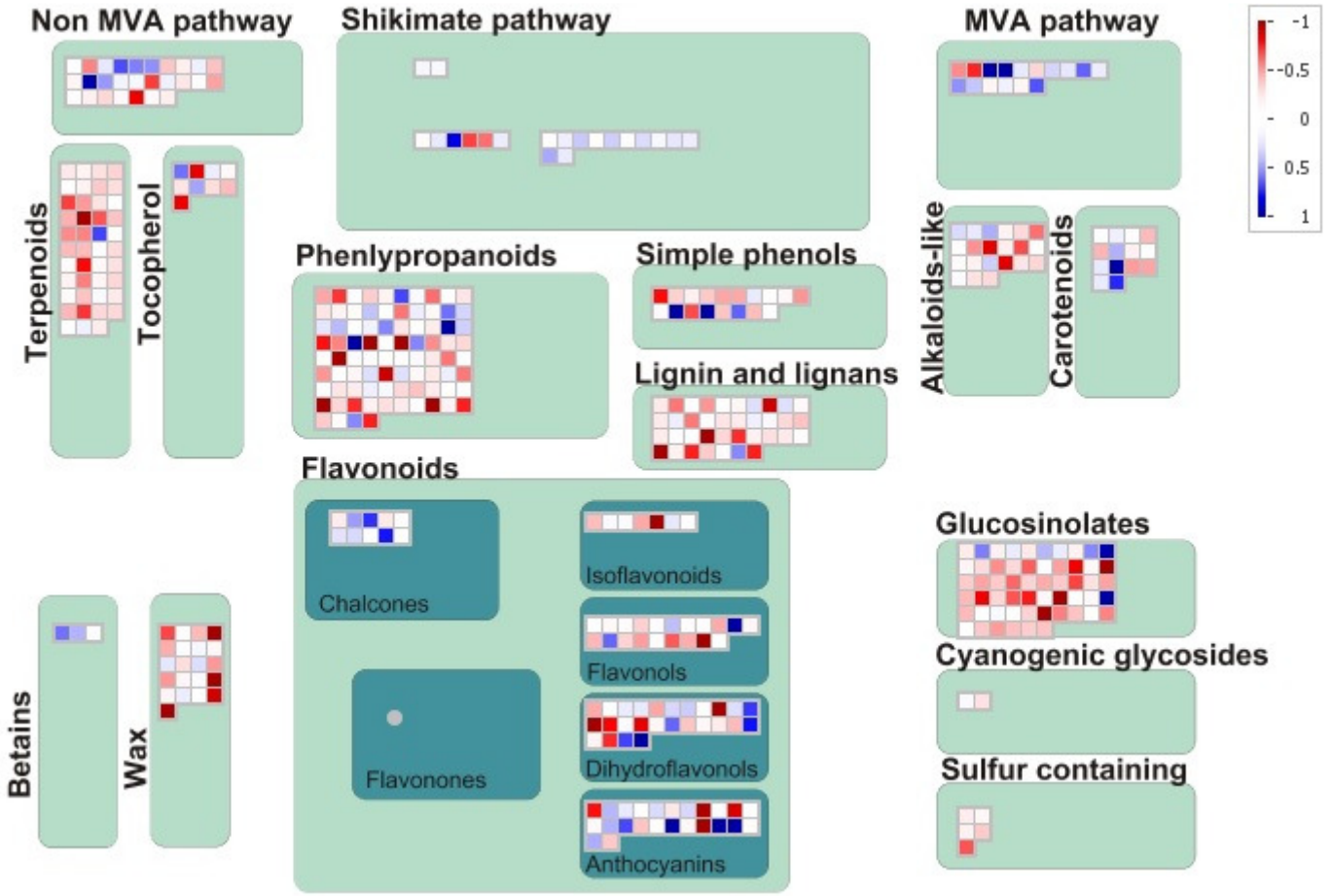

Figure 4.12. MAPMAN overview of secondary metabolism comparing up- and down-regulated genes in infected Col-0 to uninfected Col-0 hypocotyls 14DPI.
Those genes that were up-regulated are shown in blue and those that are down-regulated are shown in red.

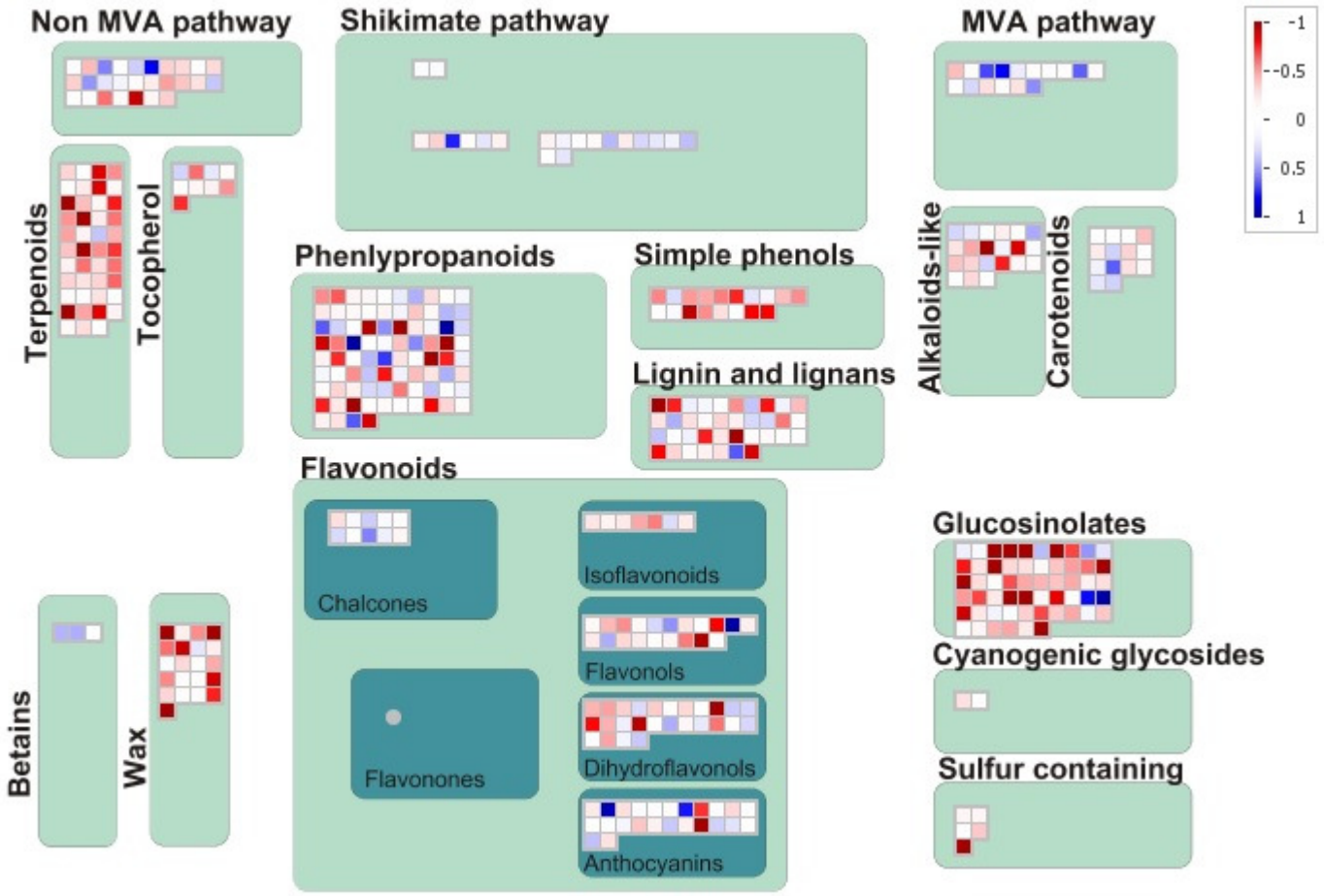

Figure 4.13. MAPMAN overview of secondary metabolism comparing up- and down-regulated genes in infected *ein5-1* to uninfected *ein5-1* hypocotyls 14DPI.
Those genes that were up-regulated are shown in blue and those that are down-regulated are shown in red.

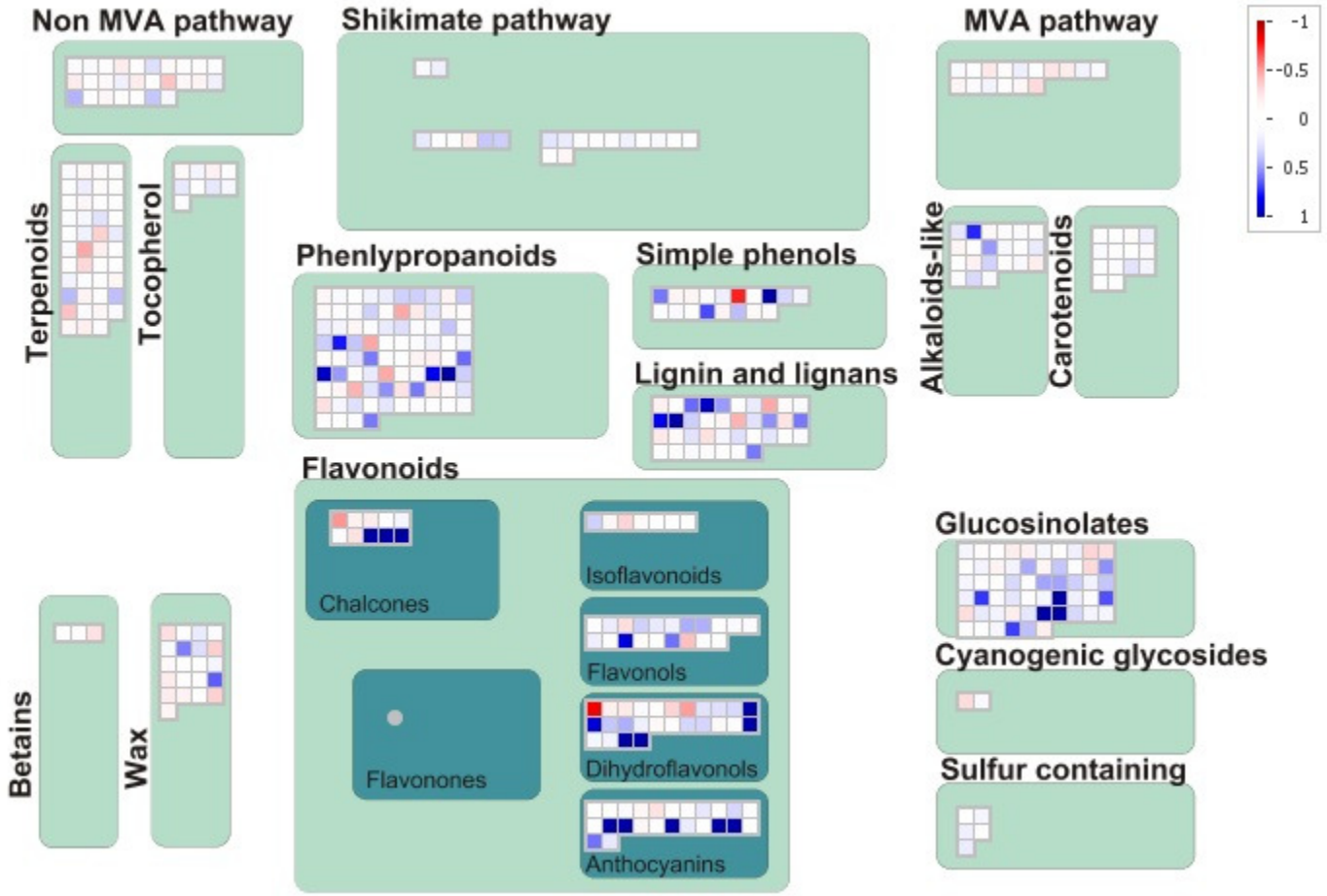

Figure 4.14. MAPMAN overview of secondary metabolism comparing up- and down-regulated genes in infected *ein5-1* to infected Col-0 hypocotyls 14DPI.
Those genes that were up-regulated are shown in blue and those that are down-regulated are shown in red.

4.4 Discussion

The aim of this chapter was to use an un-targeted approach to investigate changes in host gene expression during infection and contrast these with changes in *ein5-1* in order to examine the differences in response to infection that lead to *ein5-1* being tolerant to clubroot infection. To meet this aim a microarray analysis was carried out to analyse gene expression in 14DPI hypocotyls from uninfected and infected Col-0 and *ein5-1* plants.

Gall formation in *ein5-1* was found to be delayed by 7 days, see Chapter 2, and the delay appeared to be a consequence of the slowing down of pathogen and host symptom development. How one impacts on the other is yet to be established, i.e. does a delay in symptom development lead to a delay in pathogen development or *vice versa.* As the disease is slowed rather than being completely halted it is not surprising that changes in gene expression as a consequence of infection were very similar in both Col-0 and *ein5-1*. A 3rd component was needed in the PCA plots to separate out the Col-0 infected arrays from the *ein5-1* infected arrays, Figure 4.2C. This suggests that although Col-0 and *ein5-1* lines are different, in terms of gene expression when uninfected, infection acts to masks many of those differences pulling the two lines closer together. The heatmaps produced also showed that infection was the main driving force in comparisons between the arrays followed by the differences between Col-0 and *ein5-1*, Figure 4.6. Therefore the differences in *ein5-1* and Col-0 gene expression that lead to an altered response to infection will possibly be subtle. This was also seen in the regression analysis carried out on differentially expressed genes from Col-0 and *ein5-1* during infection, Figure 4.5. The line of regression had a R^2 value of 0.83, indicating a strong relationship between differentially expressed genes in Col-0 and *ein5-1*. The majority of differentially expressed genes also fell within 95 % confidence limits added to the regression line. Therefore gene expression is generally responding in a similar manner in both Col-0 and *ein5-1* during infection; for example, when infection causes a gene to be up-regulated in Col-0 this is usually also the case in *ein5-1*. *ein5-1* shared 78 % of up-regulated genes and 49 % of down-regulated genes with Col-0, again highlighting the similarity of response to infection in terms of alterations in gene expression. It seems likely that it is not the case that a discreet set of genes are expressed differently in *ein5-1* compared to Col-0 during infection which lead to a tolerance response. In fact when the differentially expressed genes in *ein5-1* during infection compared to Col-0 were selected (log2 fold-change ≥ 1 and adjusted P-value ≤ 0.05) only 12 genes fell within these limits, 7 which were up-regulated and 5 which were down-regulated. This suggests that changes in gene expression that lead to a tolerance response may be much subtler; a shift in expression levels perhaps rather that the complete switching off or on of genes.

4.4.1 How Does Infection Impact on Host Gene Expression in Col-0?

Previously two studies have looked to examine global host gene expression during clubroot infection (Siemens et al. 2006; Agarwal et al. 2011). Agarwal *et al* looked to examine changes in gene expression in the primary stages of infection: 4, 7 and 10 DPI roots (2011). While Siemens *et al* examined changes in gene expression at an early time point, 10DPI, before symptom development and a later time point, 23DPI, when a gall had formed (2006). Although different time-points were examined here there were many similarities in the functional groups of genes that were seen to be differentially regulated.

GO analysis of genes up-regulated in Col-0 14DPI indicated that genes associated with cell division were significantly enriched in the up-regulated genes. Siemens *et al* also found that genes involved in growth and cell cycle control were induced 10DPI (2006). During clubroot infection a gall forms as a consequence of increased cell division and expansion. The data presented in Chapter 2 indicates that gall formation is initiated around 14DPI therefore it is not surprising to see an increase in the expression of cell division related genes here. This up-regulation of cell division related genes would lead to the increase in cell number see in Col-0 hypocotyl cross-sections 21DPI.

Genes associated with decreased oxygen levels were also found to be up-regulated in infected Col-0 14DPI compared to uninfected tissue including gene associated with the GO terms: response to hypoxia, response to decreased oxygen levels and response to oxygen levels. As clubroot induces a gall to form, caused by extensive cell division and expansion, it seems likely that as the tissue size increases the diffusion of O_2 will be impaired thus resulting in reduced O_2 levels in the tissue. Very low levels of O_2 have been recorded in galls on *Acacia longifolia* caused by a Pteromalid wasp: *Trichilogaster acaciaelongifoliae* (Haiden et al. 2012). Suggesting that gall formation does lead to hypoxic conditions, which results in an up-regulation of genes in response to low O_2.

At 14DPI genes associated with the GO terms: regulation of reactive oxygen species metabolic process and regulation of hydrogen peroxide metabolic process were found to be significantly up-regulated in infected Col-0 plants. Several detoxification genes were found to be significantly up-regulated. In line with this finding four proteins associated with detoxification of reactive oxygen species (ROS) were found to be up-regulated 4DPI in *A. thaliana* hypocotyl/roots (Devos et al. 2006). Proteins associated with detoxification of ROS were also found to be differentially expressed in *B. napus* infected roots, initially being down-regulated at 12 hours after inoculation, then up-regulated 24, 48 and 72 hours after

inoculation (Cao et al. 2008). The authors stated that the initial down-regulation followed by up-regulation of detoxification enzymes was consistent with the biotrophic nature of the infection (Cao et al. 2008). ROS have been shown to increase in plants as a general defence response to pathogens, it is likely that detoxification genes/proteins are up-regulated during clubroot infection to combat the initial increase in ROS protecting host cells from potential damage but also protecting the pathogen from damage (Cao et al. 2008). Genes associated with the respiratory burst were found to be down-regulated at 14DPI in Col-0. They were also found to be repressed at 4DPI in Col-0 roots (Agarwal et al. 2011). The authors suggested that there was a down-regulation of the oxidative burst during clubroot infection so that proliferation of *P. brassicae* could occur (Agarwal et al. 2011). It seems likely that initially infection causes the production of ROS as a general defence mechanism, this leads to production of detoxification enzymes to protect the plants own cells and then a dampening of the respiratory burst genes allowing the compatible interaction between *A. thaliana* and *P. brassicae* to proceed. This was found to be the case during infection of *Phaseolus vulgaris*; French beans by *Botrytis cinerea* a fungal necrotrophic pathogen (Unger et al. 2005). There was found to be an initial unspecific induction of the oxidative burst followed by a second stronger and specific induction, it was found that in compatible plant-pathogen interactions this second oxidative burst was suppressed allowing infection to advance (Unger et al. 2005).

In keeping with the infection of *A. thaliana* by *P. brassicae* being a compatible interaction genes associated with plant defence related GO terms were found to be significantly enriched in the genes down-regulated in Col-0 14DPI. Siemens *et al* found that the majority of defence related genes were either not differentially regulated or down-regulated during infection, indicating the host was not initiating a defence response towards the pathogen (2006). Some defence-related genes were found to be up-regulated; the authors stated that there was possibly an initial defence response which was then shifted in favour of the pathogen leading to successful infection (Siemens et al. 2006).

MAPMAN analysis of secondary metabolism biosynthetic genes indicated that the general trend was a down-regulation of associated genes at 14DPI in Col-0. However, other researchers have found secondary metabolic pathways to be up-regulated during infection (Ludwig-Müller et al. 2009). GO analysis of genes down-regulated genes from infected Col-0 indicated the flavonoid biosynthesis was down-regulated. This is in contrast to Siemens *et al* who found that secondary metabolism and in particular flavonoid biosynthesis was up-regulated 23DPI (2006). Agarwal *et al* found secondary metabolism down-regulated at 4DPI but up-regulated at 7DPI (2011). These discrepancies could possibly be due to the differing

time points examined. Lignin associated genes were down-regulated at 14DPI in Col-0. Lignin biosynthesis was also found to be down-regulated in Col-0 roots 4DPI (Agarwal et al. 2011). A decrease in proteins involved in lignin biosynthesis was also seen in infected *B. napus* plants (Cao et al. 2008). It was shown that infection in *A. thaliana* leads to a reduction in xylem formation and a reduction in xylem associated transcripts (Malinowski et al. 2012). Reduced xylem production as a consequence of infection was also seen here in Chapter 2. Therefore a reduction in xylogenesis possibly leads to a decrease in lignin biosynthesis during infection. Reactive oxygen species were found to be required for lignifications during infection (Barcelo 1998). Therefore the increase ROS detoxification and down-regulation of the respiratory burst could be associated with the down-regulation of lignin biosynthesis.

4.4.2 How is Gene Expression Different in *ein5-1*?

The genes up-regulated in *ein5-1* during infection were very similar to those up-regulated in Col-0, again highlighting the similarity of infection in both lines. When a GO analysis of genes up-regulated in *ein5-1* during infection was carried out it was found that only 7 out of 143 GO terms were not also significantly enriched in up-regulated genes in infected Col-0 plants. Of these GO terms 3 were associated with salicylic acid: cellular response to salicylic acid stimulus, salicylic acid mediated signalling pathway and response to salicylic acid. Salicylic acid is a hormone involved in plant defence against pathogens and is an inducer of systemic acquired resistance, reviewed in Thatcher et al. (2005). It is tempting to speculate that *ein5-1* tolerance response is due to an increase in salicylic acid related activity during infection.

Salicylic acid related genes were found to be down-regulated 23DPI in *A. thaliana* roots/hypocotyls (Siemens et al. 2006). Agarwal *et al* also found several genes related to salicylic acid biosynthesis to be down-regulated at 4DPI (2011). In addition to this they found that *A. thaliana* plants treated with salicylic acid before infection were shown to strongly suppress clubroot disease (Agarwal et al. 2011). Infected salicylic acid treated plants were much healthier than untreated plants; at 50DPI only 50 % of the treated plants showed signs of infection while all of the un-treated plant were severely infected. It was concluded that manipulations of the salicylic biosynthesis pathway may prove to be a useful tool in increasing resistance to clubroot infection. In addition to this it was found that application of salicylic acid to the roots of *Brassica oleracea* variant *italic* (Broccoli) significantly reduced galling during infection (Lovelock et al. 2012). Again the authors conclude that manipulations salicylic acid biosynthesis pathways may provide new avenues for clubroot control and the pre-treatment of seeds with salicylic acid before treatment may lead to in field resistance.

If *ein5-1* plants were up-regulating salicylic acid biosynthesis it may account for the tolerance response during infection. Expression of selected salicylic acid biosynthesis genes were not found to be up-regulated in *ein5-1* (data not shown). This does not necessarily indicate that salicylic acid levels are not elevated, as a change in the flux of metabolites through the pathway may also cause elevated levels of salicylic acid. Further work should look to examine levels of salicylic acid levels in both Col-0 and *ein5-1* directly in order to establish whether elevated salicylic acid plays a role in the tolerance response of *ein5-1*.

Flavonoids have been shown to have functions in plant defence against pathogens, herbivores and environmental stresses, reviewed in Treutter (2005). They have been shown to possess antibacterial, antifungal and antiviral activities (Orhan et al. 2010). Several flavonoid biosynthesis genes were significantly up-regulated in infected *ein5-1* compared to Col-0. As discussed above, other researchers have found flavonoid related genes to be up-regulated during infection in Col-0 (Siemens et al. 2006). Flavonoids were also found to accumulate during gall formation in *A. thaliana*, in addition loss of flavonoids resulted in slight tolerance at low infection pressures (Päsold et al. 2010). However, treatment with flavonoids did not lead to a reduction in gall size (Päsold et al. 2010). The authors suggested flavonoids play a role in adjusting auxin efflux in galls leading to increased levels of auxin (Päsold et al. 2010). Although a role for flavonoids as protective substances was not completely ruled out (Päsold et al. 2010). Application of prohexadione-calcium, an inhibitor of flavanone-3-hydroxylase, was found to result in reduced clubroot symptoms although a direct link with reduced flavonoid levels was not established (Päsold and Ludwig-Müller 2013). This evidence suggests that the up-regulation of flavonoid biosynthesis genes does not play a role in the tolerance response to *ein5-1*. Possibly the induction of flavonoids seen in Col-0 by other researchers occurs at an earlier time point in *ein5-1,* which could lead to flavonoid biosynthesis genes being significantly up-regulated in *ein5-1* but not Col-0. Although, as flavonoids have been implicated in defence it may be of interest to further explore their roles in clubroot infection and the response of *ein5-1* to clubroot.

Both salicylic acid and flavonoids were highlighted as being of interest during infection of *ein5-1* compared to Col-0. Both are phenylpropanoid secondary metabolites produced downstream of the shikimate acid pathway, phenylpropanoids have been implicated in the plants response to abiotic and biotic stresses (Vogt 2010). MAPMAN analysis indicated that secondary metabolism was down-regulated in both Col-0 and *ein5-1*. However, it appeared that compared to Col-0 secondary metabolism in *ein5-1* was up-regulated during infection. It could possibly be that a shift in secondary metabolite content leads to *ein5-1* being tolerant to clubroot infection; as there would be an increased defence response. However, in contrast

to the findings here, many secondary metabolic pathways have been found to be up-regulated during clubroot infection (Ludwig-Müller et al. 2009). This is an area of clubroot research that needs to be explored further. A metabolomics study with both *ein5-1* and Col-0 looking to further explore the role of secondary metabolites during clubroot infection would be a possible line of investigation for future work.

4.5 Conclusions

A microarray analysis was conducted to examine changes in gene expression during infection of both Col-0 and *ein5-1*. It appeared that infection impacted on gene expression in Col-0 and *ein5-1* in a similar manner. Infection caused alterations in gene expression relating to cell division, oxygen levels, production of ROS, flavonoid and lignin biosynthesis. Two groups of secondary metabolites appeared to be involved during infection of *ein5-1*. Salicylic acid related genes were enriched in a GO analysis of up-regulated genes from infected *ein5-1* but were not found to be enriched in up-regulated genes from infected Col-0. Several flavonoid biosynthesis genes were up-regulated during infection in *ein5-1* but not in Col-0. These results suggested that secondary metabolites may be involved in the tolerance response of *ein5-1*. The results of this chapter have indicated several avenues for further investigation into the mechanisms behind the tolerance of *ein5-1* to clubroot infection.

Chapter 5: General Discussion

The work presented here used both targeted and un-targeted approaches to examine the molecular mechanisms underlying gall formation during clubroot infection in *A. thaliana*. In Chapter 2 it was shown that the mutant *ein5-1* is tolerant to clubroot infection. Gall formation was delayed by approximately 7 days in *ein5-1* compared to Col-0. This appeared to be a result of delays in host symptom development. *ein5-1* was able to maintain cellular organisation for a longer period than Col-0 and correct cell differentiation was sustained for longer in *ein5-1* than Col-0. The onset of pathogen induced cell division and expansion also appeared delayed in infected *ein5-1*. In addition pathogen development and migration seemed to be delayed, as secondary plasmodia had not colonised as much tissue in *ein5-1* plants and were much fewer in number than in Col-0. Cause and effect was not proven; a delay in pathogen development could lead to a delay in symptom development or *vice versa*.

In addition to this it was found that the miRNA-biosynthesis mutant *hen1-5* exhibited a response to clubroot that was reminiscent of that seen in *ein5-1*, see Chapter 3. With a subset of infected *hen1-5* plants producing smaller galls, which appeared to be a consequence of both delayed symptom and pathogen number/development. As both HEN1 and EIN5 are involved in miRNA-induced silencing this indicated that perturbations to the miRNA pathway may lead to tolerance to clubroot infection.

In Chapter 4 a microarray analysis was used to examine the changes in gene expression that occur in infected *ein5-1* plants and contrast these with infection-induced changes in gene expression in Col-0. The output from this analysis indicated that salicylic acid related genes were enriched in the up-regulated genes from infected *ein5-1* plants contrasted with up-regulated genes from infected Col-0 plants. As salicylic acid is involved in aspects of plant defence this indicated that an increase in the salicylic acid response may be responsible for *ein5-1* tolerance when infected with clubroot.

Throughout this work the response of *ein5-1* to clubroot has been termed a tolerance response as opposed to a resistance response. In terms of this work a tolerant plant is defined as a one which when subjected to clubroot infection displayed symptoms which were less severe than those of the infected WT plants. In addition tolerant plants were able to maintain their normal developmental processes for a longer time while under infection pressure than WT plants and appeared to contain fewer and less developed pathogens than WT. The term tolerance was used here because the disease appeared to be slowed in its progression rather than halted i.e. it is a compatible reaction. This is contrast to a plant being

resistant, which would be termed an incompatible reaction. Resistance is usually conferred by a single dominant gene and leads to a hypersensitive response, which is the death of host cells surrounding the site of infection thus preventing spread of the pathogen (Fuchs and Sacristan, 1995 and Brun *et al*, 2010). This type of resistance response in *Arabidopsis* to clubroot infection, an absence of typical disease symptoms and brown spots on the root indicting host cell necrosis, is well documented (Fuchs and Sacristan, 1995; Kobelt 2000). This typical resistance response is not seen in *ein5-1*. Other researchers have used the term partial resistance instead of tolerance. Partial resistance is defined as a compatible host-pathogen interaction but which does limit the extent of the disease either in terms of pathogen number/development or disease severity (Jubault *et al*, 2013). Partial resistance is thought to be a consequence of multiple genes having small effects (Jubault *et al*, 2013). The analysis here has indicated this may be the case with *ein5-1*; therefore it would also be appropriate to call *ein5-1* partially resistant to clubroot.

The results presented here allow a model of *ein5*-1 response to clubroot to be formed, Figure 5.1. Both *ein5-1* and *hen1-5* showed a similar response to clubroot infection, and are involved in miRNA biogenesis (Souret et al. 2004; Li et al. 2005; Yu et al. 2005 and Yang et al. 2006). This may suggest that perturbations to small-RNA induced silencing pathways lead to tolerance to clubroot infection. As salicylic acid related genes were suggested to be up-regulated during infection of *ein5-1* it could be hypothesised that these genes are usually under the regulation of a gene or genes which regulated either directly or indirectly by small-RNAs. During infection of a WT plant salicylic acid related genes are down-regulated as a consequence of silencing pathways. Therefore there is no salicylic acid response and a defence response does not occur which allows a compatible host-pathogen reaction and infection to proceed. This theory is supported by other microarray studies on clubroot infection tissue which have indicated that in a WT plant defence pathways are down-regulated (Siemens *et al*. 2006). As well as the data from Chapter 4 which indicated that defence related GO terms were enriched in down-regulated genes from Col-0 14DPI. In addition a link between salicylic acid and small-RNA pathways has been suggested (Lopez *et* al. 2011 and Bocarra *et al*. 2014). During infection of *ein5-1* this repression of the salicylic acid response is lifted and thus associated plant defence occur lead to a tolerance response to clubroot infection. This is supported by studies that showed that application of salicylic acid to plants resulted in smaller gall formation during clubroot infection (Agarwal et al. 2011; Lovelock et al. 2012). In addition to this it was also found that salicylic acid pathways are induced during clubroot infection of the partially resistant *A. thaliana* accession Bur-0 (Jubault *et al*, 2013). In order to test this model future work should look to further examine the roles of EIN5/XRN4, HEN1, miRNA-induced silencing and salicylic acid during infection.

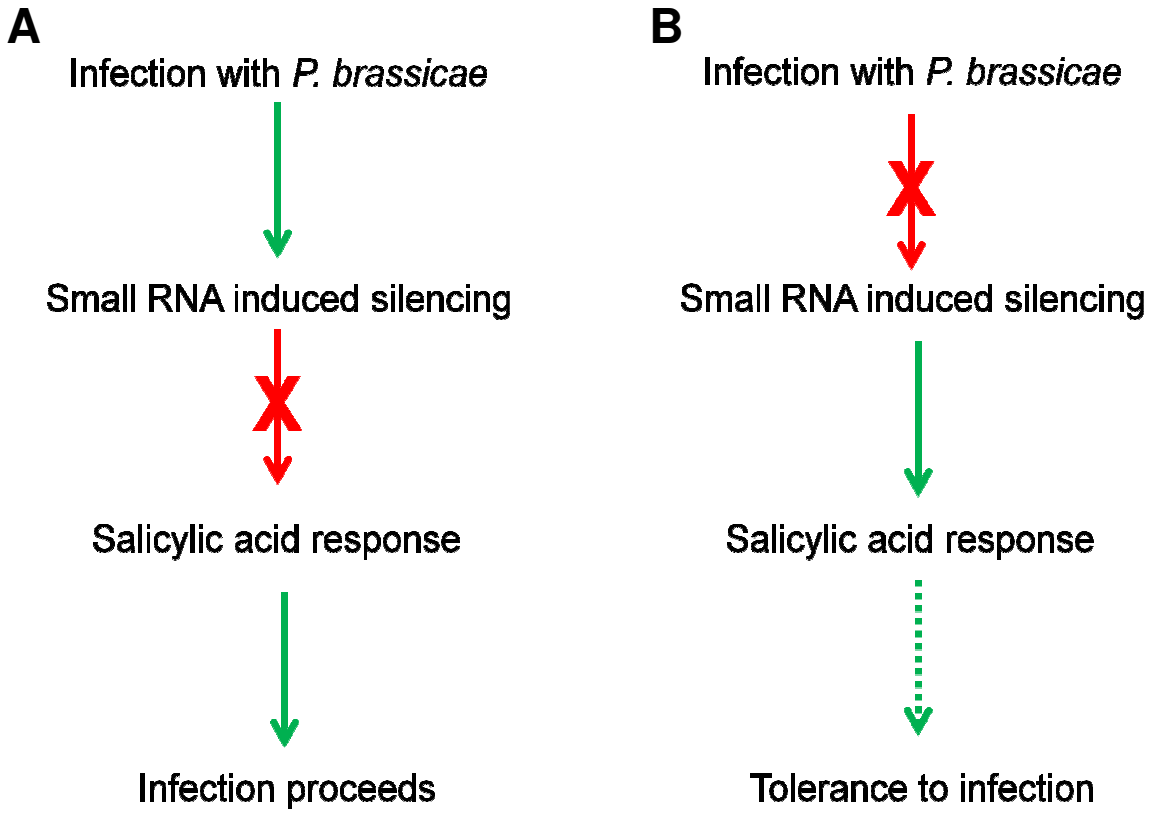

Figure 5.1 Model of the response to clubroot infection of WT and *ein5-1 Arabidopsis* plants. It is hypothesized that interruptions in small RNA induced silencing lead to tolerance to clubroot infection as inhibition of the salicylic acid response (potentially induced by small RNAs or downstream effectors) is lifted. (A) the response of WT plants to infection; small RNA induced silencing occurs which inhibits the salicylic acid response allowing infection to proceed. (B) the response of *ein5-1* to infection; small RNA induced silencing is inhibited which allows the salicylic acid response to proceed leading tolerance to infection. Arrows indicate the status of the subsequent pathway/response. Red arrows = the pathway/response is disrupted. Green arrows = pathway/response occurs. Dashed arrow = an altered disease response from WT.

To further explore the role of the miRNA pathway in clubroot infection a screen of additional miRNA biogenesis mutants would need to be conducted. *Ago1*-27 and *dcl1*-9 did not show a tolerance response when infected but this is potentially due to the redundancy seen in the AGO and DCL proteins (Schauer et al. 2002; Mallory and Vaucheret 2010b.) Therefore a screen of additional DCL and AGO should be conducted alongside a screen of those accessorry proteins discussed in Chapter 3. Additionally known miRNA targets that could play a possible role during clubroot infection could be explored.

The microarray chip used for analysis in Chapter 4 was an Affymetrix GeneChip. This chip has probes which are spread across each transcript. The analysis conducted in Chapter 4 analysed gene expression at the gene level; meaning the expression data for each probe was consolidated to give an expression value for each gene. A further analysis could examine changes in gene expression at the probe level. This may be particularly important as it is known that EIN5/XRN4 degrades the 3' ends of mRNAs produced from miRNA-directed cleavage (Souret et al. 2004). In addition the results from Chapter 3 indicated that disruptions to the miRNA pathway may be involved in lines exhibiting a tolerance response to clubroot infection. Therefore an analysis could be carried out to examine whether there is increase expression from probes which reside at the 3' ends of transcripts in *ein5-1* and if these are up-regulated during infection in *ein5-1* compared to Col-0. If this were the case these transcripts could possibly account for the tolerance response of *ein5-1*. Further analysis of these transcripts could then be performed, for example mutant lines could be examined. This analysis could also make use of the work of Rymarquis *et al* which indicated that a 150 nucleotide sequence downstream of the miRNA-complementary site conferred strong accumulation of the 3' end in the *ein5-1*/*xrn4* mutant (2011). Also 27 hexamers were found to be over-represented in transcripts and 3' ends that accumulated in the *ein5-1*/*xrn4* mutant (Rymarquis et al. 2011). These signatures could aid in the discovery of EIN5/XRN4 targets which may be important during infection.

Further experiments would look to investigate the levels of salicylic acid in both Col-0 and *ein5-1* during infection. If salicylic acid levels were higher during infection in *ein5-1* than in Col-0 it may indicate that the tolerance response of *ein5-1* is related to an induction of salicylic acid. The studies that investigated the role of salicylic acid during infection did not include a microscopic analysis of infected plants treated with salicylic acid (Agarwal et al. 2011; Lovelock et al. 2012). Therefore it would be interesting to re-examine the response of WT *A. thaliana* treated with salicylic acid to clubroot infection, this time including a microscopic examination of infected tissue. This would be useful to both understand the

mechanism of the delay in gall formation observed and to contrast this data with infection in *ein5-1*.

As *hen1-5* also showed an altered response to clubroot infection in comparison with WT, it would be interesting to include this mutant in any future work alongside WT and *ein5-1* plants.

Clubroot affects agriculturally important plants therefore it is important to examine the impact of the disease of not just the root system but of the shoot system as for most crops this portion of the plant creates the income for farmers. Although this work did include some data on the impact on dry shoot weight and rosette diameter, it would have been useful to include data on the impact of the disease on seed production. As this would measure the impact of the disease of the plants whole life cycle, so would have given an important measure of the longevity of tolerance response exhibited by *ein5-1*. Indeed other researchers have used seed production as an effective measure of disease severity in resistant versus susceptible cultivars. For example Hwang *et al* found that seed yield was higher in infected resistant cultivars versus susceptible cultivars (2011). Future screens carried out of infected plants should therefore include measures of seed yield as standard and could also possibly include additional shoot measurements such as plant height. This will help to create a much better picture of a plants response to clubroot infection.

In conclusion, it would appear the most effective way forward in this area of research is to continue to use a combination of both targeted and un-targeted approaches to uncover and establish the mechanisms underlying gall formation. Once a clear understanding of the pathogen-induced changes in host gene expression, metabolism, etc. that occur during infection has been established it will lead to the ability to engineer strategies for resistance to be implemented in the field in the hope of significantly affecting the impact of clubroot infection on crop production.

References

Agarwal, A. et al., 2011. Analysis of global host gene expression during the primary phase of the Arabidopsis thaliana – Plasmodiophora brassicae interaction. *FUNCTIONAL PLANT BIOLOGY*, 38(6), pp.462–478.

Aist, J. and Williams, P.H., 1971. CYTOLOGY AND KINETICS OF CABBAGE ROOT HAIR PENETRATION BY PLASMODIOPHORA-BRASSICAE. *Canadian Journal of Botany*, 49(11), p.2023.

Alix, K. et al., 2007. Exploiting natural genetic diversity and mutant resources of Arabidopsis thaliana to study the A.thaliana-Plasmodiophora brassicae interaction. *Plant Breeding*, 126(2), pp.218–221.

Alonso, J.M. et al., 1999. EIN2, a bifunctional transducer of ethylene and stress responses in Arabidopsis. *Science (New York, N.Y.)*, 284(5423), pp.2148–52.

An, F. et al., 2010. Ethylene-induced stabilization of ETHYLENE INSENSITIVE3 and EIN3-LIKE1 is mediated by proteasomal degradation of EIN3 binding F-box 1 and 2 that requires EIN2 in Arabidopsis. *The Plant cell*, 22(7), pp.2384–401.

Ando, S. et al., 2006. Molecular Cloning of PbSTKL1 Gene from Plasmodiophora brassicae Expressed during Clubroot Development. *Journal of Phytopathology*, 154(3), pp.185–189.

Asano, T. and Kageyama, K., 2006. Growth and movement of secondary plasmodia of Plasmodiophora brassicae in turnip suspension-culture cells. *Plant Pathology*, 55(1), pp.145–151.

Ashburner, M. et al., 2000. Gene Ontology : tool for the unification of biology. *Nature Genetic*, 25(1), pp.25–29.

Barcelo, A., 1998. Hydrogen Peroxide Production is a General Property of the Lignifying Xylem from Vascular Plants. *ANNALS OF BOTANY*, 82(1), pp.97–103.

Baumberger, N. and Baulcombe, D.C., 2005. Arabidopsis ARGONAUTE1 is an RNA Slicer that selectively recruits microRNAs and short interfering RNAs. *Proceedings of the National Academy of Sciences of the United States of America*, 102(33), pp.11928–33.

Bernstein, E. et al., 2001. Role for a bidentate ribonuclease in the initiation step of RNA interference. *Nature*, 409(6818), pp.363–6.

Binder, B.M. et al., 2007. The Arabidopsis EIN3 binding F-Box proteins EBF1 and EBF2 have distinct but overlapping roles in ethylene signaling. *The Plant cell*, 19(2), pp.509–23.

Bisson, M.M.A and Groth, G., 2010. New insight in ethylene signaling: autokinase activity of ETR1 modulates the interaction of receptors and EIN2. *Molecular plant*, 3(5), pp.882–9.

Bisson, M.M.A. et al., 2009. EIN2, the central regulator of ethylene signalling, is localized at the ER membrane where it interacts with the ethylene receptor ETR1. *BIOCHEMICAL JOURNAL*, 424(1), pp.1–6.

Bleecker, A. B. et al., 1988. Insensitivity to Ethylene Conferred by a Dominant Mutation in Arabidopsis thaliana. *Science (New York, N.Y.)*, 241(4869), pp.1086–9.

Brodersen, P. et al., 2008. Widespread translational inhibition by plant miRNAs and siRNAs. *Science (New York, N.Y.)*, 320(5880), pp.1185–90.

Buczacki, S.T., 1983. Plasmodiophora. An inter-relationship between biological and practical problems. In *Zoosporic Plant Pathogen*. pp. 161–191.

Burki, F. et al., 2010. Evolution of Rhizaria: new insights from phylogenomic analysis of uncultivated protists. *BMC evolutionary biology*, 10(1), p.377.

Butcher, D.N. et al., 1974. The role of indole glucosinolates in the clubroot disease of the Cruciferae. *Physiological plant pathology*, 4(1), pp.127–140.

Cao, T. et al., 2008. Proteome-level changes in the roots of Brassica napus as a result of Plasmodiophora brassicae infection. *Plant Science*, 174(1), pp.97–115.

Cavalier-smith, T. and Chao, E.E., 2003. Phylogeny and Classification of Phylum Cercozoa (Protozoa). *Protist*, 154, pp.341–358.

Chang, C. et al., 1993. Arabidopsis Ethylene-Response Gene ETR1: Similarity of Product to Two-Component Regulators. *Science*, 262(5133), pp.539–544.

Chao, Q. et al., 1997. Activation of the ethylene gas response pathway in Arabidopsis by the nuclear protein ETHYLENE-INSENSITIVE3 and related proteins. *Cell*, 89(7), pp.1133–44.

Chen, X. et al., 2002. HEN1 functions pleiotropically in Arabidopsis development and acts in C function in the flower. *Development (Cambridge, England)*, 129(5), pp.1085–94.

Clark, K.L. et al., 1998. Association of the Arabidopsis CTR1 Raf-like kinase with the ETR1 and ERS ethylene receptors. *Proceedings of the National Academy of Sciences of the United States of America*, 95(9), pp.5401–6.

Cook, W.R.I. and Schwartz, E.J., 1930. The Life-History, Cytology and Method of Infection of Plasmodiophora brassicae Woron., the Cause of Finger-and-Toe Disease of Cabbages and Other Crucifers. *Philosophical Transactions of the Royal Society B: Biological Sciences*, 218(450-461), pp.283–314.

Dekhuijzen, H., 1981. The occurrence of free and bound cytokinins in plasmodia of Plasmodiophora brassicae isolated from tissue cultures of clubroots. *Plant Cell Reports*, 1(1), pp.18–20.

Dekhuijzen, H. and Overeem, J., 1971. The Role of Cytokinins in Clubroot Formation. *PHYSIOLOGICAL PLANT PATHOLOGY*, 1(2), pp.151–161.

Dekhuijzen, H.M., 1980. The occurrence of free and bound cytokinins in dubroots and Plasmodiophora brassicae infected turnip tissue cultures. *PHYSIOLOGIA PLANTARUM*, 49(2), pp.169–176.

Devos, S. et al., 2006. A hormone and proteome approach to picturing the initial metabolic events during Plasmodiophora brassicae infection on Arabidopsis. *Molecular plant-microbe interactions : MPMI*, 19(12), pp.1431–43.

Devos, S. et al., 2005. Infection of Chinese cabbage by Plasmodiophora brassicae leads to a stimulation of plant growth: impacts on cell wall metabolism and hormone balance. *NEW PHYTOLOGIST*, 166(1), pp.241–250.

Diederichsen, E. et al., 2009. Status and Perspectives of Clubroot Resistance Breeding in Crucifer Crops. *Journal of Plant Growth Regulation*, 28(3), pp.265–281.

Dixon, G.R., 2009. The Occurrence and Economic Impact of Plasmodiophora brassicae and Clubroot Disease. *Journal of Plant Growth Regulation*, 28(3), pp.194–202.

Do, J.H. and Choi, D., 2006. Minireview Molecules and Normalization of Microarray Data : Single-labeled and Dual-labeled Arrays. *Molecules and Cells*, 22(3), pp.254–261.

Dobson, R.L. and Gabrielson, R.L., 1983. Role of Primary and Secondary Zoospores of Plasmodiophora brassicae in the Development of Clubroot in Chinese Cabbage. *Phytopathology*, 73(5), pp.559–561.

Donald, C. and Porter, I., 2009. Integrated Control of Clubroot. *Journal of Plant Growth Regulation*, 28(3), pp.289–303.

Donald, E.C. et al., 2008. Pathology of cortical invasion by Plasmodiophora brassicae in clubroot resistant and susceptible Brassica oleracea hosts. *Plant Pathology*, 57(2), pp.201–209.

Dong, Hong-ping et al., 2004. Downstream Divergence of the Ethylene Signaling Pathway for Harpin-Stimulated Arabidopsis Growth and Insect Defense. *Plant Physiolog*y, 13, pp.3628–3638.

Eden, E. et al., 2009. GOrilla: a tool for discovery and visualization of enriched GO terms in ranked gene lists. *BMC bioinformatics*, 10, p.48.

Evans, J. and Scholes, J.D., 1995. How does clubroot alter the regulation of carbon metabolism in its host? *Aspects of Applied Biology*, 42, pp.125–132.

Fuchs, H. and Sacristan, M., 1996. Identification of a gene in Arabidopsis thaliana controlling resistance to clubroot (Plasmodiophora brassicae) and characterization of the resistance response. *Molecular plant-microbe interactions : MPMI*, 9(2), pp.91–97.

Gagne, J.M. et al., 2004. *Arabidopsis* EIN3-binding F-box 1 and 2 form ubiquitin-protein ligases that repress ethylene action and promote growth by directing EIN3 degradation. *Proceedings of the National Academy of Scinces*, 101(17), pp.2–7.

Gao, Z. et al., 2003. Localization of the Raf-like kinase CTR1 to the endoplasmic reticulum of Arabidopsis through participation in ethylene receptor signaling complexes. *The Journal of biological chemistry*, 278(36), pp.34725–32.

Garcia-Ruiz, H. et al., 2010. Arabidopsis RNA-dependent RNA polymerases and dicer-like proteins in antiviral defense and small interfering RNA biogenesis during Turnip Mosaic Virus infection. *The Plant cell*, 22(2), pp.481–96.

Gazzani, S. et al., 2004. A link between mRNA turnover and RNA interference in Arabidopsis. *Science (New York, N.Y.)*, 306(5698), pp.1046–8.

Grsic-Rausch, S. et al., 2000. Expression and localization of nitrilase during symptom development of the clubroot disease in Arabidopsis. *Plant physiology*, 122(2), pp.369–78.

Guo, H. and Ecker, J.R., 2003. Plant Responses to Ethylene Gas Are Mediated by SCFEBF1/EBF2-Dependent Proteolysis of EIN3 Transcription Factor. *Cell*, 115(6), pp.667–677.

Guzmán, P. and Ecker, J.R., 1990. Exploiting the Triple Response of Arabidopsis to Identify Ethylene-Related Mutants. *The Plant cell*, 2(6), pp.513–523.

Haiden, S. A, et al., 2012. Benefits of photosynthesis for insects in galls. *Oecologia*, 170(4), pp.987–97.

Han, M.-H. et al., 2004. The Arabidopsis double-stranded RNA-binding protein HYL1 plays a role in microRNA-mediated gene regulation. *Proceedings of the National Academy of Sciences of the United States of America*, 101(4), pp.1093–8.

Helariutta, Y. et al., 2000. The SHORT-ROOT gene controls radial patterning of the Arabidopsis root through radial signaling. *Cell*, 101(5), pp.555–67.

Hua, J. et al., 1998. EIN4 and ERS2 are members of the putative ethylene receptor gene family in Arabidopsis. *The Plant cell*, 10(8), pp.1321–32.

Hua, J. et al., 1995. Ethylene insensitivity conferred by Arabidopsis ERS gene. *Science (New York, N.Y.)*, 269(5231), pp1712-1714.

Hua, J. and Meyerowitz, E.M., 1998. Ethylene responses are negatively regulated by a receptor gene family in Arabidopsis thaliana. *Cell*, 94(2), pp.261–71.

Hwang, S. et al., 2012. Pathogen profile Plasmodiophora brassicae : a review of an emerging pathogen of the Canadian canola (Brassica napus) crop. *Molecular Plant Pathology*, 13(2), pp.105–113.

Ingram, D.S. and Tommerup, C., 1972. The Life History of Plasmodiophora brassicae Woron. *PROCEEDINGS OF THE ROYAL SOCIETY SERIES B-BIOLOGICAL SCIENCES*, 180(1058), pp.103–112.

Irizarry, R. A., 2003. Summaries of Affymetrix GeneChip probe level data. *Nucleic Acids Research*, 31(4), p.15.

Ishikawa, T. et al., 2007. Molecular cloning of Brassica rapa nitrilases and their expression during clubroot development. *Molecular Plant Pathology*, 8(5), pp.623–637.

Ju, C. et al., 2012. CTR1 phosphorylates the central regulator EIN2 to control ethylene hormone signaling from the ER membrane to the nucleus in Arabidopsis. *Proceedings of the National Academy of Sciences of the United States of America*, 109(47), pp.19486–19491.

Kendrick, M.D. and Chang, C., 2008. Ethylene signaling: new levels of complexity and regulation. *Current opinion in plant biology*, 11(5), pp.479–85.

Kieber, J.J. et al., 1993. CTR1, a negative regulator of the ethylene response pathway in arabidopsis, encodes a member of the Raf family of protein kinases. *Cell*, 72(3), pp.427–441.

Klewer, A. et al., 2001. Restriction fragment length polymorphism markers to characterize Plasmodiophora brassicae single-spore isolates with different virulence patterns. *JOURNAL OF PHYTOPATHOLOGY-PHYTOPATHOLOGISCHE ZEITSCHRIFT*, 149(3-4), pp.121–127.

Knaust, A. and Ludwig-Müller, J., 2012. The Ethylene Signaling Pathway is Needed to Restrict Root Gall Growth in Arabidopsis after Infection with the Obligate Biotrophic Protist Plasmodiophora brassicae. *Journal of Plant Growth Regulation*, 32(1), pp.9–21.

Koch, E. et al., 1991. INFECTION OF ARABIDOPSIS-THALIANA BY PLASMODIOPHORA-BRASSICAE. *JOURNAL OF PHYTOPATHOLOGY-PHYTOPATHOLOGISCHE ZEITSCHRIFT*, 132(2), pp.99–104.

Konishi, M. and Yanagisawa, S., 2008. Ethylene signaling in Arabidopsis involves feedback regulation via the elaborate control of EBF2 expression by EIN3. *The Plant journal : for cell and molecular biology*, 55(5), pp.821–31.

Kurihara, Y. et al., 2006. The interaction between DCL1 and HYL1 is important for efficient and precise processing of pri-miRNA in plant microRNA biogenesis The interaction between DCL1 and HYL1 is important for efficient and precise processing of pri-miRNA in plant microRNA biogen. *RNA*, 12, pp.206–212.

Kurihara, Y. and Watanabe, Y., 2004. Arabidopsis micro-RNA biogenesis through Dicer-like 1 protein functions. *Proceedings of the National Academy of Sciences of the United States of America*, 101(34), pp.12753–8.

Di Laurenzio, L. et al., 1996. The SCARECROW gene regulates an asymmetric cell division that is essential for generating the radial organization of the Arabidopsis root. *Cell*, 86(3), pp.423–33.

Leboldus, J.M. et al., 2012. Adaptation to Brassica Host Genotypes by a Single-Spore Isolate and Population of Plasmodiophora brassicae (Clubroot). *Plant Disease*, 6, pp.833–838.

Li, J. et al., 2005. Methylation protects miRNAs and siRNAs from a 3'-end uridylation activity in Arabidopsis. *Current biology : CB*, 15(16), pp.1501–7.

Liu, Y. et al., 2012. Expression of Nitrilases in Brassica juncea var. tumida Tsen in Root Galls Caused by Plasmodiophora brassicae. *Journal of Integrative Agriculture*, 11(1), pp.100–108.

Llave, C. et al., 2002. Cleavage of Scarecrow-like mRNA targets directed by a class of Arabidopsis miRNA. *Science (New York, N.Y.)*, 297(5589), pp.2053–6..

Lobbes, D. et al., 2006. SERRATE: a new player on the plant microRNA scene. *EMBO reports*, 7(10), pp.1052–8.

Lovelock, D. a. et al., 2012. Salicylic acid suppression of clubroot in broccoli (Brassicae oleracea var. italica) caused by the obligate biotroph Plasmodiophora brassicae. *Australasian Plant Pathology*, 42(2), pp.141–153.

Ludwig-müller, A.J. et al., 1993. Concentrations of indole-3-acetic acid in plants of of Chinese tolerant cabbage and susceptible infected with varieties Plasmodiophora brassicae Woron. *NEW PHYTOLOGIST*, 125(4), pp.763–769.

Ludwig-Muller, J. et al., 1999. The host range of Plasmodiophora brassicae and its relationship to endogenous glucosinolate content. *NEW PHYTOLOGIST*, 141(3), pp.443–458.

Ludwig-Müller, J. et al., 1999. Indole glucosinolate and auxin biosynthesis in Arabidopsis thaliana (L.) Heynh. glucosinolate mutants and the development of clubroot disease. *Planta*, 208(3), pp.409–19.

Ludwig-Müller, J. et al., 2009. Metabolism and Plant Hormone Action During Clubroot Disease. *Journal of Plant Growth Regulation*, 28(3), pp.229–244.

Ludwig-Müller, J. and Schuller, A., 2008. What can we learn from clubroots: alterations in host roots and hormone homeostasis caused by Plasmodiophora brassicae. *European Journal of Plant Pathology*, 121(3), pp.291–302.

Malinowski, R. et al., 2012. Gall formation in clubroot-infected Arabidopsis results from an increase in existing meristematic activities of the host but is not essential for the completion of the pathogen life cycle. *The Plant journal : for cell and molecular biology*, 71(2), pp.226–38.

Mallory, A. and Vaucheret, H., 2010. Form, function, and regulation of ARGONAUTE proteins. *The Plant cell*, 22(12), pp.3879–89.

Matsumoto-Kitano, M. et al., 2008. Cytokinins are central regulators of cambial activity. *Proceedings of the National Academy of Sciences of the United States of America*, 105(50), pp.20027–31.

Maunoury, N. and Vaucheret, H., 2011. AGO1 and AGO2 act redundantly in miR408-mediated Plantacyanin regulation. *PloS one*, 6(12), p28729.

Merchante, C. et al., 2013. Ethylene signaling: simple ligand, complex regulation. *Current opinion in plant biology*, 16(5), pp.554–60.

Michael J . Prigge and D . Ry Wagner, 2013. The Arabidopsis SERRATE Gene Encodes a Zinc-Finger Protein Required for Normal Shoot Development. *The Plant Cell*, 13(6), pp.1263-1279.

Mithen, R. and Magrath, R., 1992. A contribution to the life history of Plasmodiophora brassicae: secondary plasmodia development in root galls of Arabidopsis thaliana. *Mycological Research*, 96(10), pp.877–885.

Morel, J. et al., 2002. Fertile Hypomorphic ARGONAUTE (ago1) Mutants Impaired in Post-Transcriptional Gene Silencing and Virus Resistance. *The Plant Cell*, 14, pp.629–639.

Mousdale, D., 1981. ENDOGENOUS INDOLYL-3-ACETIC ACID AND PATHOGEN-INDUCED PLANT-GROWTH DISORDERS - DISTINCTION BETWEEN HYPERPLASIA AND NEOPLASTIC DEVELOPMENT. *Experientia*, 37(9), pp.972–973.

Müller, P. and Hilgenberg, W., 1986. Isomers of zeatin and zeatin riboside in clubroot tissue : evidence for trans-zeatin biosynthesis by Plasmodiophora brassicae. *Physiologia Plantarum*, 66(2), pp.245–250.

Olmedo, G. et al., 2006. *ETHYLENE-INSENSITIVE5* encodes a 5'-3' exoribonuclease required for regulation of the EIN3-targeting F-box proteins EBF1/2. *Proceedings of the National Academy of Sciences*, 103(36), pp.13286-13293.

Orhan, D.D. et al., 2010. Antibacterial, antifungal, and antiviral activities of some flavonoids. *Microbiological research*, 165(6), pp.496–504.

Oxley, S., 2007. Clubroot disease of oilseed rape and other brassica crops. *The Scottish Agricultural Colleage TN602*.

Parent, J.-S. et al., 2012. The origin and effect of small RNA signaling in plants. *Frontiers in plant science*, 3, p.179.

Park, M.Y. et al., 2005. Nuclear Processing and Export of microRNAs in Arabidopsis. *Proceedings of the National Academy of Sciences*, 102(10), pp.3691–3696.

Park, W. et al., 2002. CARPEL FACTORY, a Dicer homolog, and HEN1, a novel protein, act in microRNA metabolism in Arabidopsis thaliana. *Current biology : CB*, 12(17), pp.1484–95.

Pashkovskiy, P.P. and Ryazansky, S.S., 2013. Biogenesis, evolution, and functions of plant microRNAs. *Biochemistry. Biokhimiia*, 78(6), pp.627–37.

Päsold, S. et al., 2010. Flavonoid accumulation in Arabidopsis thaliana root galls caused by the obligate biotrophic pathogen Plasmodiophora brassicae. *Molecular Plant Pathology*, 11(4), pp.545–562.

Päsold, S. and Ludwig-Müller, J., 2013. Reduction of clubroot (Plasmodiophora brassicae) formation in Arabidopsis thaliana after treatment with prohexadione-calcium, an inhibitor of oxoglutaric acid-dependent dioxygenases. *Plant Pathology*, 62(6), pp.1357–1365.

Pattanayak, D. et al., 2012. Plant RNA Interference Pathways: Diversity in Function, Similarity in Action. *Plant Molecular Biology Reporter*, 31(3), pp.493–506.

Penny-Evans, C.A., 2000. *Strategies for engineering resistance to Plasmodiophora brassicae woron.* PhD Thesis, The University of Sheffield.

Potuschak, T. et al., 2003. EIN3-dependent regulation of plant ethylene hormone signaling by two arabidopsis F box proteins: EBF1 and EBF2. *Cell*, 115(6), pp.679–89.

Potuschak, T. et al., 2006. The exoribonuclease XRN4 is a component of the ethylene response pathway in Arabidopsis. *The Plant cell*, 18(11), pp.3047–57.

Prigge, M.J. and Wagner, D.R., 2001. The arabidopsis serrate gene encodes a zinc-finger protein required for normal shoot development. *The Plant cell*, 13(6), pp.1263–79.

Qiao, H. et al., 2009. Interplay between ethylene, ETP1/ETP2 F-box proteins, and degradation of EIN2 triggers ethylene responses in Arabidopsis. *Genes & development*, 23(4), pp.512–21.

Qiao, H. et al., 2012. Processing and subcellular trafficking of ER-tethered EIN2 control response to ethylene gas. *Science (New York, N.Y.)*, 338(6105), pp.390–3.

Raa, J.A.N., 1971. Indole-3-acetic Acid Levels and the Role of Indole-3-acetic Acid Oxidase in the Normal Root and Clubroot of Cabbage. *Physiologia plantarum*, 25(1), pp.130–134.

Rajagopalan, R. et al., 2006. A diverse and evolutionarily fluid set of microRNAs in Arabidopsis thaliana. *Genes & development*, 20(24), pp.3407–25.

Rastas, M. et al., 2012. Occurrence of Plasmodiophora brassicae in Finnish turnip rape and oilseed rape fields. *Agricultural and Food Science*, 21(2), pp.141–158.

RAUSCH, T. et al., 1981. INFLUENCE OF CLUBROOT DISEASE ON THE GROWTH-KINETICS OF CHINESE CABBAGE. *PHYTOPATHOLOGISCHE ZEITSCHRIFT-JOURNAL OF PHYTOPATHOLOGY*, 102(1), pp.28–33.

Reinhart, B.J. et al., 2002. MicroRNAs in plants. *Genes & development*, 16(13), pp.1616–26.

Rodríguez, F.I., 1999. A Copper Cofactor for the Ethylene Receptor ETR1 from Arabidopsis. *Science*, 283(5404), pp.996–998.

Roman, G. et al., 1995. Genetic Analysis of Ethylene Signal Transduction in *Arabidopsis thaliana*: Five Novel Mutant Loci Integrated into a Stress Response Pathway. *Genetics*, 139, pp.1393-1409.

Rymarquis, L. A. et al., 2011. Evidence that XRN4, an Arabidopsis homolog of exoribonuclease XRN1, preferentially impacts transcripts with certain sequences or in particular functional categories. *RNA (New York, N.Y.)*, 17(3), pp.501–11.

Sakai, H. et al., 1998. ETR2 is an ETR1-like gene involved in ethylene signaling in Arabidopsis. *Proceedings of the National Academy of Sciences of the United States of America*, 95(10), pp.5812–7.

Schauer, S.E. et al., 2002. DICER-LIKE1: blind men and elephants in Arabidopsis development. *Trends in plant science*, 7(11), pp.487–91.

Siemens, J. et al., 2011. Extracellular invertase is involved in the regulation of clubroot disease in Arabidopsis thaliana. *Molecular Plant Pathology* , 12, pp.247–262.

Siemens, J. et al., 2009. Monitoring expression of selected Plasmodiophora brassicae genes during clubroot development in Arabidopsis thaliana. *Plant Pathology*, 58(1), pp.130–136.

Siemens, J. et al., 2002. The Interaction of Plasmodiophora brassicae and Arabidopsis thaliana : Parameters for Disease Quantification and Screening of Mutant Lines. *JOURNAL OF PHYTOPATHOLOGY-PHYTOPATHOLOGISCHE ZEITSCHRIF*, 150(11-12), pp.592–605.

Siemens, J. et al., 2006. Transcriptome analysis of Arabidopsis clubroots indicate a key role for cytokinins in disease development. *Molecular plant-microbe interactions : MPMI*, 19(5), pp.480–94.

Solano, R. et al., 1998. Nuclear events in ethylene signaling: a transcriptional cascade mediated by ETHYLENE-INSENSITIVE3 and ETHYLENE-RESPONSE-FACTOR1. *Genes & Development*, 12(23), pp.3703–3714.

Souret, F.F. et al., 2004. AtXRN4 degrades mRNA in Arabidopsis and its substrates include selected miRNA targets. *Molecular cell*, 15(2), pp.173–83.

Sunkar, R. and Zhu, J., 2004. Novel and Stress-Regulated MicroRNAs and Other Small RNAs from Arabidopsis. , 16, pp.2001–2019.

Supek, F. et al., 2011. REVIGO summarizes and visualizes long lists of gene ontology terms. *PloS one*, 6(7), p21800.

Thatcher, L. et al., 2005. Review : Plant defence responses : what have we learnt from Arabidopsis? *FUNCTIONAL PLANT BIOLOGY*, 32(1), pp.1–19.

Thimm, O. et al., 2004. Mapman: a User-Driven Tool To Display Genomics Data Sets Onto Diagrams of Metabolic Pathways and Other Biological Processes. *The Plant Journal*, 37(6), pp.914–939.

Timpte, C.S. et al., 1992. Effects of the axr2 mutation of Arabidopsis on cell shape in hypocotyl and inflorescence. *Planta*, 188(2), pp.271–8.

Tommerup, I.C. and Ingram, D.S., 1971. THE LIFE-CYCLE OF PLASMODIOPHORA BRASSICAE WORON . IN BRASSICA TISSUE CULTURES AND IN INTACT ROOTS. *NEW PHYTOLOGIST*, 70(2), pp.327–332.

Treutter, D., 2005. Significance of flavonoids in plant resistance and enhancement of their biosynthesis. *Plant biology (Stuttgart, Germany)*, 7(6), pp.581–91.

Unger, C. et al., 2005. Suppression of the Defence-Related Oxidative Burst in Bean Leaf Tissue and Bean Suspension Cells by the Necrotrophic Pathogen Botrytis cinerea. *Journal of Phytopathology*, 153(1), pp.15–26.

Vazquez, F. et al., 2008. Evolution of Arabidopsis MIR genes generates novel microRNA classes. *Nucleic acids research*, 36(20), pp.6429–38.

Vazquez, F. et al., 2004. The nuclear dsRNA binding protein HYL1 is required for microRNA accumulation and plant development, but not posttranscriptional transgene silencing. *Current biology : CB*, 14(4), pp.346–51.

Vogt, T., 2010. Phenylpropanoid biosynthesis. *Molecular plant*, 3(1), pp.2–20.

Wallenhammar, A.C., 1996. Prevalence of Plasmodiophora brassicae in a spring oilseed rape growing area in central Sweden and factors influencing soil infestation levels. *Plant Pathology*, 45(4), pp.710–719.

Wen, X. et al., 2012. Activation of ethylene signaling is mediated by nuclear translocation of the cleaved EIN2 carboxyl terminus. *Cell research*, 22(11), pp.1613–6.

Xie, Z. et al., 2005. Expression of Arabidopsis MIRNA Genes . *Plant Physiology*, 138 , pp.2145–2154.

Xie, Z. and Qi, X., 2008. Diverse small RNA-directed silencing pathways in plants. *Biochimica et biophysica acta*, 1779(11), pp.720–4.

Yang, Z. et al., 2006. HEN1 recognizes 21-24 nt small RNA duplexes and deposits a methyl group onto the 2’ OH of the 3' terminal nucleotide. *Nucleic acids research*, 34(2), pp.667–75.

Yu, B. et al., 2005. Methylation as a crucial step in plant microRNA biogenesis. *Science (New York, N.Y.)*, 307(5711), pp.932–5.

Appendix

GO terms enriched in down-regulated genes from infected Col-0 vs. uninfected Col-0:

GO Term	Description
GO:0016570	histone modification
GO:0016569	covalent chromatin modification
GO:0016568	chromatin modification
GO:0009909	regulation of flower development
GO:0006325	chromatin organization
GO:0051276	chromosome organization
GO:0048831	regulation of shoot system development
GO:0048580	regulation of post-embryonic development
GO:2000241	regulation of reproductive process
GO:0034968	histone lysine methylation
GO:0016571	histone methylation
GO:0006479	protein methylation
GO:0008213	protein alkylation
GO:0006725	cellular aromatic compound metabolic process
GO:0006139	nucleobase-containing compound metabolic process
GO:0032259	Methylation
GO:0043414	macromolecule methylation
GO:0046483	heterocycle metabolic process
GO:0034641	cellular nitrogen compound metabolic process
GO:0009220	pyrimidine ribonucleotide biosynthetic process
GO:0009218	pyrimidine ribonucleotide metabolic process
GO:0046390	ribose phosphate biosynthetic process
GO:0009260	ribonucleotide biosynthetic process
GO:0006221	pyrimidine nucleotide biosynthetic process
GO:0006220	pyrimidine nucleotide metabolic process
GO:0072528	pyrimidine-containing compound biosynthetic process
GO:0009259	ribonucleotide metabolic process
GO:0019693	ribose phosphate metabolic process
GO:0006807	nitrogen compound metabolic process
GO:1901360	organic cyclic compound metabolic process
GO:0072527	pyrimidine-containing compound metabolic process
GO:2000026	regulation of multicellular organismal development
GO:0006996	organelle organization
GO:0051239	regulation of multicellular organismal process
GO:0044699	single-organism process
GO:0006259	DNA metabolic process
GO:0050793	regulation of developmental process
GO:0051567	histone H3-K9 methylation
GO:0009165	nucleotide biosynthetic process
GO:1901293	nucleoside phosphate biosynthetic process

GO:0006275	regulation of DNA replication
GO:0022402	cell cycle process
GO:0043412	macromolecule modification
GO:0051052	regulation of DNA metabolic process
GO:0044763	single-organism cellular process
GO:1901137	carbohydrate derivative biosynthetic process
GO:0008283	cell proliferation
GO:0090304	nucleic acid metabolic process
GO:0016458	gene silencing
GO:0040029	regulation of gene expression, epigenetic
GO:0006464	cellular protein modification process
GO:0036211	protein modification process
GO:0050789	regulation of biological process
GO:0010605	negative regulation of macromolecule metabolic process
GO:0051726	regulation of cell cycle
GO:0009892	negative regulation of metabolic process
GO:0048645	organ formation
GO:0034654	nucleobase-containing compound biosynthetic process
GO:0006342	chromatin silencing
GO:0045814	negative regulation of gene expression, epigenetic
GO:0010629	negative regulation of gene expression
GO:0032502	developmental process
GO:0065007	biological regulation
GO:0044238	primary metabolic process
GO:0006606	protein import into nucleus
GO:0051170	nuclear import
GO:0048449	floral organ formation
GO:0044271	cellular nitrogen compound biosynthetic process
GO:0006270	DNA replication initiation
GO:0018130	heterocycle biosynthetic process
GO:0032506	cytokinetic process
GO:0000911	cytokinesis by cell plate formation
GO:1902410	mitotic cytokinetic process
GO:0045934	negative regulation of nucleobase-containing compound metabolic process
GO:0009117	nucleotide metabolic process
GO:0055086	nucleobase-containing small molecule metabolic process
GO:0006753	nucleoside phosphate metabolic process
GO:0010558	negative regulation of macromolecule biosynthetic process
GO:2000113	negative regulation of cellular macromolecule biosynthetic process
GO:0051172	negative regulation of nitrogen compound metabolic process
GO:0031324	negative regulation of cellular metabolic process
GO:1901135	carbohydrate derivative metabolic process
GO:0009890	negative regulation of biosynthetic process
GO:0031327	negative regulation of cellular biosynthetic process

GO:0016043	cellular component organization
GO:0006913	nucleocytoplasmic transport
GO:0051169	nuclear transport
GO:0016572	histone phosphorylation
GO:0010564	regulation of cell cycle process
GO:0045892	negative regulation of transcription, DNA-dependent
GO:0051253	negative regulation of RNA metabolic process
GO:0031323	regulation of cellular metabolic process
GO:0009987	cellular process
GO:0010389	regulation of G2/M transition of mitotic cell cycle
GO:0072594	establishment of protein localization to organelle
GO:0048646	anatomical structure formation involved in morphogenesis
GO:0019222	regulation of metabolic process
GO:0019438	aromatic compound biosynthetic process
GO:1901990	regulation of mitotic cell cycle phase transition
GO:1901987	regulation of cell cycle phase transition
GO:0044237	cellular metabolic process
GO:1901566	organonitrogen compound biosynthetic process
GO:0003006	developmental process involved in reproduction
GO:0048523	negative regulation of cellular process
GO:0006796	phosphate-containing compound metabolic process
GO:0016482	cytoplasmic transport
GO:0006793	phosphorus metabolic process
GO:0071840	cellular component organization or biogenesis
GO:0022414	reproductive process
GO:0048519	negative regulation of biological process
GO:0048453	sepal formation
GO:0048451	petal formation
GO:0050794	regulation of cellular process
GO:0007017	microtubule-based process
GO:0071704	organic substance metabolic process
GO:0017038	protein import
GO:0008152	metabolic process
GO:1901362	organic cyclic compound biosynthetic process
GO:0060255	regulation of macromolecule metabolic process
GO:0031047	gene silencing by RNA
GO:0044260	cellular macromolecule metabolic process
GO:0090407	organophosphate biosynthetic process
GO:0044267	cellular protein metabolic process
GO:0000226	microtubule cytoskeleton organization
GO:0043170	macromolecule metabolic process
GO:0006306	DNA methylation
GO:0006305	DNA alkylation
GO:0044728	DNA methylation or demethylation

GO:0006304	DNA modification
GO:0007346	regulation of mitotic cell cycle
GO:0006260	DNA replication
GO:0048610	cellular process involved in reproduction
GO:0019219	regulation of nucleobase-containing compound metabolic process
GO:0051171	regulation of nitrogen compound metabolic process
GO:0007010	cytoskeleton organization
GO:1901564	organonitrogen compound metabolic process
GO:0015031	protein transport
GO:0045184	establishment of protein localization
GO:0006886	intracellular protein transport
GO:0080090	regulation of primary metabolic process
GO:0010556	regulation of macromolecule biosynthetic process
GO:2000112	regulation of cellular macromolecule biosynthetic process
GO:0031326	regulation of cellular biosynthetic process
GO:0019637	organophosphate metabolic process
GO:0046907	intracellular transport
GO:0006346	methylation-dependent chromatin silencing
GO:0009889	regulation of biosynthetic process
GO:0051649	establishment of localization in cell
GO:0010468	regulation of gene expression
GO:0044281	small molecule metabolic process
GO:0019538	protein metabolic process
GO:0042991	transcription factor import into nucleus
GO:0009560	embryo sac egg cell differentiation
GO:0022412	cellular process involved in reproduction in multicellular organism
GO:0009957	epidermal cell fate specification
GO:0031048	chromatin silencing by small RNA
GO:0006355	regulation of transcription, DNA-dependent
GO:2001141	regulation of RNA biosynthetic process
GO:0051252	regulation of RNA metabolic process
GO:0006839	mitochondrial transport
GO:0044767	single-organism developmental process
GO:0001708	cell fate specification
GO:0006626	protein targeting to mitochondrion
GO:0072655	establishment of protein localization to mitochondrion
GO:0044710	single-organism metabolic process
GO:0006468	protein phosphorylation
GO:0032501	multicellular organismal process
GO:0010310	regulation of hydrogen peroxide metabolic process
GO:2000377	regulation of reactive oxygen species metabolic process
GO:0071702	organic substance transport
GO:0016310	phosphorylation
GO:0048869	cellular developmental process

GO:0007051	spindle organization
GO:0051225	spindle assembly
GO:0070925	organelle assembly
GO:0007126	meiosis
GO:0044707	single-multicellular organism process
GO:0009791	post-embryonic development
GO:0006974	cellular response to DNA damage stimulus
GO:0001510	RNA methylation
GO:0006261	DNA-dependent DNA replication
GO:0009451	RNA modification
GO:0001666	response to hypoxia
GO:0036293	response to decreased oxygen levels
GO:0010089	xylem development
GO:0070482	response to oxygen levels
GO:0048856	anatomical structure development
GO:0009862	systemic acquired resistance, salicylic acid mediated signaling pathway
GO:0010087	phloem or xylem histogenesis
GO:0006281	DNA repair
GO:0009640	Photomorphogenesis
GO:0030154	cell differentiation
GO:0009888	tissue development
GO:0006310	DNA recombination
GO:0000338	protein deneddylation
GO:0010388	cullin deneddylation
GO:0048511	rhythmic process
GO:0007623	circadian rhythm
GO:0000741	Karyogamy
GO:0048284	organelle fusion
GO:0090305	nucleic acid phosphodiester bond hydrolysis
GO:0051716	cellular response to stimulus
GO:0014070	response to organic cyclic compound
GO:0051234	establishment of localization
GO:0044765	single-organism transport
GO:0006810	transport
GO:0007049	cell cycle
GO:0072521	purine-containing compound metabolic process

GO terms enriched in down-regulated genes from infected Col-0 vs. uninfected Col-0:

GO Term	Description
GO:0009719	response to endogenous stimulus
GO:0010033	response to organic substance
GO:0010200	response to chitin
GO:0010243	response to organonitrogen compound
GO:0042221	response to chemical
GO:1901700	response to oxygen-containing compound
GO:0050896	response to stimulus
GO:1901698	response to nitrogen compound
GO:0009611	response to wounding
GO:0009612	response to mechanical stimulus
GO:0009725	response to hormone
GO:0009873	ethylene mediated signaling pathway
GO:0000160	phosphorelay signal transduction system
GO:0009963	positive regulation of flavonoid biosynthetic process
GO:0006950	response to stress
GO:0009962	regulation of flavonoid biosynthetic process
GO:0071369	cellular response to ethylene stimulus
GO:0006857	oligopeptide transport
GO:0015833	peptide transport
GO:0042886	amide transport
GO:0044765	single-organism transport
GO:0002679	respiratory burst involved in defense response
GO:0045730	respiratory burst
GO:0009755	hormone-mediated signaling pathway
GO:0010363	regulation of plant-type hypersensitive response
GO:0006612	protein targeting to membrane
GO:0090150	establishment of protein localization to membrane
GO:0010941	regulation of cell death
GO:0043067	regulation of programmed cell death
GO:0080135	regulation of cellular response to stress
GO:0032870	cellular response to hormone stimulus
GO:0071495	cellular response to endogenous stimulus
GO:0002682	regulation of immune system process
GO:0045088	regulation of innate immune response
GO:0050776	regulation of immune response
GO:0006812	cation transport
GO:0002252	immune effector process
GO:0071705	nitrogen compound transport

GO terms enriched in up-regulated genes from infected *ein5-1* vs. uninfected *ein5-1*:.

GO Term	Description
GO:0016570	histone modification
GO:0016569	covalent chromatin modification
GO:0016568	chromatin modification
GO:0051276	chromosome organization
GO:0022402	cell cycle process
GO:0016572	histone phosphorylation
GO:0006325	chromatin organization
GO:0009909	regulation of flower development
GO:0034968	histone lysine methylation
GO:0048831	regulation of shoot system development
GO:0048580	regulation of post-embryonic development
GO:0031323	regulation of cellular metabolic process
GO:2000241	regulation of reproductive process
GO:0050789	regulation of biological process
GO:0051567	histone H3-K9 methylation
GO:0019222	regulation of metabolic process
GO:2000026	regulation of multicellular organismal development
GO:0051239	regulation of multicellular organismal process
GO:0016571	histone methylation
GO:0006479	protein methylation
GO:0008213	protein alkylation
GO:0006259	DNA metabolic process
GO:0006996	organelle organization
GO:0050794	regulation of cellular process
GO:0065007	biological regulation
GO:0050793	regulation of developmental process
GO:0032259	Methylation
GO:0043414	macromolecule methylation
GO:0006275	regulation of DNA replication
GO:0051052	regulation of DNA metabolic process
GO:0044763	single-organism cellular process
GO:0044699	single-organism process
GO:0010605	negative regulation of macromolecule metabolic process
GO:0008283	cell proliferation
GO:0016458	gene silencing
GO:0009892	negative regulation of metabolic process
GO:0007017	microtubule-based process
GO:0010629	negative regulation of gene expression
GO:0032502	developmental process
GO:0048449	floral organ formation
GO:0010310	regulation of hydrogen peroxide metabolic process
GO:0048519	negative regulation of biological process

GO:0040029	regulation of gene expression, epigenetic
GO:0048645	organ formation
GO:2000377	regulation of reactive oxygen species metabolic process
GO:0010558	negative regulation of macromolecule biosynthetic process
GO:2000113	negative regulation of cellular macromolecule biosynthetic process
GO:0009890	negative regulation of biosynthetic process
GO:0031327	negative regulation of cellular biosynthetic process
GO:0060255	regulation of macromolecule metabolic process
GO:0010564	regulation of cell cycle process
GO:0031324	negative regulation of cellular metabolic process
GO:0006342	chromatin silencing
GO:0045814	negative regulation of gene expression, epigenetic
GO:0043412	macromolecule modification
GO:0048646	anatomical structure formation involved in morphogenesis
GO:0006725	cellular aromatic compound metabolic process
GO:0019219	regulation of nucleobase-containing compound metabolic process
GO:0006464	cellular protein modification process
GO:0036211	protein modification process
GO:0051171	regulation of nitrogen compound metabolic process
GO:0048453	sepal formation
GO:0048451	petal formation
GO:0003006	developmental process involved in reproduction
GO:0010389	regulation of G2/M transition of mitotic cell cycle
GO:0045892	negative regulation of transcription, DNA-dependent
GO:0051253	negative regulation of RNA metabolic process
GO:0051726	regulation of cell cycle
GO:0045934	negative regulation of nucleobase-containing compound metabolic process
GO:0000226	microtubule cytoskeleton organization
GO:1901360	organic cyclic compound metabolic process
GO:0001666	response to hypoxia
GO:0036293	response to decreased oxygen levels
GO:0051172	negative regulation of nitrogen compound metabolic process
GO:0022414	reproductive process
GO:0006270	DNA replication initiation
GO:1901990	regulation of mitotic cell cycle phase transition
GO:1901987	regulation of cell cycle phase transition
GO:0032506	cytokinetic process
GO:0000911	cytokinesis by cell plate formation
GO:1902410	mitotic cytokinetic process
GO:0009862	systemic acquired resistance, salicylic acid mediated signaling pathway
GO:0080090	regulation of primary metabolic process
GO:0070482	response to oxygen levels
GO:0010556	regulation of macromolecule biosynthetic process

GO:2000112	regulation of cellular macromolecule biosynthetic process
GO:0010089	xylem development
GO:0031326	regulation of cellular biosynthetic process
GO:0010087	phloem or xylem histogenesis
GO:0048523	negative regulation of cellular process
GO:0009889	regulation of biosynthetic process
GO:0006606	protein import into nucleus
GO:0051170	nuclear import
GO:0007010	cytoskeleton organization
GO:0046483	heterocycle metabolic process
GO:0006139	nucleobase-containing compound metabolic process
GO:0034641	cellular nitrogen compound metabolic process
GO:0006807	nitrogen compound metabolic process
GO:0006468	protein phosphorylation
GO:0016043	cellular component organization
GO:0048610	cellular process involved in reproduction
GO:0042991	transcription factor import into nucleus
GO:0016310	Phosphorylation
GO:0006913	nucleocytoplasmic transport
GO:0051169	nuclear transport
GO:0007346	regulation of mitotic cell cycle
GO:0010468	regulation of gene expression
GO:0071446	cellular response to salicylic acid stimulus
GO:0009863	salicylic acid mediated signaling pathway
GO:0009220	pyrimidine ribonucleotide biosynthetic process
GO:0009218	pyrimidine ribonucleotide metabolic process
GO:0090304	nucleic acid metabolic process
GO:0006221	pyrimidine nucleotide biosynthetic process
GO:0006220	pyrimidine nucleotide metabolic process
GO:0072528	pyrimidine-containing compound biosynthetic process
GO:0006260	DNA replication
GO:0007051	spindle organization
GO:0051225	spindle assembly
GO:0070925	organelle assembly
GO:0017038	protein import
GO:0009987	cellular process
GO:0046390	ribose phosphate biosynthetic process
GO:0009260	ribonucleotide biosynthetic process
GO:0072527	pyrimidine-containing compound metabolic process
GO:0010033	response to organic substance
GO:0009259	ribonucleotide metabolic process
GO:0019693	ribose phosphate metabolic process
GO:0071840	cellular component organization or biogenesis
GO:0031047	gene silencing by RNA

GO:0009751	response to salicylic acid
GO:0050896	response to stimulus
GO:0044238	primary metabolic process
GO:0044267	cellular protein metabolic process
GO:0009888	tissue development
GO:0051716	cellular response to stimulus
GO:0007126	meiosis
GO:0008152	metabolic process
GO:0014070	response to organic cyclic compound
GO:0006793	phosphorus metabolic process
GO:0065001	specification of axis polarity
GO:0009944	polarity specification of adaxial/abaxial axis
GO:0048856	anatomical structure development
GO:0072594	establishment of protein localization to organelle

GO terms enriched in down-regulated genes from infected *ein5-1* vs. uninfected *ein5-1*:

GO Term	Description
GO:0044036	cell wall macromolecule metabolic process
GO:0030001	metal ion transport
GO:0000041	transition metal ion transport
GO:0006857	oligopeptide transport
GO:0015833	peptide transport
GO:0042886	amide transport
GO:0010413	glucuronoxylan metabolic process
GO:0045492	xylan biosynthetic process
GO:0045491	xylan metabolic process
GO:0070592	cell wall polysaccharide biosynthetic process
GO:0070589	cellular component macromolecule biosynthetic process
GO:0044038	cell wall macromolecule biosynthetic process
GO:0010410	hemicellulose metabolic process
GO:0006812	cation transport
GO:0071705	nitrogen compound transport
GO:0034637	cellular carbohydrate biosynthetic process
GO:0010383	cell wall polysaccharide metabolic process
GO:0010106	cellular response to iron ion starvation
GO:0006826	iron ion transport
GO:0044765	single-organism transport
GO:0015698	inorganic anion transport
GO:0006811	ion transport
GO:0044262	cellular carbohydrate metabolic process
GO:0010167	response to nitrate
GO:0015706	nitrate transport
GO:0033692	cellular polysaccharide biosynthetic process
GO:0016051	carbohydrate biosynthetic process
GO:0010087	phloem or xylem histogenesis
GO:0071365	cellular response to auxin stimulus
GO:0009734	auxin mediated signaling pathway
GO:0000271	polysaccharide biosynthetic process
GO:0006810	transport

GO terms enriched in down-regulated genes from uninfected *ein5-1* vs. uninfected Col-0:

GO Term	Description
GO:0006950	response to stress
GO:0010200	response to chitin
GO:0010243	response to organonitrogen compound
GO:1900674	olefin biosynthetic process
GO:1900673	olefin metabolic process
GO:0043449	cellular alkene metabolic process
GO:0043450	alkene biosynthetic process
GO:0009693	ethylene biosynthetic process
GO:0009692	ethylene metabolic process
GO:0009612	response to mechanical stimulus
GO:0009611	response to wounding
GO:1901698	response to nitrogen compound
GO:0009873	ethylene-activated signaling pathway
GO:0000160	phosphorelay signal transduction system
GO:0050896	response to stimulus
GO:0071369	cellular response to ethylene stimulus
GO:0009719	response to endogenous stimulus
GO:1901700	response to oxygen-containing compound
GO:0010033	response to organic substance
GO:0046482	para-aminobenzoic acid metabolic process